DEVELOPMENT OF HURRICANE BASED FRAGILITY CURVES FOR WOOD-ZINC HOUSES IN PUERTO RICO

by

Rolando García González

A thesis submitted in partial fulfillment
of the requirements for the degree of

DOCTOR OF PHILOSOPHY
in
CIVIL ENGINEERING
UNIVERSITY OF PUERTO RICO
MAYAGÜEZ CAMPUS
2007

Approved by:

_____	_____
Felipe J. Acosta, Ph.D. Member, Graduate Committee	Date
_____	_____
Luis A. Godoy, Ph.D. Member, Graduate Committee	Date
_____	_____
Ricardo R. López, Ph.D. Member, Graduate Committee	Date
_____	_____
Ricardo Ramos, Ph.D. Member, Graduate Committee	Date
_____	_____
Ali Saffar, Ph.D. President, Graduate Committee	Date
_____	_____
Ismael Pagán, M.S.C.E. Chairperson of the Department	Date
_____	_____
Víctor Huérfano, Ph.D. Representative, Graduate Studies	Date

ABSTRACT

The costliest natural disasters to strike Puerto Rico in the last century have been caused by tropical storms and hurricanes. Over the years, many attempts were made to reduce vulnerability by improving the infrastructures. The results have been mixed for what can be best described as lack of focus on areas needing the most attentions. Wood-zinc houses are constructed using stud walls and a roof system formed by fastening corrugated, galvanized steel sheets, referred to as zinc, to wood spacers and rafters. In the aftermath of hurricane Georges, in 1998, nearly 5,000 houses were destroyed and more than 95,000 houses suffered extensive roof damage. The majority of the houses involved were wood-zinc houses.

Consequence-based Risk Management, CRM, is a new multidisciplinary approach to multi-hazards risk reduction that was developed over the last decade by the researchers at the Mid-America Earthquake Center, MAE. In the CRM approach, a succession of processes and decisions are used to predict the consequences of a particular hazard, be it an earthquake, fire, flood, or a hurricane. The UPRM, being a member of MAE, was assigned the task of examining the portability of the CRM into a multi-hazards environment. The wood-zinc structures were selected as the best example to test the consequence minimization

The purpose of this investigation is to select prototypes, quantify demand and resistance functions, and develop fragility curves for different classes of wood-zinc structures used in Puerto Rico. From historical records, the roof system and the roof-to-

wall connections have been the most vulnerable components for these structures. Other components considered are the wall systems, the wall sidings, and the openings. Full scale laboratory testing was used to model the roof systems based on a new dynamic load protocol. The structural systems tested varied from weak, W, to common, C1 and C2, to strong, S1 and S2, to ultimate, U. The S2 and U systems use zinc straps as a roof retrofitting measure. Different design and built configurations were also examined for roof-to-wall connections and wall systems. Simulations show substantial improvements in the performance of systems whenever high code standards are followed.

RESUMEN

Los desastres naturales más dañinos en azotar la isla de Puerto Rico el último siglo han sido tormentas tropicales y huracanes. Con el pasar de los años, se han realizado muchos intentos con el propósito de mitigar los daños mejorando la infraestructura del país. Los resultados han sido variados debido mayormente a falta de atención y enfoque en las áreas críticas. Estas residencias son construidas con paredes de madera y un sistema de techo compuesto por viguetas y alfajías de madera que sostienen las planchas de zinc criollo, como son conocidas en la Isla. Luego del azote del huracán Georges en 1998, cerca de 5,000 residencias fueron destruidas, mientras que sobre 95,000 casas sufrieron daños extensos en el techo. La mayoría de estas residencias eran de madera con techos de madera y zinc.

El manejo de riesgo basado en consecuencias (*CRM*, por sus siglas en inglés) es un enfoque multidisciplinario nuevo, basado en la reducción de riesgos de diversos desastres. El mismo fue desarrollado durante la última década por investigadores en el *Mid-America Earthquake Center*, (*MAE*, por sus siglas en inglés). Durante la implementación del CRM, una serie de procesos y decisiones se utilizan para predecir las consecuencias de un desastre en particular, sea éste un terremoto, un fuego, una inundación o un huracán, entre otros. La Universidad de Puerto Rico, recinto de Mayagüez, siendo miembro del centro MAE, emprendió la tarea de estudiar la aplicación del CRM a un ambiente expuesto a múltiples desastres. Las estructuras de madera y zinc

fueron seleccionadas como el mejor ejemplo para probar las técnicas de mitigación y minimización de consecuencias.

El propósito de esta investigación fue el seleccionar prototipos, cuantificar demandas de cargas y capacidad y desarrollar curvas de fragilidad para las diversas estructuras de madera y zinc en Puerto Rico. Históricamente, los componentes más vulnerables de estas estructuras han sido el sistema de techo y las conexiones techo-pared. Tanto el sistema de paredes como su cubierta y aperturas fueron considerados. Pruebas experimentales a escala real utilizando un protocolo de carga novel fueron realizadas para modelar el sistema de techo. Los sistemas estructurales estudiados variaron entre las configuraciones débiles (W), comunes (C1 y C2), fuertes (S1 y S2) y última (U). Varias configuraciones para las conexiones entre techo y pared y para los sistemas de pared también fueron evaluadas. Las simulaciones realizadas demuestran mejoras substanciales en el desempeño de los sistemas que son construidos con mayor calidad.

This work is dedicated to the people who gave me the strength to finish it:
my father, Rodolfo García Pacheco,
my mother, Carmen Migdalia González de la Cruz,
my grandmother, Paula de la Cruz Pérez,
my brother and sister, Rodolfo and Migdalia,
my good friends, you are too many to list,
and my beloved wife, Bessie R. López, this is for you.

ACKNOWLEDGEMENTS

Such an extensive work could not have been completed without the help and support of various people. I would like to extend my gratitude to the Mid America Earthquake Center and to FEMA for financing this research. I would like to thank my advisor, Dr. Ali Saffar, for believing in me and for his unconditional support and guidance throughout all these years. I would also like to thank the members of my graduate committee, Dr. Ricardo López, Dr. Luis A. Godoy, Dr. Ricardo Ramos, and Dr. Felipe Acosta for their constructive criticism and insight. My most sincere gratitude is also extended to Dr. Daniel Wendichansky for accepting me into the structural laboratory office and for his support.

For their help during the experimental phase of the research, I thank the laboratory technicians Mr. Elvis Ramos, Mr. Iván Santiago, Mr. Monserrate Cruz, and the reproductions technician Mr. Miguel Báez. I am also thankful to many friends that have made these years more bearable. Thanks to my housemates of many years, Juan A. Román, Yadiel Rivera, and our unofficial housemate Gilberto Martínez; you are my brothers. I am also thankful for the friendship and support that Daniel Avilés, Samuel Cuadrado, Paul Kohan, Guillermo Gerbaudo, Rosana Aguilar, and Jaffet Martínez have offered me. I really appreciate it. A very special thank you goes to two fellows that shared this odyssey first hand with me, and I owe them more than a thank you for their support, camaraderie, and friendship. Thanks to Edgardo Vélez Vélez and Jorge Ayala Burgos. Mi gente, lo hicimos, acabamos…

I also want to thank my family, Rodolfo and Migdalia García, Jordi and Gabriel Maura, Miguel Hernández, and Luis Pérez. Thanks to my parents for all their support, love, and righteous upbringing, Rodolfo García Pacheco and Carmen Migdalia González de la Cruz. Thanks to my grandmother, Paula de la Cruz Pérez for being an inspiration. Last, but not least, I thank my lovely wife, Bessie R. López Meléndez for putting up with this for so long.

TABLE OF CONTENTS

LIST OF TABLES

APPENDIX B ROOF TESTS SUMMARY

LIST OF FIGURES

CHAPTER 11 ADDITIONS AND INSTITUTIONAL BUILDINGS

CHAPTER 12 CONCLUSIONS

APPENDIX B ROOF TESTS SUMMARY

CHAPTER 1

INTRODUCTION

1.1 General

The costliest hurricane to hit Puerto Rico, Hurricane Georges made landfall on the southeastern coast of the island on the night of September 22, 1998. Wind velocities of 110 to 115 mph were sustained during a 6-hour trek across the island. Widespread property and agricultural damages are estimated at over two billion dollars. Nearly 5000 houses were destroyed and more than 95,000 houses suffered extensive roof damage. The majority of the houses involved were wood houses with wood-zinc roofs.

In the aftermath of hurricane Georges, many prominent political and business leaders questioned the wisdom of building wood houses in Puerto Rico. As presented, it appeared indeed wasteful to keep rebuilding in wood when you can build it in concrete and save long term in rebuilding costs. Numerous pictures of wood-zinc roofs flown away by the hurricane winds helped lend validity to such arguments. However, in close analysis there was no solid evidence to suggest that concrete provided a better value than wood or for that matter any other type of construction material.

The United States Census Bureau data from 1990 lists more than 150,000 houses in Puerto Rico as either wood frame or mixed construction with wood-zinc roofs. This constituted roughly fifteen percents of all the Island's housing. Although more recent surveys do not provide building classification details, construction trends over the last few decades have remained relatively unchanged. It may therefore be concluded that the reported losses from past hurricanes in Puerto Rico are disproportionately related to low-cost wood-zinc houses and auxiliary structures. Since 1989, hurricanes Hugo, Georges and Hortense have provided ample evidence of this. The engineering profession has tried to address the problem by disseminating information on correcting measures through construction guides and workshops. Most of these guides, however, prescribe to the so called common sense approach and can not predict with any degree of certainty the cost-to-benefit ratio.

The purpose of this investigation is to select prototypes, develop fragility curves, and quantify loss functions for different classes of wood structures that are commonly used in Puerto Rico. Fragility curves are traditionally defined to project the probability that the structure under consideration will undergo a specific damage state at a given hazard level. Up to four damage states are typified in descriptive terms such as minor, moderate, extensive and total. Each damage state will have an associated fragility curve. Given the likelihood of various hazard levels, weights can be assigned to the expected damage states for each building class. Factoring in the loss functions, lifetime maximum probable loss may be estimated. For the purposes of this investigation, the prototype structures are assumed to follow at the minimum the basic guidelines from the Federal Emergency Management Agency (FEMA) and the Puerto Rico Engineering and Land

Surveying Board (CIAPR, from its Spanish acronym). To be sure, there are still structures on the Island which would violate those guidelines. However, since the federally mandated approval of a national building code, their numbers have been in sharp decline.

The lifetime maximum probable loss data is essential in providing risk assessment guidelines for both government and insurance agencies. By presenting the real cost of a low-cost building for a region, rational decisions can be made on whether or not any rebuilding plan should include the same kind of construction. The ratio of life cycle cost to original cost may also be used as an adjustment factor by insurance agents allowing them to write mortgage policies which are not available now. The home owners or buyers could also profit by having reduced mortgage rates for refinancing or purchase of the house. As it is, most banks do not issue mortgages without insurance, and most insurance companies in the island will not cover the wood and wood-zinc roof houses because of the uncertainties in both construction and behavior.

1.2 Consequence-Based Risk Management

Consequence-based Risk Management (CRM) is a new multidisciplinary approach to multi-hazards risk reduction. The methodology was developed over the last decade by the researchers at the Mid-America earthquake Center to which UPRM is a member institution. CRM is defined by a succession of processes and decisions that predict the consequences of a particular hazard, be it an earthquake or as in this research

a hurricane. It can also be used to investigate the impact of specific mitigation techniques on reducing the losses across a system of interest.

Generally, the CRM framework connects four interacting disciplines. These are hazard definition, engineering engines, social sciences, and information technology. Hazard definition is the foundation upon which the entire framework rests. It defines such things as ground motion maps and hurricane path records. The engineering engine is concerned with uniform fragilities, dynamic networks, inventory technologies, and multi-hazards interactions. It also provides the social sciences with enough information to facilitate decision dynamics through quantitative social and economic impact models. Both the engineering engine and social sciences feed into information technology to implement loss models.

There are uncertainties associated with the CRM methodology. The hazard definitions are not readily available. The divisions between groups with known system fragilities must narrow down considerably. The system inventories are expensive to generate and would be even more so once the fragility groups are extended. Over time, the uncertainties related to the key components may be reduced. This will require considerable investments in inventory technologies and damage synthesis areas. As with this research, the consequence minimization objective should remain the driving force behind any such endeavors.

1.3 Objectives

The primary goal of this investigation is to provide damage and risk estimation tools for wooden buildings with wood-zinc roofs in Puerto Rico under hurricane-wind loading. These structures include houses, additions to houses, schools, and other institutions. To achieve this objective, a newly devised dynamic loading protocol is extended to rate metal roof systems in an efficient and methodical manner. The secondary goal of this investigation is to enable consequence minimization framework in order to carry out cost-benefit analysis in the use of the retrofits. In the process, we shall examine the portability of the CRM methodology beyond the Mid-America region by calibrating and refining structural elements of loss estimation and visualization in a well-defined multi-hazard environment.

1.4 Attempts at System Fragility

One of the earliest attempt to use fragility curves in an extreme wind fragility model dates back to 1976, when G. C. Hart used the data provided by a panel of experts. The Delphi method is a technique for obtaining forecasts from a panel of independent experts. Experts are asked their opinions over two or more rounds. The process ends when the opinions change little between rounds. Final round forecasts are then combined by averaging. The Delphi method was also used by Schiff and Newsom (1979) to predict the fragility of electrical power equipments under extreme lateral loads such as those caused by earthquakes or hurricanes. Their findings demonstrated the shortcomings of the Delphi method when the data provided by different panels of experts differed by as

much as a factor of three for some cases. Around the same time, Leicester et al. (1979) used a linear correlation between wind speed and damage index to develop fragility curves for certain classes of buildings in Australia.

Applied Technology Council was the first group to generate a systematic approach for quantifying structural fragility in a report directed to the Seismic Safety Commission of the state of California (ATC-13, 1985). Again the Delphi method was used. The results were later tested and verified by the Committee on Earthquake Engineering (CoEE, 1989) using different panels of experts but much of the same terminology. Modern fragility and reliability analyses were becoming more common in relation with wooden structures also. For example, Bulleit and Yate (1991) analyzed metal-plate connected wood trusses using a finite element approach and then compared the results with the ones obtained from Monte Carlo simulation derived from experimental tests, reporting their results as satisfactory. Years later, Bulleit and Liu (1995) used a similar approach to study the lifetime behavior of wood floor and roof systems subjected to sustained uniform loads and simply supported at two edges. Rosowsky and Cheng (1999a and 1999b) conducted in parallel papers the characterization of the statistical properties of light-framed wooden gable roofs and possible failure modes, proceeding later to establish the system reliability. The authors determined the reliability index, β, for the roof systems, using the ASCE 7–95 for calculating the wind demands on their analyses.

More recently, Shinozuka et al. (2000) presented a statistical analysis of structural fragility curves for a complete bridge, using the empirical data from the 1995 Kobe earthquake. Khanduri and Morrow (2002) developed a fragility function for Puerto Rico

based on loss data of insurance companies. A methodology for disaggregating the curve into several curves that represent better individual building types by combining it with local data and particular building inventory information of a specific area was also presented. Rosowsky and Lee (2004) used the sensitivity analysis (varying exposure, nailing schedule, etc.) to develop a fragility model for roof sheathing uplift.

1.5 Component-Based Fragility

While most of the research on fragility has historically been focused on complete structures, research on component-based fragility (CBF) has gained ground in recent years. In a CBF model, the structure is considered to be an assembly of individual parts (sheathings, connections, etc.) interacting together. Individual fragilities of various components are determined separately and then combined, based on certain rules of interaction, to obtain the fragility of the structure as a whole (Davidson et al., 2003). The newer, more sophisticated wind fragility analyses are based on CBF. Unanwa and McDonald (2000) used upper and lower probability damage bands from previously determined fragility curves and wind resistance indices to predict wind damage to buildings. The buildings are divided into several components, stressing the importance of the connections between the components. The CBF model was also used by the Federal Emergency Management Agency (FEMA) and the National Institute of Building Sciences (NIBS) in developing the wind hazard component of their new HAZUS-MH loss estimation software. Both HAZUS and Unanwa and McDonald models were

utilized by Zhao (2002), who formulated a Markov chain based methodology to predict region wide changes in fragility of buildings over time.

A conceptual framework for the definition of the basic damage states and the corresponding fragility curves under extreme wind loads was presented by Filliben et al. (2002). Similarly, Ellingwood and Rosowsky (2004) proposed a methodology to carry out fragility analysis for light-frame wood structures subjected to extreme hazards. Their limit states were based on a performance review of the residential buildings during near past hurricanes and earthquakes. Individual fragility curves for different structural components, such as roof panels and wood panel shear walls, and non-structural components were developed. Abdullah and Norton (2004) formulated a methodology to predict damages based on system fragility by using a fault tree analysis and relating component fragilities to one another. Their main focus was on low to medium-rise structures exposed to extreme loading events, such as earthquakes and hurricanes.

1.6 Methodology

By CRM terminology, this investigation was designed to feed into damage synthesis and consequence minimization objectives. The wood-zinc structures were identified as the local construction type most suspect to hurricane wind loading. For evaluating the performances of these structures, critical components and their failure modes had to be identified. Historical data has shown that the most critical component is the wood-zinc roof ensemble. Although the damages to the roofs are more often localized, there are well publicized images of the complete roof assemblies having been

torn out of place. In strict terms, the latter is not a problem of the roof system itself but rather of the roof-to-wall connections.

Fragility curves represent the form of data most suited to consequence minimization objectives. Imagine two distinct sets of curves, one for a vulnerable system and the other for the same system with a suggested retrofit. Now imagine several sets with different retrofitting options. Cost to benefit ratios can be calculated for various scenarios, for a given hurricane or for all potential hurricanes over certain time periods, for one building or for clusters of buildings. The development of fragility curves themselves would be an exercise in damage synthesis.

Table 1.1 shows the damage matrix from which the fragility curves in this study are developed. The damage matrix has rows defining damage states and columns defining the corresponding demands on building components. The first two columns are for the components previously discussed. The next two columns are for wall system and wall sidings. These two components rarely result in total loss of the system. The last column describes damage states for the windows and other openings.

The damage matrix describes two types of component failure. The more common is the progressive type of failure, which sets limits on all four damage states. The roof system, wall siding, and window components fall under this category. The second type of component failure is the yes or no proposition type, as in roof-to-wall connections and wall structure. Failure of these components will result in the loss of the system.

Except for the column describing the roof system, the rest of the damage matrix follows the industry norm for hurricane fragilities. The roof system column is generated based on the experimental study described in Chapters 4 and 5. The definition of the roof

performance index used in this classification, I_{RP}, is given in Chapter 6. Using the damage state limits in Table 1.1, the fragility relationships for wood-zinc houses, additions, and institutions are developed.

Table 1.1 - Damage matrix for wood-zinc structures

Damage State	Roof System	Roof-to-Wall Connections	Wall Siding	Wall Structure	Windows
Slight	$0.25 < I_{RP} < 0.5$	No	<5%	No	1
Moderate	$0.5 \leq I_{RP} < 1$	No	5%-10%	No	Up to 3 or 15%
Extensive	$1 \leq I_{RP} \leq 1.5$	No	10%-20%	No	>3 or 15%-50%
Total	$I_{RP} > 1.5$	Yes	>20%	Yes	>50%

Log-normal distributions representing fragility curves are defined by two sets of parameters. For a given component under a specific demand, a performance index varying from 0 to 4 may be assigned, with 0 meaning no damage and 4 the total damage. Table 1.2 shows an example for a conventional roof system at a wind speed of 200 mph. Each house ID in this table refer to one out of one hundred selections from a data base of wood zinc-houses. Notice that the same house may be counted under several damage states, depending on its performance index. For example, a sample with a performance index of 3 will be counted in the minor and moderate damage states as well as the extensive damage state. The reason lies in the cumulative nature of the fragility curves as depicted in Figure 1.1. For the system represented by this figure, the total damage state is likely 20 percent of the time at a wind speed of 150 mph. There is also 10 percent chance of having extensive damage state, 25 percent chance of having moderate damage state, 21

percent chance of having minor damage state, and 24 percent chance of having no damages.

Table 1.2 – Example on developing fragility curves

Conventional Roof System at 200 mph					
House ID	Performance Index	Damage States			
		Slight	Moderate	Extensive	Total
1	2	1	1	0	0
2	2	1	1	0	0
3	3	1	1	1	0
4	2	1	1	0	0
5	2	1	1	0	0
6	3	1	1	1	0
7	2	1	1	0	0
⋮ ⋮	⋮ ⋮	⋮ ⋮	⋮ ⋮	⋮ ⋮	⋮ ⋮
99	2	1	1	0	0
100	1	1	0	0	0
Σ D.S./100 =		0.99	0.97	***0.31***	0

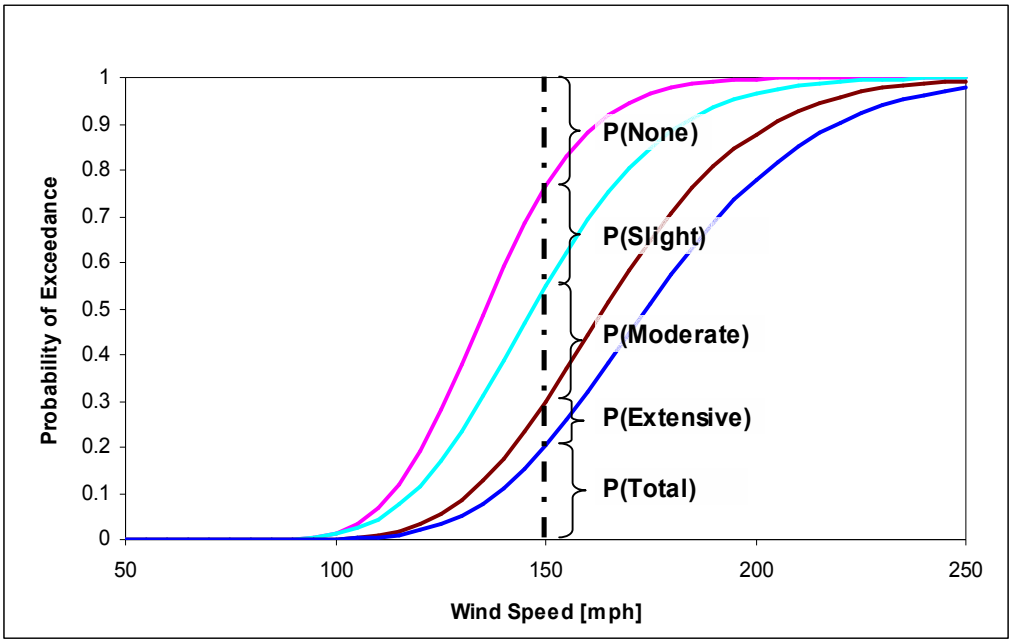

Figure 1.1 – Example on reading the fragility curves

The results from Table 1.2 will give one data point for each damage state. Table 1.3 presents the outcome for the extensive damage state if the process is repeated at different wind speeds. For further clarification, the result from Table 1.2 is underlined. Once a table similar to Table 1.3 is generated, the corresponding fragility curve is drawn by curve fitting a log-normal CDF equation, varying the statistical parameters until the mean squares of differences are minimized. Figure 1.2 shows an example of the curve fitting into the data points along with the statistical parameters defining the curve.

Table 1.3 – Cumulative number of extensive damage states at different wind speed

Wind Speed	50-180	185	190	195	200	205	210	215	220	225	230	235	240	245	250
Extensive D.S.	0	2	7	16	31	40	52	59	70	78	87	93	96	99	100

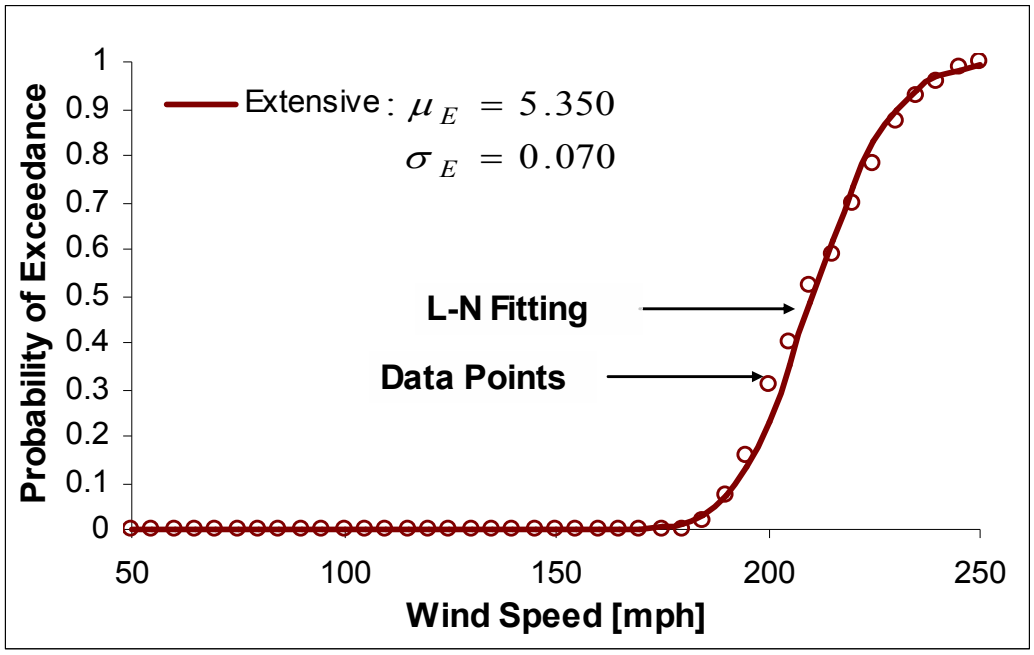

Figure 1.2 – Example of curve fitting into the data points

1.7 Scope

The main focus of this research is on the fragility of wood-zinc structures in Puerto Rico under extreme wind events. To that end, certain components of these systems need to be studied and analyzed. The deliverables of this investigation will provide the necessary tools for assessing and minimizing the consequences of such events. To achieve these goals, the following tasks were completed:

1) Collection and archiving of systems inventory in Puerto Rico from which building prototypes may be selected.
2) Laboratory testing of full-scale wood-zinc roof specimens under a new dynamic loading protocol in order to determine the resistance capacity of such systems under various design configurations.
3) Model testing of connections between roofing system and the walls.
4) Using both experimental and analytical data to feed into the simulation models of selected prototypes.
5) Developing damage matrices and fragility functions for the prototype structures.

1.8 Organization

This thesis is divided into twelve chapters. The introductory chapter presents the motivation for the study as well as some background materials. Chapter 2 reviews general wood-zinc construction in Puerto Rico and the selection of building prototypes for simulation studies. The extreme wind loading for both systems and components is

discussed in Chapter 3. The selection of roof prototypes for experimental studies, including retrofitted systems, as well as the testing apparatus and the dynamic loading schedules are presented in Chapter 4. The performances of roof specimens and the ratings assigned to them are discussed in Chapter 5. The final chapter on roof systems, Chapter 6 presents the translation of data from the laboratory experiments to fragility relationships.

A partially composite stud wall model is used to evaluate the wall system fragility in Chapter 7. Also discussed in that chapter is a simple model based on nailing schedules to determine the extent of damages to wall sidings. Chapter 8 presents the laboratory findings along with fragility properties for the roof-to-wall connections. Failure modes for windows and other openings are discussed in Chapter 9. Using the combination rules in Table 1.1, the system fragilities for wood-zinc houses are developed in Chapter 10. All other wood-zinc buildings along with similar structures are discussed in Chapter 11. The final chapter reports the conclusions derived from this research, including some consequence mitigation examples and design recommendations. A summary of fragility parameters are presented in Appendix A. Detailed schematics of each roof test, listing the damage types in order of occurrence, is provided in Appendix B.

CHAPTER 2

WOOD-ZINC CONSTRUCTION IN PUERTO RICO

2.1 Introduction

Wood-zinc roof systems are assembled by fastening zinc coated, corrugated, galvanized steel sheets to wood spacers and rafters. Most wood houses and some of the reinforced masonry and concrete structures in Puerto Rico are constructed using these systems. The dwellings are usually low-cost and contractor made, without engineering blueprints or certified inspection of the work. Given their poor performances in the past hurricanes, the Federal Emergency Management Agency (FEMA), the Civil Defense, and the Puerto Rico Engineering and Land Surveying Board (CIAPR, abbreviation from its Spanish name) have prepared technical construction guidelines designed to meet the minimum requirements stipulated by the governing building codes. The guidelines are discussed in this chapter. Also presented are the selection of prototypes for houses, additions, and institutional buildings.

2.2 Building Guidelines

In most circumstances, the gravity loads carried by wood-zinc systems are very light. Light frame structures are traditionally the domain of building contractors. In fact, in the absence of an extreme wind event, many preset configurations of components may suffice. To build against hurricanes, however, sophisticated engineering solutions are required.

The building guidelines proposed by FEMA/CIAPR (1989) stress the importance of the key components of the structure. For a wood-zinc roof assembly this will mean designing connections to secure zinc sheets, spacers, joists, and rafters. Figure 2.1 shows one such assembly. The wood members are sized in accordance with the house width. The suggested dimensions for wood rafters are listed in Table 2.1. Depending on their size, the rafters are spaced at 16", 24", or 32" on center. Wood spacers are aligned perpendicular to the rafters. They add stiffness to the roofing system and provide more area for fastening the zinc sheets and roof membranes. The typical size for wood spacers is 1"x4", although 2"x4" boards may also be used depending on the spacing between rafters. The usual grading of the timber used in Puerto Rico for the construction of wood houses is the pressure treated No.1 Southern Pine.

Zinc-coated galvanized steel sheets are the most common roof sheathing used on the Island. It is corrugated in order to obtain a higher moment of inertia. For drainage purposes, they are placed with the grooves parallel to the joists. The zinc sheets, as they are commonly called on the Island, are typically gauge 26 or less in thickness. They are placed to overlap a minimum of 12-in longitudinally and 6-in transversally.

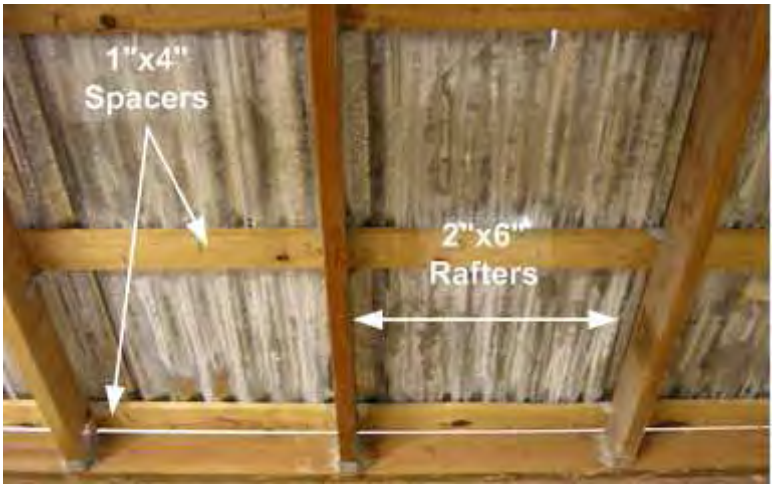

Figure 2.1 – Wood-zinc roof specimen

Table 2.1 – Recommended rafter size for various residence dimensions

Dwelling Width [ft]	Recommended Nominal Rafter Size [in]
16' ~ 22'	2” x 6”
23' ~ 28'	2” x 8”
29' ~ 32'	2” x 10”

Figure 2.2 depicts the typical 3-in long spiral-shank nails used to connect the sheathing to the roof framing alongside the conventional corrugated steel sheet. The recommended spacing for nails is 6-in on the edge and 12-in elsewhere, with additional nails in the overlapping of the galvanized sheathing if needed. They are to be placed on the top crest of the corrugations to reduce the likelihood of water percolating into the interior of the building. These nails are then bent perpendicularly to the grain direction of the wood spacers at their protruding segment through the inside of the residence to provide additional withdrawal resistance.

(a) Umbrella-headed grooved nail **(b) Galvanized corrugated sheet**

Figure 2.2 – Recommended roofing nail and sheathing

The uplift demands resulting from hurricane wind loading are such that metal connection plates and straps are required between various roof components as well as roof to wall connections. The FEMA/CIAPR guidelines recommend several galvanized stainless steel connector models to be used with 8d or 10d wire nails.

The basic wall structure is composed of wall plates, studs, and wall sheathings or sidings. The recommended wall studs are 2-in x 4-in and larger in size, spaced 24-in on center. All the outer walls must have double top plates, with their end joints arranged with an offset of no less than 48-in. The top plates help to distribute lateral shear loads along the whole length of the exterior walls. Corner bracings coming down from the roof and leaning between 45º and 60º are advised for added stiffness and limiting the deformations caused by lateral forces. The plywood panels used as exterior sheathing for wood shear walls must have more than 3 plies and their thickness should exceed 1/2-in, generally 5/8-in for wall sheathing and 7/8-in for wall sidings. Their vertical edges must always be solidly blocked and nailed into the studs with 8d wire nails spaced at 4-in on the edge and 8-in on the field to develop their full capacity. Interior sheathing is

recommended to be 1/4-in thick at least. Our field studies showed that with the exception of interior wall sheathings, these recommendations are generally followed.

2.3 Residential Building Prototypes

As part of the collaborative efforts with the Mid-America Earthquake Center, building types most receptive to hurricane damages were identified using field reports from past hurricanes, interviews conducted in various municipalities, and written surveys submitted to insurance companies. Accordingly, system inventories in Puerto Rico were extended to all types of light frame structures. Collecting and archiving information on wood-zinc houses were an integral part of that effort.

Low cost and relatively fast and easy construction are some of the characteristics of wood-zinc houses that are very appealing to people with limited resources. The houses are located mainly in rural areas and use similar geometric configurations, whether they are engineered or not. The floor sizes typically vary from 20-ft x 24-ft to 24-ft x 36-ft. The average eave height is about 8 ft, with additional eave-to-ridge heights between 3-ft to 4-ft. As previously stated, gable roofs are the most common form with the angle of roof from horizontal, parallel to the least dimension of the residence, varying from 11 to 18 degrees.

Many engineered wood-zinc houses in Puerto Rico are prefabricated. A sample floor plan for this type of buildings is shown in Figure 2.3. The roof rafters are 2-in x 6-in, spaced 24-in on center. Wall studs are 2-in x 4-in, also spaced 24-in on center. All members are pressure treated Southern Pine. The wall siding are 5/8-in thick in this case,

although sidings of 7/8-in or sheathings of 1/2-in to 5/8-in thickness are also on record. On the inside of the dwellings, panels with a minimum thickness of 3/8-in are generally used for covering up the wall studs, electrical ducts, and other unsightly features. Contractor built houses have similar configurations, although 2-in x 4-in roof rafters are sometimes used instead. The interior panels were not always present in our survey.

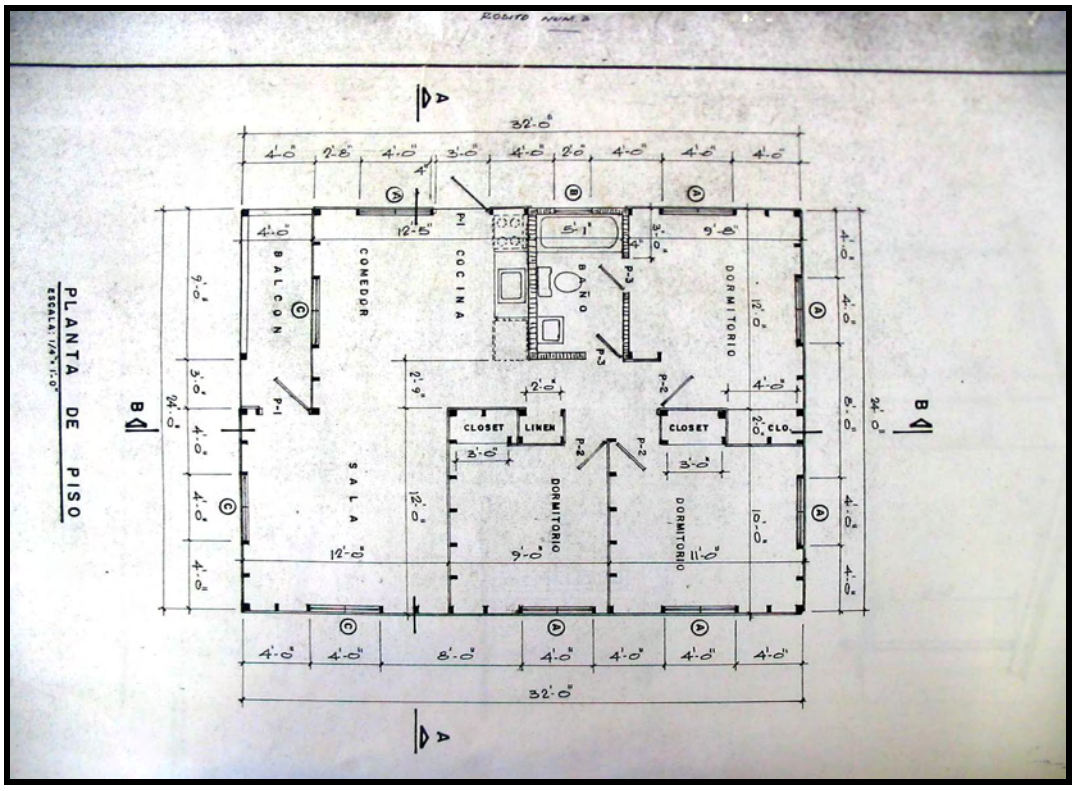

Figure 2.3 – Typical plan view of wood-zinc residence

The one disadvantage of contractor built houses is the improper use, or rather the lack of, steel connector plates and straps at spacer-to-rafter, stud-to-wall plate, and roof-to-wall connections. The windows used in all residences have similar characteristics. Glass louvered windows are used in the front entrance of the building. Aluminum

louvered windows are used in the sides and in the back. The placement of windows tends to be symmetric in these structures, counting the same number of windows in opposing walls. Louvered windows are excellent for ventilation, but are poor insulators and do not close very well. The damage model for these windows will differ from the more traditional windows, although airborne debris is still the principal cause of damages. Table 2.2 presents a listing of the actual building sizes used during wind fragility simulations.

Table 2.2 – Summary of sampled residences

Sample	Dimensions [ft]		Eave Height [ft]	Roof Angle	Number of Windows			
	Façade	Side			Façade	R. Side	Back	L. Side
1	22	30	8	11º	2	3	1	2
2	24	26	8	14º	2	2	2	2
3	24	32	8	15º	2	3	2	3
4	20	26	8	14º	2	2	2	3
5	24	36	8	15º	4	2	3	2
6	24	34	8	18º	2	3	2	3
7	22	24	8	11º	2	1	2	3
8	22	30	8	14º	2	2	2	3
9	24	32	8	15º	2	3	2	3
10	20	32	8	11º	2	2	2	1
11	24	36	8	12º	2	3	2	2
12	22	26	8	18º	2	2	3	3

2.4 Institutional and Other Mixed Construction

Many older institutional buildings in Puerto Rico were constructed using wood-zinc roof systems and either stud walls or unreinforced masonry walls. These buildings were designed by engineers and should be considered high code when compared to their

residential counterparts. The member sizes are the same as those in prefabricated houses. Aluminum louvered windows are used for the most part except in assembly type facilities where glass windows may be used. In our field studies, the connections at spacer-to-rafter, roof-to-wall, and stud-to-wall plates were found to be adequately built. Institutional wood-zinc structures are divided into two groups based on their sizes. A small size institutional will have a size similar to wood-zinc houses. A full size institutional will have a floor area of at least 1,000 ft^2, representing a mass hall, assembly hall, and a few lecture rooms or offices. Their dimensions vary from 24-ft x 42-ft to 56-ft x 98-ft.

Mixed construction in the form of wood-zinc additions to existing reinforced concrete frame or shear wall structures are another familiar site in Puerto Rico. These additions are considered good investments, often used to meet the housing needs of a growing family or as an additional source of income. In fact, the Puerto Rico Building Code prior to being replaced by UBC-97 allowed two different roof live loads for residential houses, anticipating future expansions. A second story addition can have either stud walls or masonry walls. The third story additions in our surveys are all wood-zinc. The sizes for these additions are very similar to wood-zinc houses, and except for the increase in height, fragility simulation parameters will stay the same.

CHAPTER 3

SIMULATING WIND EFFECTS

3.1 Introduction

ASCE-7 standards are the basis for wind design in much of the United States. The standards use three second gusts to calculate wind surface pressures. Gusts are wind peaks generally measured in 3 to 5 seconds. The sustained wind data reported by the National Hurricane Center, however, are based on one minute averaging time. The value of the maximum 3 second gust in a hurricane environment is about 30 percent higher than the one minute sustained wind (Hsu, 2003; and Boose et al., 2004). A typical hurricane has one minute sustained winds of 100 to 150 mph.

The Saffir-Simpson hurricane intensity scale is based on one minute sustained wind. It is the scale utilized for the Atlantic and Northeast Pacific basins to give an estimate of the potential flooding and property damage. Table 3.1 list the maximum sustained wind speeds for different hurricane categories and the expected structural losses.

Table 3.1 – Saffir-Simpson Scale*[1]

Hurricane category	Maximum sustained wind speeds [mph]	Maximum 3-sec. gust wind speeds [mph]	Storm surge [ft]	Expected structural damage
1	74-95	82-108	4-5	Minimal. Damage primarily to some crops and trees.
2	96-110	109-130	6-8	Moderate. Loss of roofing materials, some doors and windows, Extensive damage to signs.
3	111-130	131-156	9-12	Extensive. Partial or complete failures of roofs on many small houses. Extensive damage to windows.
4	131-155	157-191	13-18	Extreme. Some structural damage to small buildings as well as loss of roofs.
5	156+	191+	18+	Catastrophic. Some complete building failures.

* The 3-sec.gust and surge values are for reference only.

Both the system and component fragility curves developed in this research are based on the maximum 3 seconds gust speeds. The approximate conversions in Table 3.1 may be used to place those fragilities in the context of hurricane categories. To derive the fragility relationships, the loadings on the building components are calculated from the ASCE-7 by changing the 3 second gust speeds at 5 mph intervals. A summary of the computational algorithms as well as a review of the ASCE-7 is provided in this chapter.

[1] Adopted from ASCE 7-02, Tables C6-1 and C6-2

3.2 ASCE 7-02 Methodology

The wind-induced surface pressures are calculated using the ASCE 7-02 specifications. The basic wind speed, V, is the 3 seconds gusts at 33 ft above ground in exposure C that exemplifies open terrain with scattered obstructions having heights of less than 30 ft. The wind exposure factor, K_z, is used to account for changes in height and exposure from defaults. It is given by:

$$K_z = \begin{cases} 2.01\left(\frac{z}{z_g}\right)^{2/\alpha} & for\ 15' \le z \le z_g \\ 2.01\left(\frac{15}{z_g}\right)^{2/\alpha} & for\ z < 15' \end{cases} \tag{3-1}$$

Variable z is the height above ground level. For a definition of different wind exposures and the corresponding z_g and α values refer to Table 3.2.

Table 3.2 – Wind exposure[2]

Exposure	Definition	α	z_g
B	Cities, urban and suburban areas, wooded areas: having closely spaced construction the size of a single family dwellings or larger. Exposure B must prevail upwind of the site for a minimum of 2630 feet or 10 times the height of the building.	7	1200
C	Open terrain with scattered obstruction typically less than 30 feet or less in height. Exposure C is the **default exposure** for the standard and should be used when the site does not fit into any of the other exposure categories.	9.5	900
D	Unobstructed sites with wind flowing over open water for a distance of at least one mile. Exposure C extends inland a distance of 1500 feet or 10 times the height of the building. Exposure D need not be used for the design of components and cladding.	11.5	700

[2] Adopted from ASCE 7-02

The design velocity wind pressure is computed from the wind stagnation pressure, $0.00256 \cdot V^2$:

$$q_z = 0.00256 K_z K_{zt} K_d V^2 I \tag{3-2}$$

The constant 0.00256 is the air density in a standard atmosphere. K_{zt} is the topographic factor, K_d is the directionality factor, and I is the importance factor. A brief discussion on the values assigned to these factors is given in the next section. For complete definition of terms, the reader should consult ASCE 7-02.

ASCE 7-02 presents three different methods for calculating the design wind pressures for the main wind force resisting system of a building. Low rise, regular-shaped buildings having fundamental frequencies of 1Hz or more qualify for the simplified Method 2. In this case, the design wind pressure for the main wind force resisting system (MWFRS) is calculated from:

$$p = q_h \left[\left(GC_{pf} \right) - \left(GC_{pi} \right) \right] \tag{3-3}$$

where q_h is the velocity wind pressure at mean roof height, h; and GC_{pf} and GC_{pi} are the external and internal pressure coefficients. For components and cladding (C&C):

$$p = q_h \left[\left(GC_p \right) - \left(GC_{pi} \right) \right] \tag{3-4}$$

The only difference between C&C and MWFRS equations is the use of different external pressure coefficients, GC_p as opposed to GC_{pf}. In general, C&C design pressures are larger because of localized high pressures acting over small areas. Components can be part of MWFRS when they act as shear walls and roof diaphragms.

When calculating design wind pressures for MWFRS, all wind directions are considered by alternating each corner of the building as the reference corner. This will

result in eight basic load cases in longitudinal and transverse directions (ASCE 7-02). Figure 3.1 shows the two cases with the same reference corners. The structure is divided into 10 different zones (1 through 6 and 1E through 4E), each with a different pressure coefficient. The *a*-parameter shown in Figure 3.1 is defined as 10% of the least horizontal dimension or 40% of the height, whichever is smaller, but not less than either 4% of the least horizontal dimension or 3 ft. The external pressure coefficient for each zone is calculated by multiplying a gust factor of G =0.85 by the C_{pf} factor listed in Table 3.3. Plus and minus signs indicate pressures toward and away from the surface, respectively.

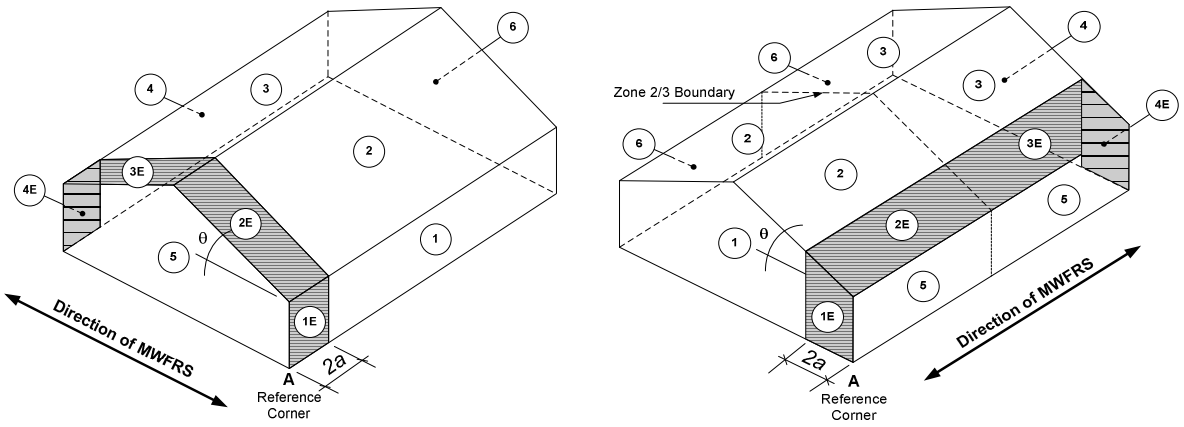

(a) Transverse direction **(b) Longitudinal direction**

Figure 3.1 – Effect of wind orientation on pressure distribution[3]

[3] Adapted from ASCE 7-02

Table 3.3 – External pressure coefficients for MWFRS[4]

Roof Angle	External Pressure Coefficients, C_{pf} for Low-Rise Building Surfaces per Zone									
θ [º]	1	2	3	4	5	6	1E	2E	3E	4E
0	0.4	-0.69	-0.37	-0.29	-0.45	-0.45	0.61	-1.07	-0.53	-0.43
5	0.4	-0.69	-0.37	-0.29	-0.45	-0.45	0.61	-1.07	-0.53	-0.43
20	0.53	-0.69	-0.48	-0.43	-0.45	-0.45	0.8	-1.07	-0.69	-0.64
30	0.56	0.21	-0.43	-0.37	-0.45	-0.45	0.69	0.27	-0.53	-0.48
45	0.56	0.21	-0.43	-0.37	-0.45	-0.45	0.69	0.27	-0.53	-0.48
90	0.56	0.56	-0.37	-0.37	-0.45	-0.45	0.69	0.69	-0.48	-0.48

The external pressure coefficients for wall C&C are listed in Table 3.5. The table was adopted from Cope (2004). It assumes an effective wind area for C&C of 10 ft^2 or less. The tabulated values are conservative for larger C&C areas and are consistent with Table 6-11A of ASCE 7-02. The external pressure coefficients for roof C&C are not used for evaluating the performance of wood-zinc roof systems except for the localized pressure grid and the supporting connections. The methodology presented in Chapter 6 rates roof performances based on demands from the MWRFS, except for the localized pressure grid where C&C external pressure coefficient of -2.1 is used.

Table 3.4 - Wall C&C pressure coefficient values[5]

Location	GC_p
Windward wall	1.0
Leeward wall	-0.8
Side wall	-1.1
Side wall leading edge (distance "a" from corner)	-1.4

[4] Adapted from ASCE 7-02
[5] Adopted from Cope (2004)

The internal pressures coefficient, GC_{pi}, for both MWFRS and C&C are dependent on the enclosure type defined by ASCE 7-02 as enclosed, partially enclosed, or open. All the buildings in the inventory considered for this study are enclosed. This will set the GC_{pi} value at ± 0.18. Once again, plus and minus signs indicate pressures toward and away from the surface, respectively. The possibility of a system changing enclosure type during the simulation was discarded because the requirements for partial enclosure are such that the system will fail before the changes take place.

3.3 Simulation Process

Because of the regular form and small size, a wood-zinc structure would not usually require sophisticated analysis. As it was previously discussed in Section 3.2, the simplified Method 2 of ASCE 7-02 will allow for easy and efficient wind fragility simulation algorithms. The prototype structures are placed in a database, each having an index assigned to it. Table 2.2 provided an example of one such listing. At each wind speed, n number of structures will be selected from the database, some more than once. A wind direction is assigned to every building selected. The roof angle will not enter the calculations for external wind pressure coefficients if the wind direction is parallel to the ridge. Table 3.5 shows a sample computation of the C_{pf} and the average pressure demands for perpendicular-to-ridge and parallel-to-ridge loading conditions.

Table 3.5 – Sample C_{pf} and pressure demand computation for 250 mph wind speed

Roof Angle [º]	Case 1 - Perpendicular to Ridge - C_{pf} and Pressures for Low-Rise Buildings									
14	1^{W}	2^{*}	3^{*}	4^{L}	5^{S}	6^{S}	$1E^{W}$	$2E^{*}$	$3E^{*}$	$4E^{L}$
C_{pf}	***0.40***	***-0.69***	***-0.37***	***-0.29***	***-0.45***	***-0.45***	***0.61***	***-1.07***	***-0.53***	***-0.43***
$q \cdot G \cdot C_{pf}$	46.91	-67.71	-42.79	-36.70	-44.16	-44.16	71.05	-105.00	-61.43	-54.56
$(+)\ q_i \cdot GC_{pi}$	20.78	20.78	20.78	20.78	20.78	20.78	20.78	20.78	20.78	20.78
$(-)\ q_i \cdot GC_{pi}$	-20.78	-20.78	-20.78	-20.78	-20.78	-20.78	-20.78	-20.78	-20.78	-20.78
$q \cdot G \cdot C_p + q_i \cdot GC_{pi}$	67.69	-46.93	-22.00	-15.92	-23.38	-23.38	91.83	-84.22	-40.65	-33.78
$q \cdot G \cdot C_p - q_i \cdot GC_{pi}$	26.13	-88.49	-63.57	-57.48	-64.94	-64.94	50.27	-125.78	-82.21	-75.34
Roof Angle [º]	**Case 2 - Parallel to Ridge - C_{pf} and Pressures for Low-Rise Building**									
0	1^{W}	2^{*}	3^{*}	4^{L}	5^{S}	6^{S}	$1E^{W}$	$2E^{*}$	$3E^{*}$	$4E^{L}$
C_{pf}	***0.40***	***-0.69***	***-0.37***	***-0.29***	***-0.45***	***-0.45***	***0.61***	***-1.07***	***-0.53***	***-0.43***
$q \cdot G \cdot C_{pf}$	39.25	-67.71	-36.31	-28.46	-44.16	-44.16	59.86	-105.00	-52.01	-42.20
$(+)\ q_i \cdot GC_{pi}$	20.78	20.78	20.78	20.78	20.78	20.78	20.78	20.78	20.78	20.78
$(-)\ q_i \cdot GC_{pi}$	-20.78	-20.78	-20.78	-20.78	-20.78	-20.78	-20.78	-20.78	-20.78	-20.78
$q \cdot G \cdot C_p + q_i \cdot GC_{pi}$	60.03	-46.93	-15.53	-7.68	-23.38	-23.38	80.64	-84.22	-31.23	-21.42
$q \cdot G \cdot C_p - q_i \cdot GC_{pi}$	18.47	-88.49	-57.09	-49.24	-64.94	-64.94	39.08	-125.78	-72.79	-62.98

The reliability theory requires the generation of random pressure demands in order to evaluate resistance in a simulation engine. The design wind pressures calculated from equations 3.3 and 3.4 are deterministic in nature. To inject uncertainties into these equations, the wind speed V_0 at which a building component is evaluated, will become random itself. Equation 3-5 generates a different velocity demand, V, for every building analyzed at V_0:

$$V = V_0\left[1 + \zeta\, COV(V)\right] \tag{3-5}$$

In the above equation, ζ is a random number ranging from -1 to 1. The coefficient of variation for V, $COV(V)$, is taken as 0.1 (Cope, 2004).

Additionally, the velocity pressure Equation 3-2 is modified as:

$$q_z = 0.8\left(0.00256K_z V^2\right) \tag{3-6}$$

The factor 0.8 is added to counteract the safety factor embedded into ASCE 7-02 (Cope 2004). The directionality factor, K_d, is not recognized because the wind direction is modeled separately during the simulation. The importance factor, I, is also discarded because it is an additional safety factor related to occupancy and function. The topographic factor, K_{zt}, is set to unity. It is possible to factor K_{zt} back in when reading the fragility data if one were to use an equivalent velocity, V_{eq}, instead. Comparing Equations 3.2 and 3.6:

$$V_{eq} = \sqrt{K_{zt}} \cdot V \tag{3-7}$$

3.4 Component Loading

In simulating the performances of assorted building components, the wind speeds are varied from 50 mph to 250 mph at 5 mph intervals. From the expanded building inventories discussed in Chapter 2, one hundred random selections are made at each wind speed. It is assumed that the wind will act either in longitudinal or in transverse direction. Accordingly, a wind direction is assigned to every building selected. In short, the performance data at any given wind speed will be the result of analysis on 100 randomly selected buildings and wind directions.

The damage matrix presented in Chapter 1 forms the basis for analysis of building components. The flowchart in Figure 3.2 should help to clarify the process. The roof system is divided into pressure grids and tested against the uplift pressure demands in zones 2, 2E, 3, and 3E of Figure 3.1. That is except for one grid in zone 2E that will be

subject to C&C localized pressure. Further details on the load distribution can be found in Chapter 6. The uplift load on the roof is transferred to roof-to-wall connections based on the tributary areas assigned to every connector. This procedure is explained in detail in Chapter 7. The stability of the wall structure is tested against the combination of axial load in each stud resulting from the roof-to-wall connections and the transverse loads corresponding to zones 1, 1E, 4, 4E, 5, and 6, also presented in Figure 3.1. The loss of wall sheathings is investigated based on the shear-wall action requirements. The pressure demands on both the wall sheathings and the openings are calculated in accordance with the C&C external pressure coefficients for walls. In addition to the uniform transverse loading, the effects of airborne debris on the windows fragility are included.

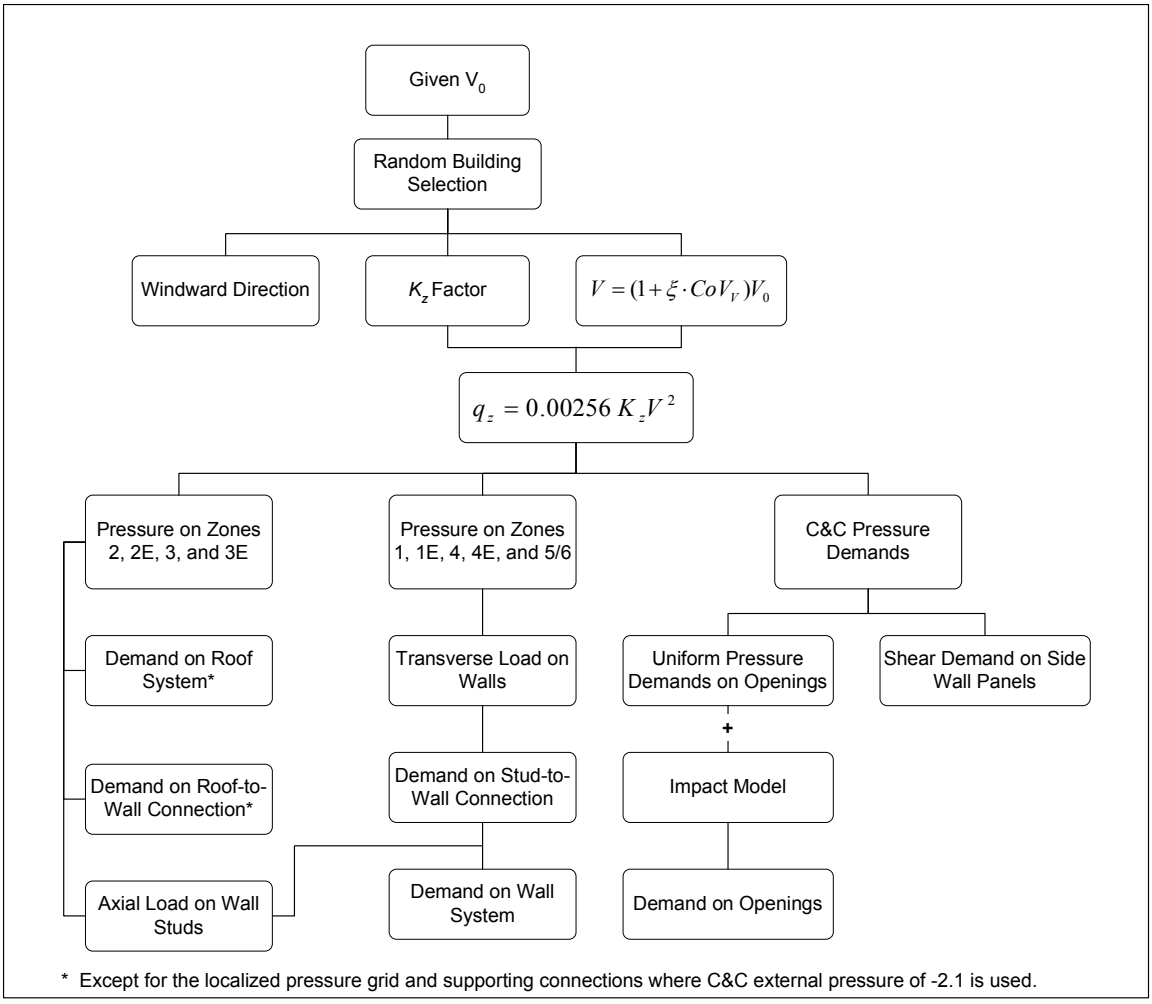

Figure 3.2 – Calculating demands on building components

CHAPTER 4

SELECTION OF ROOF PROTOTYPES

4.1 Introduction

Over the last fifteen years, the researchers at the Civil Engineering and Surveying Department of the University of Puerto Rico at Mayagüez have designed, built, and continuously upgraded a flexible loading apparatus for hurricane wind studies. The dynamic response of wood-zinc roof systems was first investigated as part of a research sponsored by FEMA (Avilés, 2006). The emphases were on developing load-cycle relationships; identifying potential weaknesses; and designing retrofitting schemes to improve performance. In this study, the design fragility curves for such systems are ultimately developed using the same basic set up and a modified SIGDERS dynamic protocol for performance rating.

The decision on what roof prototypes to test is a key aspect of the investigation. Except for the prefabricated wood-zinc houses, engineering blueprints are rarely reviewed by the regulatory agency. Small time contractors which have learned their trade by practice and generally lack any engineering background dominate the field.

Construction guidelines such as the ones developed by FEMA and CIAPR provide basic guidelines on member size and spacing, and the use of mechanical fasteners and steel connectors. The roof prototypes designed by Avilés (2006) follow those guidelines. Limited field studies during the course of this investigation found his models to be well represented. A review of those prototypes as well as a summary of various dynamic loading protocols is presented in this chapter.

4.2 Evolution of Roof Prototypes

The first wood-zinc roof prototype designed by Avilés (2006) was built by running 2-in x6-in wood rafters across a wood frame at two feet intervals. The same 2-in x 6-in lumber sizes were used to construct the outside frame measuring 12 feet horizontally and 8 feet vertically. Running across the rafters, also at 2 feet intervals, are 1-in x 4-in wood spacers. In this fashion, a grid system is assembled over which the zinc sheets are attached in accordance with the FEMA/CIAPR guidelines. The rafters are fastened to the outer frame by using two 3-in spiral shank nails and an additional U-shaped metal connector at each end. These connectors are nailed with 1½-in long, 10d nails, although the number of nails per connector varies, as shown in Figure 4.1.

The connection between spacers and rafters are also made with two 3-in spiral shank nails. FEMA/CIAPR guidelines recommend an additional anchoring strap to reinforce the connection. However, the strap type recommended for anchoring the spacer to the rafter is not readily available in the Island. Recognizing the importance of duplicating the real field experiences, two separate straps of the more common types

were used in place of the single strap. Figure 4.2 shows the two strap configuration adopted. The use of straps was proven essential to the integrity of the systems tested by Avilés (2006). Additional tests also proved the necessity of reinforcing outside frame corners with special corner anchorages.

Figure 4.1 - Variable connectors between joist and rafter

(a) Nailed connection **(b) Two strap configuration**

Figure 4.2 – Spacer to joist connections[1]

[1] Adopted from Avilés (2006)

Prototypes 2 and 3 designed by Avilés (2006) were the elevated rafter prototypes. The rafters were placed either on top of the outer frame or they were notched at the extreme. The other key difference between these two prototypes and Prototype 1 was their dimensions. Because of the limitations imposed by the actuator used in the lab, the size of the specimens was reduced to 8-ft x 8-ft instead of the original 8-ft x 10-ft, thus reducing the number of grids from twenty to sixteen. The new size became the standard for all other prototypes.

Prototype 4 was similar to Prototype 1, except for the overall dimension, the exclusive use of two strap configuration in spacer-to-rafter joints, and the stiffening of the side supports in the testing apparatus. The findings from the Prototype 4 specimens prompted further modifications in which the sample roof specimen was rotated by 90 degrees and the additional side supports were eliminated. The resulting Prototype 5 was easy to construct and install and was shown to better represent roof boundaries and performance. Prototype 5 is the design prototype for this study and is shown in Figure 4.3.

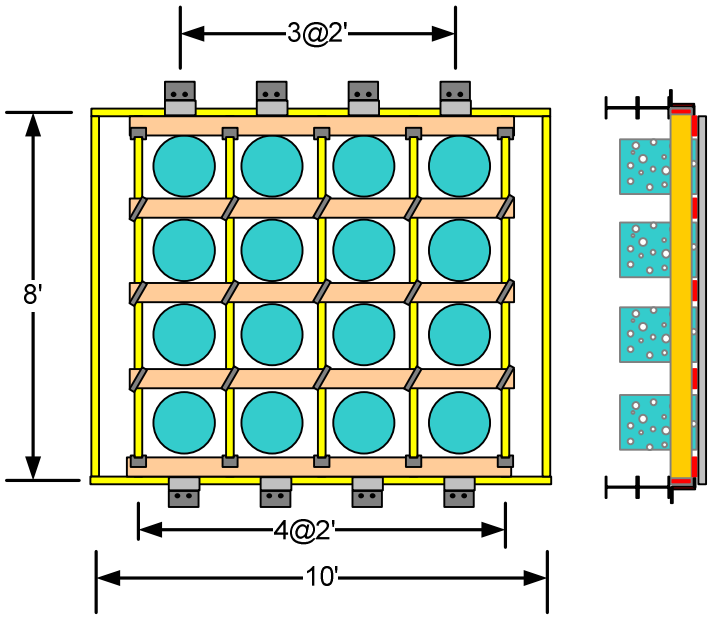

Figure 4.3 - Prototype 5 Specimen[2]

4.3 Design Prototype

Following the second generation Prototype 5 guidelines discussed by Avilés (2006), the wood-zinc roof specimens are assembled by running seven parallel 94½-in. long 2-in x6-in wood rafters spaced at two feet intervals, with the rafters at the extremes being distanced from the outside frame by only 1 foot. The ends of the joists are nailed to two 10 feet 2-in x6-in pieces which run perpendicular to the others and they represent either the top plate or wall member to which the roof is fastened. The system is fastened together using two 3-in spiraled shank nails per connection, plus the additional recommended U-hangers. By placing 1-in x4-in wood spacers transversely to the joists, also at 2 feet intervals, a grid system is formed. The spacers are also connected to the

[2] Adopted from Avilés (2006)

rafters by two 3-in spiraled shank nails per intersection plus the corresponding metal connectors. This grid provides a framework over which the zinc sheets can be fastened. The wood selected for both rafters and spacers was pressure treated Southern Pine No. 1, which is the most widely used in the Island. The corners of the specimens are reinforced with special corner connectors.

In a typical construction, commercial grade galvanized steel decks, called zinc sheets, are placed with the grooves parallel to the slope of the roof for drainage reasons. The zinc sheets are gage 26, commercial grade galvanized steel decks, which conform to the ASTM 653/653M standards. Laboratory testing of strips taken from the zinc sheets delivered yield stresses that varied from 40 ksi to 60 ksi. Such gage is not appropriate for a structural component and it is not sold as such but because it's low price and availability they have become the standard.

Following the FEMA/CIAPR guidelines, consecutive zinc sheets are overlapped by two corrugations and are fastened to the wooden frame by 2½-in long, umbrella-headed spiral-shank nails. The recommended spacing between the nails is 6 inches which will roughly amount to one nail every two humps. For the purposes of this research, the nailing schedule was varied to asses the poor construction practices. The roof specimens are designated as 6-6-6, 6-12-6, or 12-12-12, depending on the spacing between the fasteners in the vertical edge-inside-edge lines. A typical house will use 6-in. spacing at the edge of the roof and 12-in. spacing elsewhere. In most cases, the effects may be simulated combining the data from 6-12-12 and 12-12-12 specimens. A poorly constructed house, on the other hand will not use adequate number of fasteners at the

edge, and will be best modeled using the data from 12-12-12 specimens alone. Further discussions on this topic will be given in Chapter 6.

The nails are to be bent at the back of the spacers, perpendicular to the wood fibers to avoid potential withdrawal of the nails. This particular step is critical for achieving the best performance in the system yet it is sometimes overlooked because of inadequate supervision during roof construction. An additional nail might be necessary in the overlapping zones between zinc sheets. It is important to note that the nails are placed on top of the corrugations to avoid drainage problems. Figure 4.8 depicts a schematic drawing of the different members of the prototype

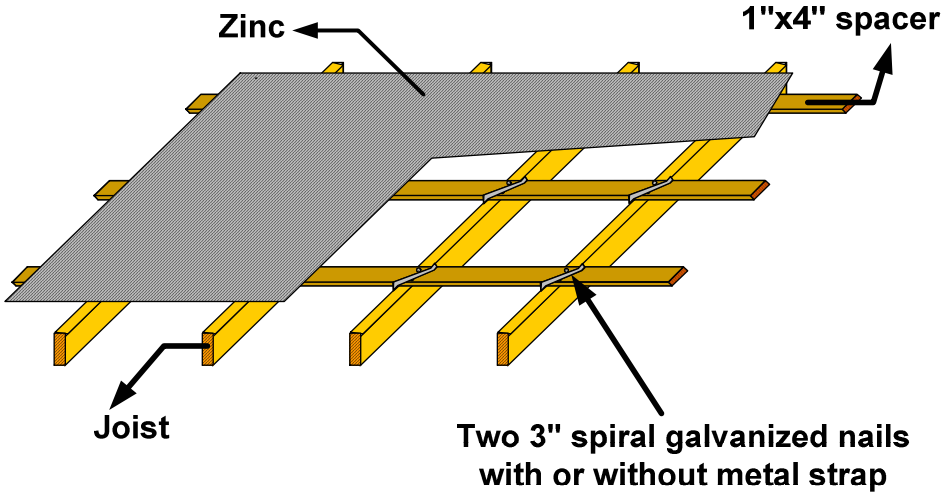

Figure 4.4 – Schematic of wood-zinc roof specimen[3]

[3] Adopted from Avilés (2006)

4.4 Retrofitting Measures

The dominant failure mode for Prototype 5 specimens tested by Avilés (2006) was found to be fatigue at zinc-to-spacer connections. The use of multi-layered zinc reinforcement straps along the connection lines to strengthen the contact area was henceforth recommended. The straps are made by cutting 4-in strips out of the zinc sheets and layering them in stacks of three. The straps are bound together and are pre-drilled in place wherever the nailing schedule requires. As recommended by NDS (2001), the drill bit used is of lesser diameter than the nail itself. The same overlapping principles used with zinc sheets are also used with zinc straps. The construction and application of the strips is shown in Figure 4.5.

Figure 4.5 – Retrofitting scheme proposed[4]

The results obtained from the laboratory testing showed remarkable improvements in the overall behavior of the system, changing the failure modes to wood member connections in most cases and splitting of wood members in others. Specimens retrofitted with the zinc straps and loaded at constant amplitude from 0 to 6.5 kip showed

[4] Adopted from Avilés (2006)

an increase in the number of cycles to failure by at least 5 times the number for unretrofitted specimens.

Anticipating the potential impact of the retrofitting scheme proposed by Avilés (2006), the mechanism was studied in this research along with variations in the nailing schedule. Each variation is marked in a similar manner to unretrofitted systems discussed in the previous section. Three configurations are considered. These are 6-12-6R, 6-6-6R, and 12-12-12R with letter R indicating the retrofitted system. As before, a typical design case would be represented by a combination of the 6-12-6R and 12-12-12R configurations.

4.5 Testing Apparatus

The loading apparatus for hurricane wind studies at the Structural Engineering Laboratory of UPRM consists of a single span steel frame supporting two W6x12 steel beams in front. The positions of the beams can be adjusted to fit variable sample heights. Aviles modified the system by pairing two beams in place of one, positioning them further to the front. The roof specimens are lifted and placed on angles attached to the front beams. The frame is braced against out of plane movements on the sides. Additional vertical supports for the beams are provided by the short column at the center of the frame. The loading frame in the back is supported by railings on each side. Figure 4.6 shows schematic drawings of the test frame.

In order to uniformly distribute the load from the hydraulic jack at the back of the loading frame to the roof prototypes, 16 cylindrical air bags were housed inside the roof

grids, between the loading plates and zinc sheets. The air bags are protected with layers of duct tape and fiber-reinforced tape to guarantee their fitting within the grid and to resist puncture. The load is generated by an MTS hydraulic actuator capable of applying a maximum load of 36 kips, with a maximum stroke of 10 inches. A more complete description of the loading apparatus can be found in the second chapter of Avilés (2006).

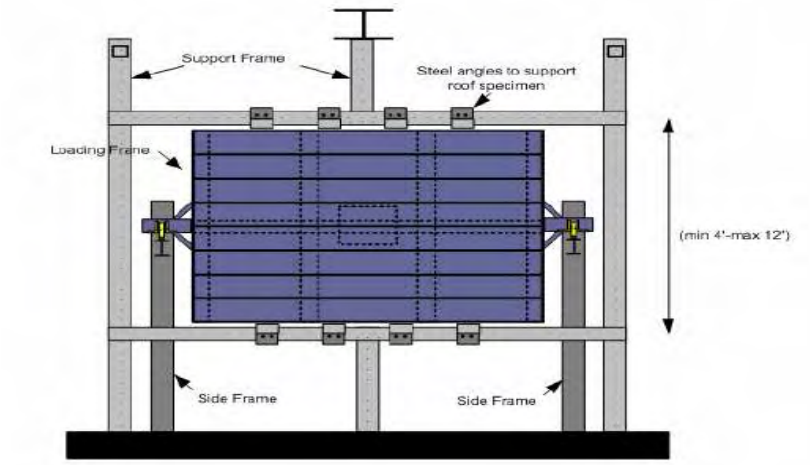

(a) Front view of the testing apparatus

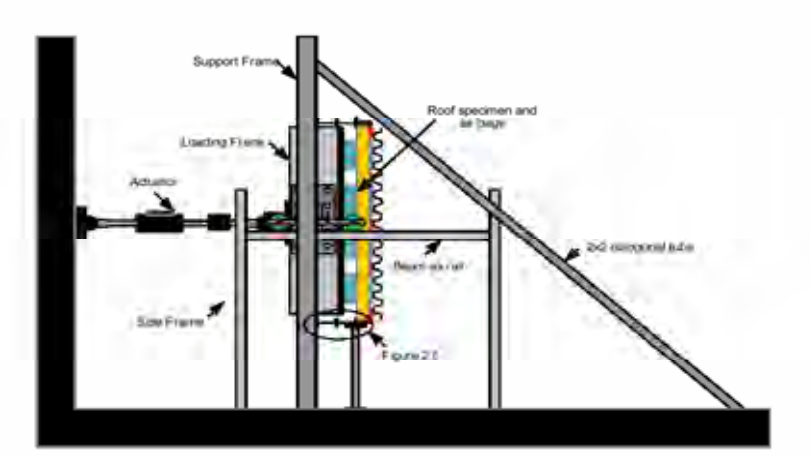

(b) Side view of the testing apparatus

Figure 4.6 – Front and side view schematics of the testing[5]

[5] Adopted from Avilés (2006)

4.6 SIGDERS-5 Dynamic Protocol

Dynamic protocols for simulating wind load effects dates back to the regional Australian standards established by Darwin Reconstruction Committee in the aftermath of Cyclone Tracy in 1974. According to that standard, the metal roof system should be stressed from no load to a predetermined allowable stress level for 10,000 cycles, followed by a proof load of 1.8 times the design load. The cycle count comes from studies by Morgan and Beck (1977) that showed low cycle fatigue in the vicinity of the 10,000 cycles for metal roof systems. The well known Australian Standards TR440 was subsequently developed and enacted, with additional input from Morgan and Beck (1977) and Melbourne (1977). The TR440 protocol consists of 8,000 cycles from no load to 62.5 percent of the design load, followed by 2,000 cycles at 75 percent, 200 cycles at 100 percent, and finally the proof load of 1.8 times the design load.

Other protocols were proposed in years since, perhaps none more complicated than the Random Block Loading method (Mahendran 1993). The method is so named because the numbers of cycles and magnitudes of the loading are randomly selected from the cells of a pressure matrix. The European standard UEAtc-551 uses a five-year return period to establish the wind load cycles. Less complicated than Random Block Loading, a typical UEAtc-551 test takes more than a day to complete.

In his doctoral dissertation, Avilés (2006) discussed the possibility of using a more recent dynamic protocol developed by the Special Interest Group for Dynamic Evaluation of Roofing Systems (SIGDERS) in Canada. The group interest was in developing a standard for dynamic testing of Poly Vinyl Chloride (PVC) and Ethylene Propylene Diene Monomer (EPDM) membranes used as water-proof covering in steel

deck roofs. The SIGDERS protocol is comprised of eight sets of load cycles that vary in number and amplitude. Each set defines a level, divided into two different sub-groups. As stated by Baskaran et al. (1997), the first group represents wind-induced suction over a roof assembly. It consists of four sequences, where the pressure level alternates between zero and a fixed pressure. The second group represents the effects of exterior wind fluctuations combined with a constant interior pressure on a building. For this second group, a constant minimum static pressure is applied to the roof system, and the pressure intensity alternates between this minimum and the maximum pressure established for each sequence.

The maximum and minimum values for the applied pressure at any given level are dictated by the initial testing load specified. The subsequent levels are dependant on the initial load, increasing the maximum pressure per level at 25% increments. Each additional level adds the necessary cycles for simulating a higher demand on the system, which proves to be the most appealing aspect of the protocol. This loading protocol allows for the sample to be continuously tested under an increasing demand until a final rating is obtained. Figure 4.7 shows the original loading regimen proposed by the SIGDERS group.

Over the years, the low cycle fatigue number of 10,000 used in TR440 was proven to be a proper measure for the rating performance of metal roofs. Initial testing by Aviles showed the need to maintain this number of cycles for the SIGDERS protocol to work on metal roofs. The proposed solution that was later verified was to multiply the number of cycles in the SIGDERS sequences by 5. This will increase the total number of cycles in level A from 2,200 to 11,000. The sample completing level A will receive a

rating of P which is the assumed rating at the beginning of level. The same sample completing level B, after 5,500 cycles instead of 1,100 shown in Figure 4.7, will receive a rating of 1.25P. Increased ratings may be obtained by completing other levels in sequence.

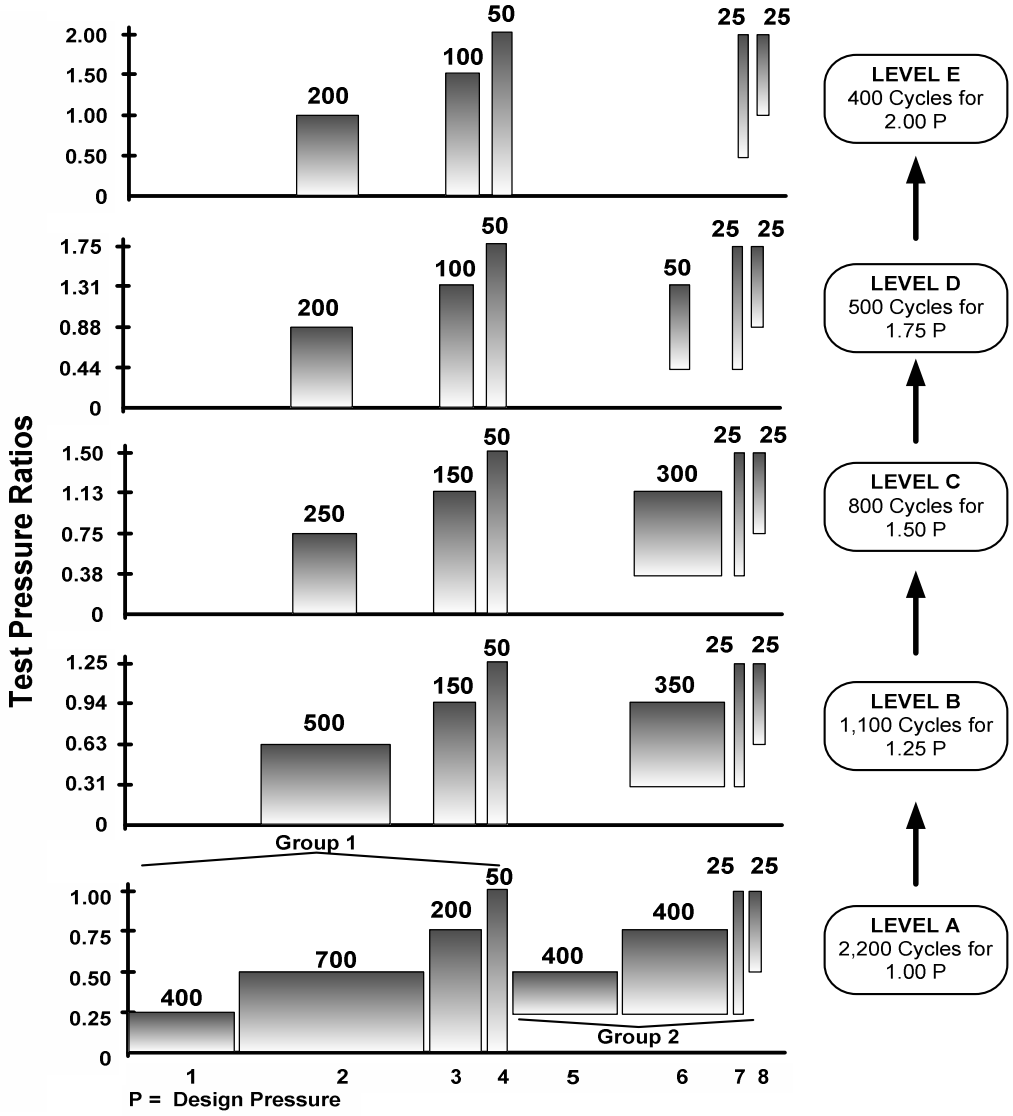

Figure 4.7 - SIGDERS loading protocol[6]

[6] Adapted from Baskaran et al. (1997)

For validation purposes, the acquired ratings of two specimens tested under SIGDERS-5 protocol were used as the design load for identical specimens tested using TR440. The first pair was reported on by Avilés (2006). For completion sake, the results from SIGDERS-5 test on specimen 30 and TR440 test on specimen 31 will be discussed here. The nailing schedule for both specimens was 6-in on center at the edges and 12-in on center elsewhere plus additional nails in the overlaps where necessary. This resulted in a total of 72 nails for each specimen.

The SIGDERS-5 loading for specimen 30 started at 4 kips. The testing could not carry through level D, which using the 1.5 multiplier from level C resulted in a rating of 6 kips. Specimen 31 was then tested using TR440 at 6 kips. Figure 4.8 shows the sequence of damages for both specimens following the rules set forth in Chapter 5 and Appendix B. For the new protocol to be valid, the maximum load and the failure patterns should coincide with those obtained from the universally recognized TR440 schedule. Note the similarities in the total number of failures (10.5 for specimen 30, 11 for specimen 31), failure types, and locations for both specimens. Damages coincided in 15 instances and the main damage type recorded was Type 1, which corresponds to low-cycle fatigue cracks. Further details on each test can be found in Appendix B.

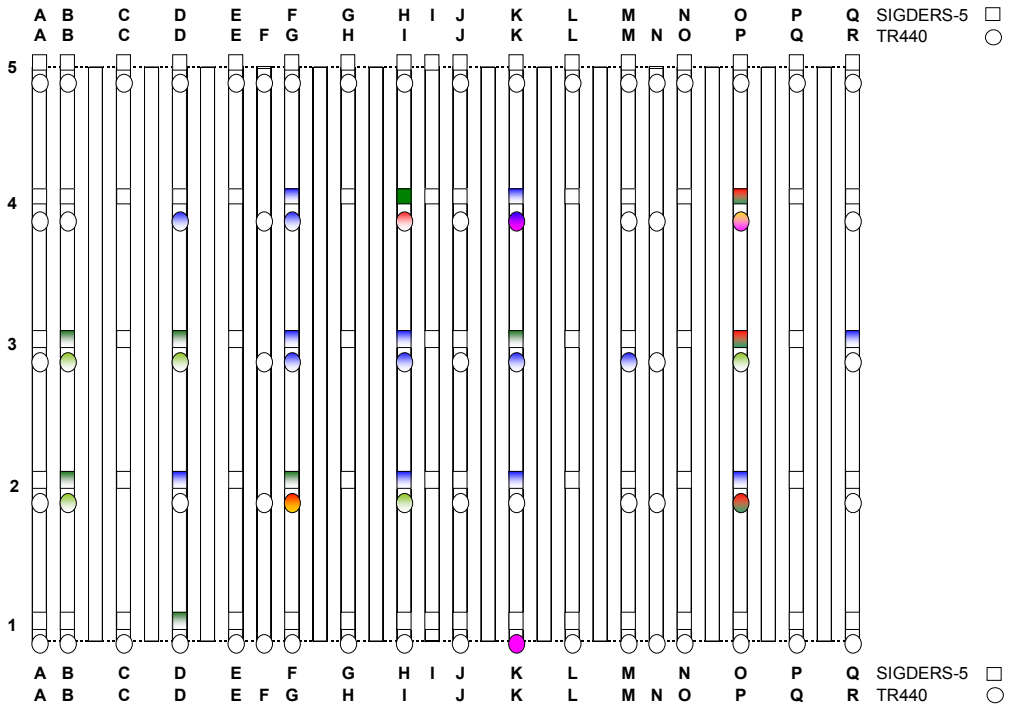

Figure 4.8 – Comparison of failure location in Specimen 30 and Specimen 31

CHAPTER 5

EXPERIMENTAL RESULTS

5.1. Introduction

The testing regimens for the wood-zinc roof prototypes included three different nailing schedules, with and without zinc strap retrofits. In total, nine full-scale laboratory specimens were tested under the newly proposed SIGDERS-5 dynamic protocol. The first specimen tested was numbered 30 to maintain continuity with the previous UPRM research on the subject (Avilés, 2006). The failure definitions used in this investigation are presented in this chapter along with a summary of results from each experiment.

5.2. Failure Definitions

For the purposes of this investigation, connections between the zinc sheets and wood members are considered partially lost when low-fatigue cracks are developed in the sheathing around the fasteners. Avilés (2006) reported this failure mode as the most common type exhibited by the specimens tested during his extensive research on these

types of roofing system. It includes diamond-shaped and longitudinal low-fatigue cracks around fasteners, and is marked as Type 1 failure. Figure 5.1a gives an example of Type 1 failure. Since at this stage the fastener is still capable of transferring part of its tributary loading, the damage state is counted as half local failure and is assigned an index of 0.5.

The loss of the umbrella-head of a fastener is marked as Type 2 failure. Although it may be argued that the full load transfer is still taking place, the decrease in contact area increases the stresses around the head of the fastener and the separation of sheathing is certain to follow. Figure 5.1b shows the effects of the fasteners punching through as the consequence of the head loss. As with a type 1 failure, a damage index of 0.5 is assigned.

Type 3 local failures mark the cases when the fasteners fail to transfer any load between the sheathing and the wood members. A Type 3 failure is often an outgrowth of Type 1 or 2 failures. It may occur in one of several ways. For example, the fastener can break, it can punch through the sheathing, or it can straighten and pull out from the spacer. Examples of Type 3 failures are shown in Figure 5.1c. A damage index of 1 is assigned to Type 3 failures.

At the end of each SIGDERS-5 level, the damage index for that level is calculated by summing the indices from all local failures. Because of the needs to protect the testing apparatus as well as to maintain the uniformity of the applied load, specimens are only tested to the point where at least three fasteners are lost in a vertical line or at an edge grid. The loss of five fasteners in two neighboring grids will also establish failure. If possible, the testing would continue until the end of that particular SIGDERS-5 level. Because most roof specimens can still be repaired at this stage, the final ratings are meant

to define either the moderate or the extensive damage state. For clarifications on the subject refer to Sections 5.3 and 5.4.

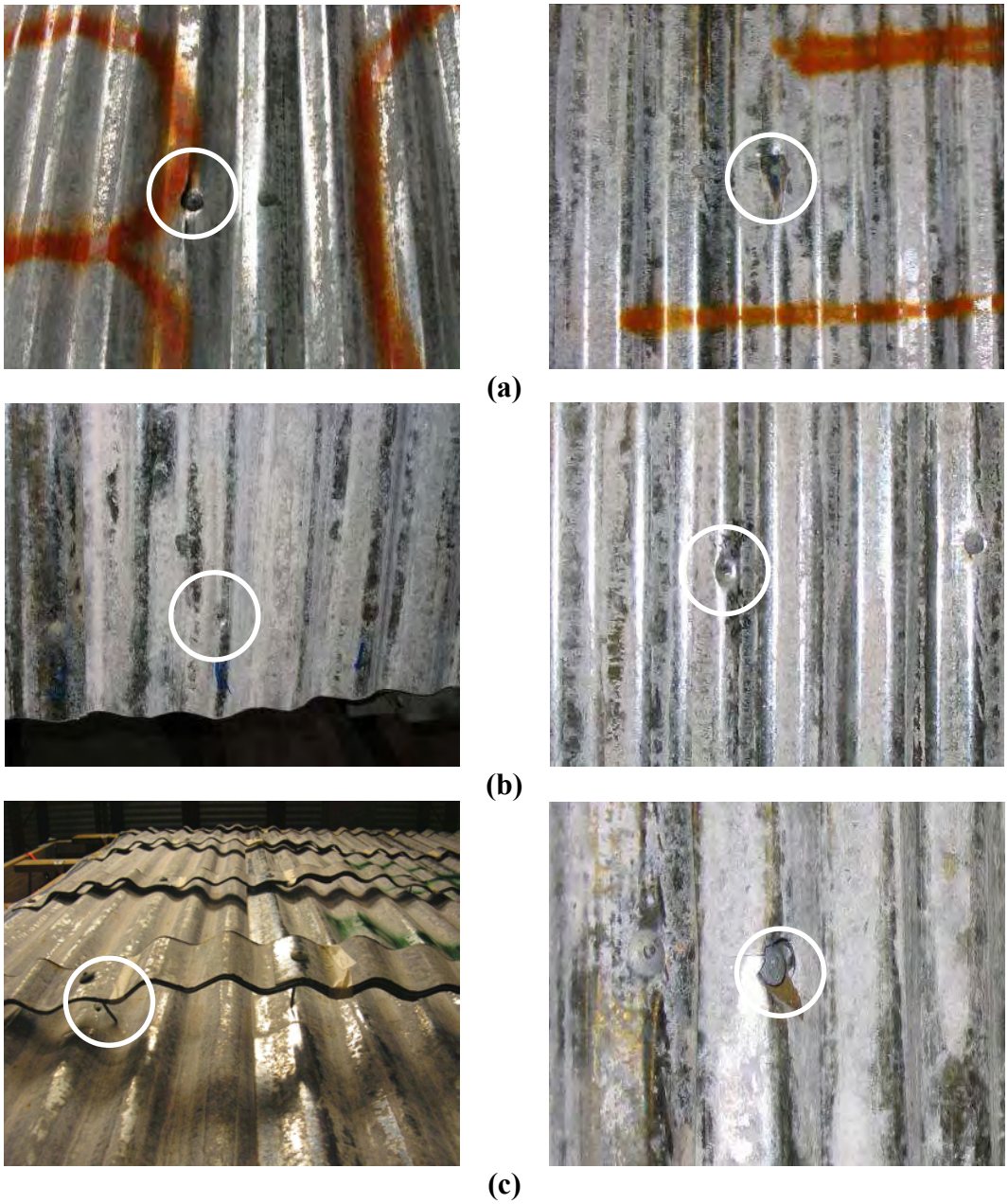

(a)

(b)

(c)

Figure 5.1 – Example of failure modes

5.3. Conventional Systems

The conventional wood-zinc roof systems are the systems without zinc straps meeting the minimum requirements of using metal straps at spacer-to-rafter joints and the bending of the sheathing nails at the back of spacers. A complete description of these systems was presented in Chapter 4. The prototype specimens vary only in their nailing schedules. A summary of the results obtained for each of the six conventional prototypes is presented in this section. The damage state observed at the end of each test was extensive for conventional systems. The lowest SIGDERS-5 level at which the level index was at least half of the final index is used to rate the moderate damage state. For detailed schematics of each test including the failure types and sequence, refer to Appendix B. An example of the conventional roof specimens is shown in Figure 5.2.

Figure 5.2 – Conventional specimen ready to be tested

5.3.1. Specimen 30

Specimen 30 was the first specimen tested under the modified SIGDERS-5 protocol. The nailing schedule used for this specimen was 6-in spacing at the edges and 12-in spacing at the field plus additional nails in the overlaps whenever necessary. This is marked as 6-12-6 schedule. A total of 67 fasteners were used. The specimen passed the Level A of SIGDERS-5 at 4 kips with only two Type 1 failures. By the end of the Level B of loading, 11 Type 1 failures were developed. Level index at the end of the Level C was 10.5. This was the last completed level and the specimen was rated at 6 kips for extensive damage state and 5 kips for the moderate damage state.

5.3.2. Specimen 32

The nailing schedule for specimen 32 was also 6-12-6, only no additional nails in the overlaps were used. A total of 61 spiraled-shank nails were used. The starting load for specimen 32 was 4.5 kips. Seven Type 1, two Type 2, and one Type 3 failures were recorded after the completion of the Level A, six of them before even reaching subset A-5 of the protocol. Between subsets B-1 and B-4, three additional Type 1 and two additional Type 3 failures were recorded. The specimen passed Level C, earning a rating of 5.63 for the extensive damage state. The final rating compares favorably with the one obtained from the previous test.

5.3.3. Specimen 33

The nailing schedule for specimen 33 was 12-in spacing at the edges and at the field plus additional nails in the overlaps. This is marked 12-12-12. A total of 45 spiraled-shank nails were used. The starting load for this specimen was 4 kips. Nine Type 1 and one Type 2 failures were observed at the end of Level A, accounting for 20 percent of all fasteners in its envelope. The damages were well spread over the specimen. One additional Type 1 and two Type 3 failures were recorded at the completion of Level B. The final load rating of the system corresponded to this level at 5 kips.

A close inspection of the results from the first three tests resulted in reducing the starting loads for other conventional system specimens. This was to produce more refined ratings by closing the gaps between different levels of loading.

5.3.4. Specimen 36

The nailing schedule for specimen 36 was 6-in spacing at the edges and at the field plus additional nails in the overlaps. This is marked 6-6-6 and represents the best schedule in the field. A total of 85 spiraled-shank nails were used. In order to better capture the failure sequence, the starting load was set to 2 kips. The behavior of the system was superior to all previous specimens. The first failure, a Type 2 failure, appeared at Level G which in this case corresponds to 4.5 kips. Two additional Type 1 failures were recorded in Level K (7 kips). The next two levels brought ten new failures;

eight Type 1 and two Type 3 failures. The final ratings for the system were 7.5 kips for extensive damage states and 7 kips for the moderate damage state.

5.3.5. Specimen 38

Similar to specimen 32, the nailing schedule for specimen 38 was 6-12-6 with no additional nails in overlaps. The starting load was 2 kips, and the first three SIGDERS-5 levels were completed without recording any failure. Four Type 1 failures occurred in the second half of Level D, with a maximum level load of 3.5 kips. Two of these failures became Type 3 in Level E, with two additional Type 1 and two additional Type 2 failures also appearing. Two additional Type 3 failures were recorded in the Level G. The next level of loading produced five additional Type 1 and four Type 3 failures before subset H-4 could be completed. A total of 10.5 failures in 63 connectors were observed. The final ratings for the system were 5 kips for extensive damage states and 4.5 kips for the moderate damage state.

5.3.6. Specimen 39

Similar to specimen 33, the nailing schedule for specimen 39 was 12-12-12 with additional nails at overlaps. This was the last conventional system tested. The starting load was 2 kips, and the first two SIGDERS-5 levels were completed without recording any failure. Level C loading at 3 kips maximum resulted in five Type 1 failures. Three Type 1 failures were recorded in Level D. The second to last level was Level F at 4.5 kips maximum, which had two Type 3 failures in subsets 3 and 4. The Level G loading

could not be completed. The final ratings for the system were 4.5 kips for extensive damage states and 4 kips for the moderate damage state.

5.3.7. Discussion of Results

The final ratings from similar specimens (30, 32 and 38 on one count and 33 and 39 on another) are close enough to conclude that regardless of how the initial loading is selected, the SIGDERS-5 dynamic protocol succeeds in consistently predicting the performance. Still, it is important to note that if the initial loading is close to ultimate capacity, the protocol may miss the correct rating by overshooting it in the next level. A smaller starting load is therefore recommended, although this may result in longer loading time.

5.4. Retrofitted Systems

The recently proposed zinc-strapped retrofitted systems are investigated for their potential impacts on the behavior and reliability of the roofing systems. Three separate specimens with different nailing schedules are tested. These are 6-6-6R, 6-12-6R and 12-12-12R. The numbers have similar meaning to what was used for conventional systems, with the letter R at the end signaling the use of zinc-strap retrofits. A summary of the results from all three retrofitted specimens is presented in this section. The damage state observed at the end of each test was moderate for zinc-strapped systems. In fact, the extensive damage state assigned to this study was caused by the failure of some wood

members and is based on static load tests. The corresponding extensive damage rating is the same for all three nailing schedules. For detailed schematics of each test including the failure types and sequence refer to Appendix B. An example of the retrofitted roof specimens is shown in Figure 5.3.

Figure 5.3 - Retrofitted specimen ready to be tested

5.4.1. Specimen 34

Specimen 34 was the first retrofitted specimen to be tested under the SIGDERS-5 dynamic protocol. The nailing schedule was 6-in spacing at the edges and at the field plus additional nails in the overlaps. This is marked 6-6-6R. A total of 85 fasteners were used. Because of the presumed strength of this system, the starting load was set to 4 kips. The first two failures were recorded next to each other at Level F, at 2.25 times the initial

load. These were Type 3 failures caused by nails breaking in two due to fatigue. The zinc sheathings themselves were not damaged. In the next load level, three more Type 3 failures appeared in proximity to the previous two. One failure was caused by the nail straightening at the back of spacers and pulling out. The other two were again the results of nails breaking in two. The final rating of the system that corresponded to a moderate damage state was 9 kips with a level index of 5.

5.4.2. Specimen 35

The nailing schedule on Specimen 35 was 12-in at the edges and at the field plus additional nails in the overlaps. This is marked 12-12-12R. A total of 45 fasteners were used. The starting load selected for this test was 2 kips. The system progressed without any appreciable damages until subset 4 of Level M, where four Type 3 failures were recorded. The moderate damage state rating for this specimen was at Level M rating of 8 kips.

5.4.3. Specimen 37

Specimen 37 was the last retrofitted specimen tested. A total of 59 nails were used. The nailing schedule was 6-in at the edges and 12-in at the field plus additional nails in the overlaps. This is marked 6-12-6R. The initial load for this test was 3 kips. Similar to other retrofitted specimens, zinc sheathings did not suffer any damages. All eight fastener failures were observed in the subset of level H (2.75 times the original

load) defined by the straightening and withdrawal of the nails from the specimen. The final rating of the 6-12-6R system for moderate damage state was 7.5 kips.

5.5. Conclusions

Both conventional and zinc-strapped roof prototypes were tested under SIGDERS-5 dynamic protocols. The most prominent failure mode observed for the conventional systems was low-cycle fatigue in the zinc sheets around the fastener holes. Given the inspection results at the end of the tests, the final ratings of these systems will correspond to the extensive damage state. The zinc sheets in the zinc-strapped roof specimens did not suffer any damages. Fastener failures due to breakage or pull out presented the only problems with these systems. At worst, the rating at the end of these tests will correspond to the moderate damage state. It can be concluded that the zinc-strap retrofits provide considerable improvements in performances over the conventional systems. Table 5.1 presents a summary of results.

Table 5.1 – Test summary

Test No.	Specimen Type	Starting Load [kips]	Load at Moderate Damage State [kips]	Load at Extensive Damage State [kips]
30	6-12-6U	4	4.88	6
32	6-12-6U	4.5	4.22	5.63
33	12-12-12U	4	4	5
34	6-6-6R	4	9	9.5*
35	12-12-12R	2	7.5	9.5*
36	6-6-6U	2	7.58	8
37	6-12-6R	3	7.5	9.5*
38	6-12-6U	2	4.28	5
39	12-12-12	2	3.56	4.5

* From static load test.

CHAPTER 6

ROOF SYSTEM FRAGILITY

6.1 Introduction

A methodology for generating fragility curves for wood-zinc roof systems is presented. The model divides each roof into a finite number of grids. The demands on grid capacities will either be managed or result in one of two damage states. The indices associated with governing damage states will be combined to produce a roof performance index. Assigning probabilistic values to grid capacities and high wind demands will result in an algorithm to calculate the roof performance index. The fragility curves for various system configurations are generated using the calculated performance indices. The method covers both conventional and retrofitted systems.

6.2 Sampling Resistance

Under hurricane wind loading, the roofing system may be the most vulnerable component of a wood-zinc structure. As reported earlier in Chapter 5, extensive full

scale laboratory testing was used to quantify the capacity of these roofs. The study included the effects of various nailing schedules and retrofitting schemes. To use the resistance capacity of these specimens during the simulation process, both the nature of these tests and their results need to be closely inspected.

Because of the needs to protect the testing apparatus as well as to maintain the uniformity of the applied load, most specimens could not be loaded to the point of absolute collapse. Instead, certain rules were put in place to insure failure at neighboring grids which in turn could lead to significant loss of load bearing functions. These rules were discussed in Chapter 5. Table 5.1 listed the ratings of the roof specimens at the moderate and extensive damage states.

Our field studies have indicated a serious lack of quality control during construction for this type of structure. Both workmanship and material quality are highly variable. The zinc sheets, for example, are commercial grade and not subject to usual scrutiny afforded for structural products. To account for the variability between systems, the coefficient of variation (*COV*) for the resistance of wood-zinc roofs is set equal to 0.4, a higher value than what is typically assumed for structural components.

The roof ratings obtained from our experiments cannot be used as the mean sample values during simulations because they would not represent average field conditions. The specimens were constructed by strictly adhering to high standards. There were no missing or damaged roof nails, inadequate member connections or anchorage, or any other construction vices. Recognizing that the performance of these specimens will be superior to the majority of the cases encountered in the field, the results were assumed to represent the 90 percent fractile values. In structural reliability

terms, this will mean that no more than 10 percent of the roofs in the field can match or exceed experimental ratings.

Since resistance parameters are generally modeled as log-normally distributed, the capacity of the roofing systems was simulated as such. In order to do this, the available values have to be transformed to log-normal parameters. Let us designate R to represent capacity of the roofs in general. Then $R_{0.90}$ will be the recorded capacities from the experiments. Equation 6-1 shows the relationship between the mean of R, μ_R, and the mean of ln(R) , $\mu_{\ln(R)}$:

$$\mu_{\ln R} = \ln\left[\frac{\mu_R}{\sqrt{[COV(R)]^2 + 1}}\right] \tag{6-1}$$

The standard deviation of ln(R) is only a function of COV(R). This is shown in Equation 6-2:

$$\sigma_{\ln R} = \sqrt{\ln\left(COV^2 + 1\right)} \tag{6-2}$$

Using the principles of structural reliability, one can write the following equation to calculate $\mu_{\ln(R)}$ from the known values of $R_{0.90}$ and $\sigma_{\ln(R)}$:

$$R_{0.90} = \exp\left[\mu_{\ln R} + \sigma_{\ln R} \cdot \Phi^{-1}(0.90)\right] \tag{6-3}$$

where Φ^{-1} is the inverse of the normal distribution. Substitute back into equation 6-1, the mean resistance of the systems is obtained.

Table 6.1 lists resistance summaries for various roofing systems at extensive and moderate damage states. The 90% fractile values for the roof systems that were tested more than once are combined. The distributed means in this table are calculated by dividing the means over the pressure area of 64 ft^2 for the roof specimens.

Table 6.1 - Summary of resistances of roofing systems

Roof Type	Damage State	90% Fractile [kip]	Mean [kip]	Distributed Mean [psf]
6-6-6U	Moderate	7.58	4.98	77.8
	Extensive	8.50	5.59	87.4
6-12-6U	Moderate	4.57	3.00	46.9
	Extensive	5.25	3.45	54.0
12-12-12U	Moderate	3.59	2.36	36.9
	Extensive	4.75	3.13	46.2
6-6-6R	Moderate	9.00	5.92	92.5
	Extensive	9.50	6.25	97.6
6-12-6R	Moderate	7.50	4.93	77.1
	Extensive	9.50	6.25	97.6
12-12-12R	Moderate	7.50	4.93	77.1
	Extensive	9.50	6.25	97.6

6.3 Predicting Damage States

Previous studies on wood structures had considered the behavior of the roofing panels as individual, independent entities. Due to complexities inherent to wood-zinc roofs, it was decided to incorporate the test data directly by dividing the roof into a grid system and checking the resistance of each grid. The grids are approximately sized to match the pressure area for the laboratory specimens of 8-ft x 8-ft. During the analytical simulation, the size of the sampled structure, the wind direction, and the corresponding roof angles are determined. The area of the roof is calculated and divided by 64 sq. ft to determine the number of grids in the structure. The result is rounded to an even integer number which is then used to calculate the grid area. In terms of the geometrical positioning of the grids, the minimum number of grids running perpendicular to the ridge

line is assumed to be two. This assumption was made after reviewing the buildings in our inventory. Figure 6.1 shows an example of the grid system.

When running the simulation, the capacity of each grid is assigned independently. For the most common nailing schedule, with 6-in spacing on the edge and 12-in spacing elsewhere, average resistance may vary depending on the overall location of the grid. In such a case, 6-12-6 data are used for grids in pressure zones 2E and 3E and 12-12-12 data are used in zones 2 and 3. Given the typical width of the higher pressured zone 2E, the outer edge of a grid in that zone is most likely subject to the lower pressure of zone 2, thus the use of 6-12-6 data as opposed to 6-12-12. The same rules are followed for retrofitted systems with identical nailing schedule. For all other nailing schedules, both common and retrofitted, the resistance properties used in the simulation would correspond to the specified nailing schedule.

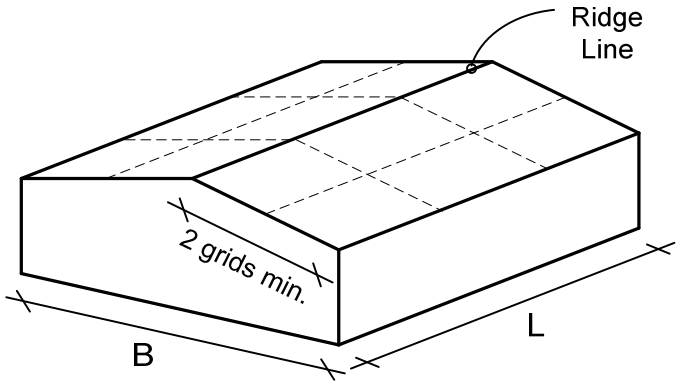

Figure 6.1 – Schematic drawing of grid distribution and structural symmetry

A description of MWFRS pressure zones was given in Chapter 3. Figure 6.2 shows the grid system with pressure zones overlaid. To account for the localized high pressures that can act over a small area on the roof, C&C external pressure coefficient of

-2.1 is used to calculate demands on one of the grids in zone 2E. From our field observations and interviews, the grid area is large enough that such an assignment will result in a conservative estimate of the pressure demands. The use of C&C coefficients for all grids is considered overly conservative when calculating the roof performance index discussed in Section 6.3.1.

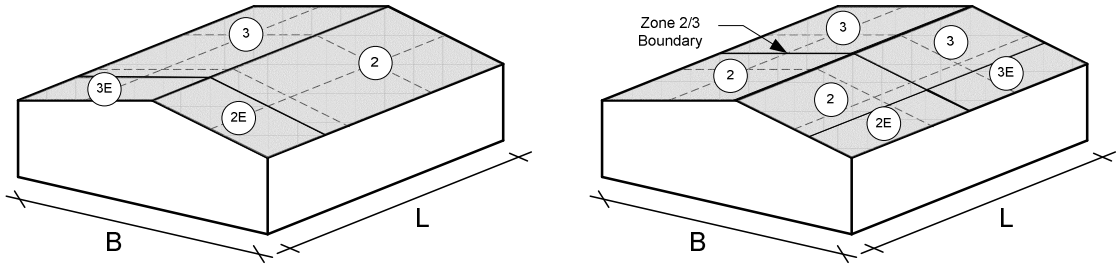

(a) Wind perpendicular to ridge **(b) Wind parallel to ridge**

Figure 6.2 – Pressure distribution according to wind direction

6.3.1. Roof Performance Index

In order to predict the system performances for the roofs, a novel approach is proposed. During the simulation process, random resistance-to-demand ratios are calculated for each grid at all wind speeds. Accordingly, a damage index is assigned to each grid that will later be combined to predict the damage states of various pressure zones on the roof. To asses the behavior of the complete roof ensemble, a roof performance index is calculated from:

$$I_{RP} = \sum_{i=1}^{4} I_{Zi} \tag{6-4}$$

where I_{Zi} is the performance associated with each individual roof zone i, with i=1 corresponding to zone 2E, i=2 to zone 2, i=3 to zone 3E, and i=4 to zone 3 as defined by the ASCE 7-02. The zone performance index is an average of the damage indices for the grids in that zone.

In equation form:

$$I_{Zi} = \frac{\sum_{j=1}^{n} I_{Dj}}{n} \tag{6-5}$$

where n is the number of grids in zone i. The damage index for a grid, I_{Dj}, can have values of 0, 0.25 or 0.5, depending on the resistance to demand ratio. If the demand exceeds or equals the mean resistance for the extensive damage state in Table 6.1, a damage index of 0.5 is used. A lower demand that still exceeds or equals the mean resistance for the moderate damage state in Table 6.1 will result in a damage index of 0.25. All lower demands on a grid are assumed incapable of producing enough damages to affect the overall roof performance and are assigned a zero damage index.

The limits on the roof performance indices are listed in Table 6.2. Accordingly, the roof system is assumed to be totally lost if three zones are in the extensive damage states and one zone suffers at least minor to moderate damages; or if two zones are in the extensive damage states and the other two zones suffer moderate to extensive damages. Similarly, a moderate damage state requires at least two zones moderately damaged. For a minor damage state, moderately damaged grids should not be present beyond zone 2E.

Table 6.2 – Roof performance index, I_{RP}

Damage State	Roof System
Minor	$0.25 < I_{RP} < 0.5$
Moderate	$0.5 \le I_{RP} < 1$
Extensive	$1 \le I_{RP} \le 1.5$
Total	$I_{RP} > 1.5$

6.4 Roof Fragility Curves

During the simulation process, a roof performance index is calculated for each house at a given wind speed. Depending on this index, the house will be assigned a 0 or 1 value for each of the four roof damage states, with 1 indicating the occurrence. In this way, one will record 0,0,0,0 for $I_{RP} < 0.25$; 1,0,0,0 for $0.25 < I_{RP} < 0.5$; 1,1,0,0 for $0.5 \le I_{RP} < 1$; 1,1,1,0 for $1 \le I_{RP} \le 1.5$; and 1,1,1,1 for $I_{RP} > 1.5$. At any wind speed, the number of 1's in each column is counted, returning the cumulative number of houses subject to a particular damage state or worse. The cumulative numbers for each damage state are tabulated at all wind speeds, creating a data array that is fitted into a cumulative log-normal distribution using the 3-second gust wind speeds as the variable. When plotted, the distribution will give the fragility curve for that particular damage state.

The use of log-normal distribution to model fragilities is fairly standard. Consequently, the probability that a certain level of damage will be met or exceeded at the 3-second gust speed *w* will be given by:

$$F_X(w) = \Phi\left(\frac{\ln w - \mu_{\ln X}}{\sigma_{\ln X}}\right) \tag{6-6}$$

The function Φ(u) represents the cumulative distribution for the standardized normal variable U:

$$\Phi(u) = \frac{1}{\sqrt{2\pi}} \int_{-\infty}^{u} \exp\left(\frac{-v^2}{2}\right) dv \tag{6-7}$$

The statistical parameters $\mu_{\ln X} = \mu$ and $\sigma_{\ln X} = \sigma$ are evaluated by curve fitting the damage data using log-normal CDF. For a more detailed review of the process, refer to the numerical example presented in Section 1.6.

The flowchart in Figure 6.3 shows the procedure followed to generate fragility curves for the roof systems. Examples of these curves for wood-zinc houses roofs are given in Figure 6.4 through Figure 6.9. The conventional system in Figure 6.4 uses the best nailing schedule 6-6-6. As shown, only 3 percent of the roofs damaged at 250 mph gust winds are totally lost. Compare this to 46 percent for the usual 6-12-6 schedule (Figure 6.5) and 99 percent for the weak 12-12-12 schedule (Figure 6.6).

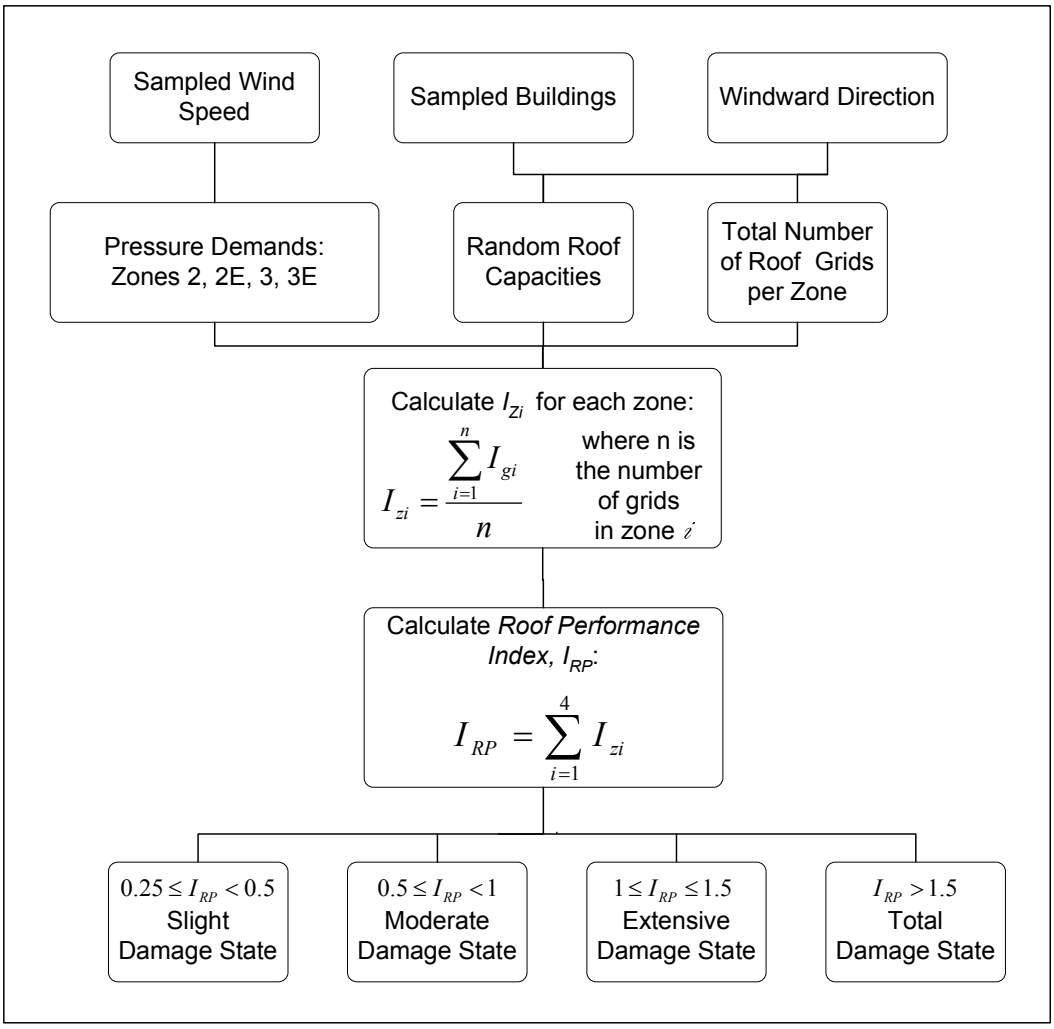

Figure 6.3 - Flowchart for simulating the roof system performance

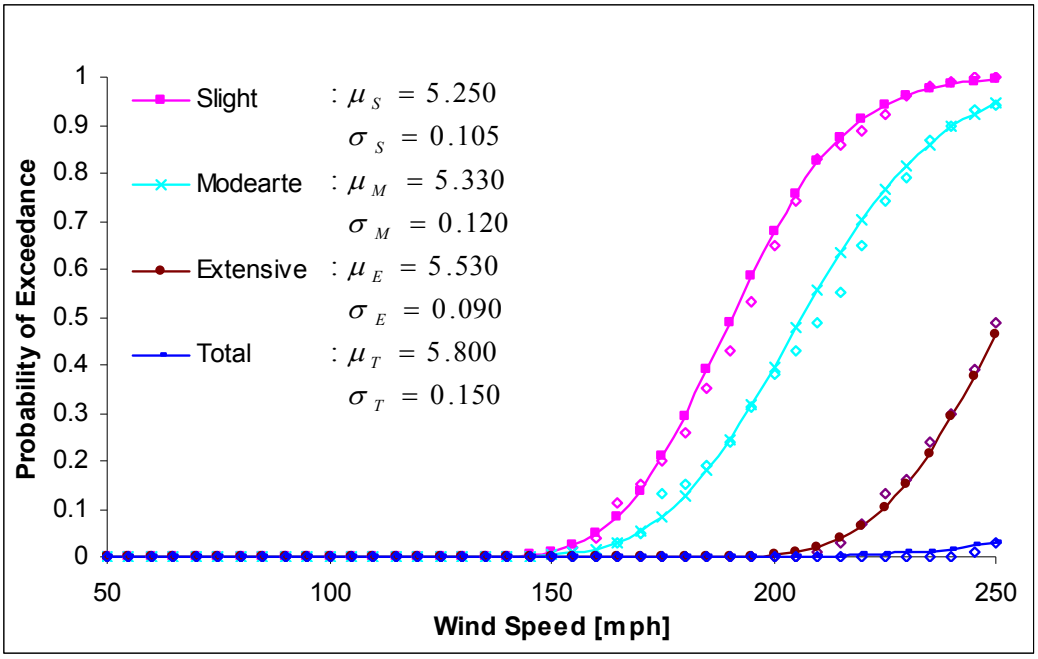

Figure 6.4 – Fragility curves for conventional systems with 6-6-6 schedule

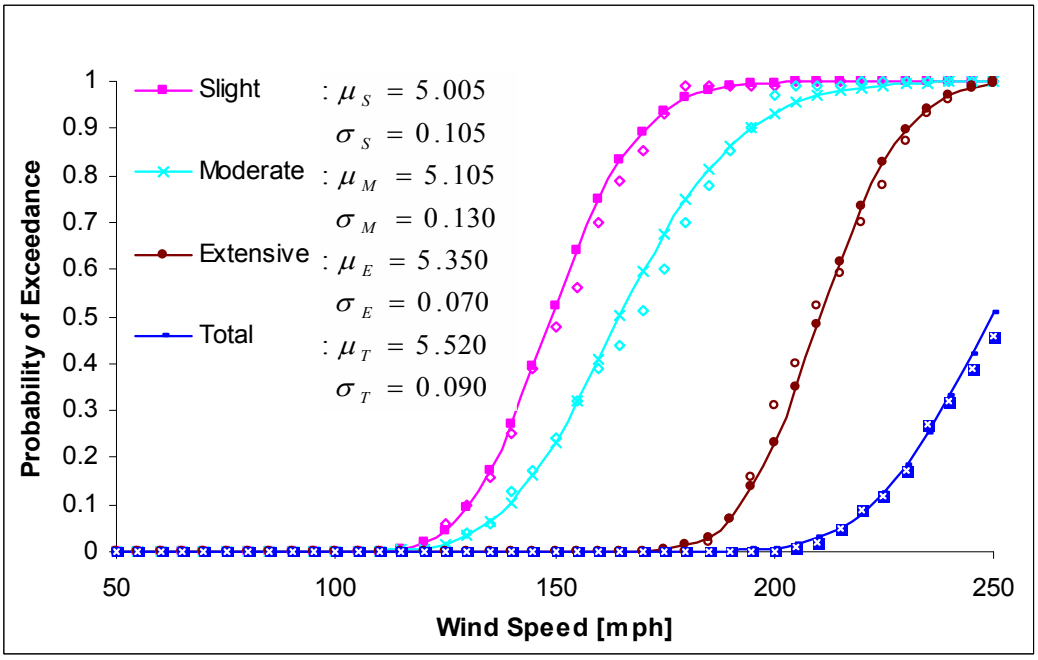

Figure 6.5 – Fragility curves for conventional system with 6-12-6 configuration

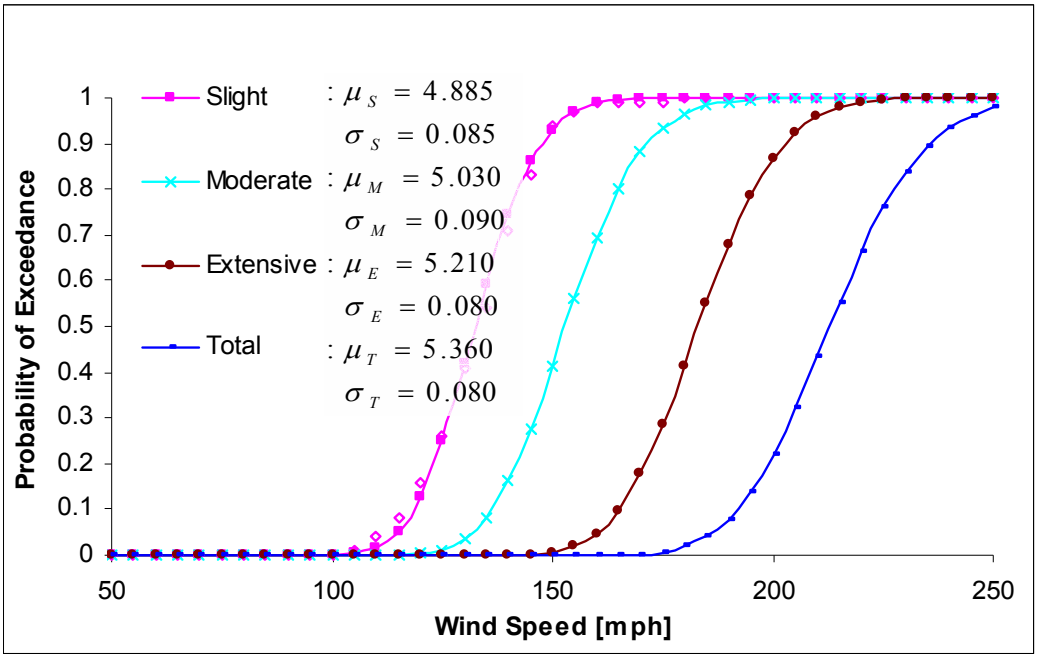

Figure 6.6 – Fragility curves for conventional system with 12-12-12 configuration

The fragility curves for the retrofitted roof systems depict marked improvements over the conventional systems. The extensive and total damage states are not present for gust wind speeds of up to 200 mph. This will correspond to high category 4 hurricanes. The only conventional system of comparable performance uses the 6-6-6 nailing schedule. Based on our field interviews, this is the system rarely used because of concerns with increased leaks and labor costs.

Table 6.3 lists the statistical parameters that when substituted in Equation 6.6 will give roof system fragility relations for wood-zinc houses.

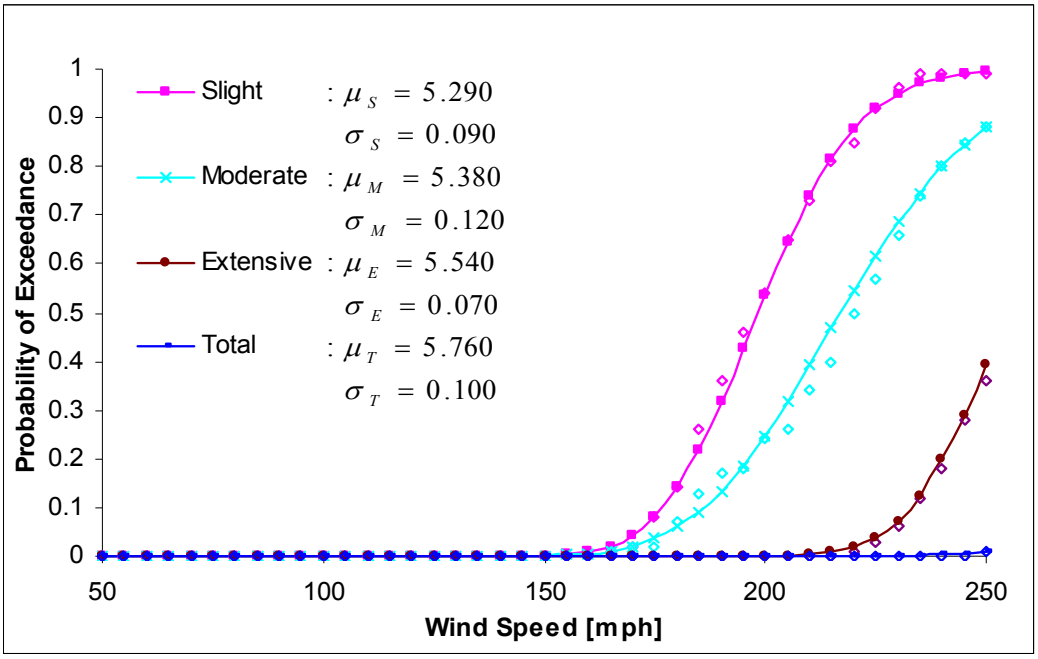

Figure 6.7 - Fragility curves for retrofitted system with 6-6-6 configuration

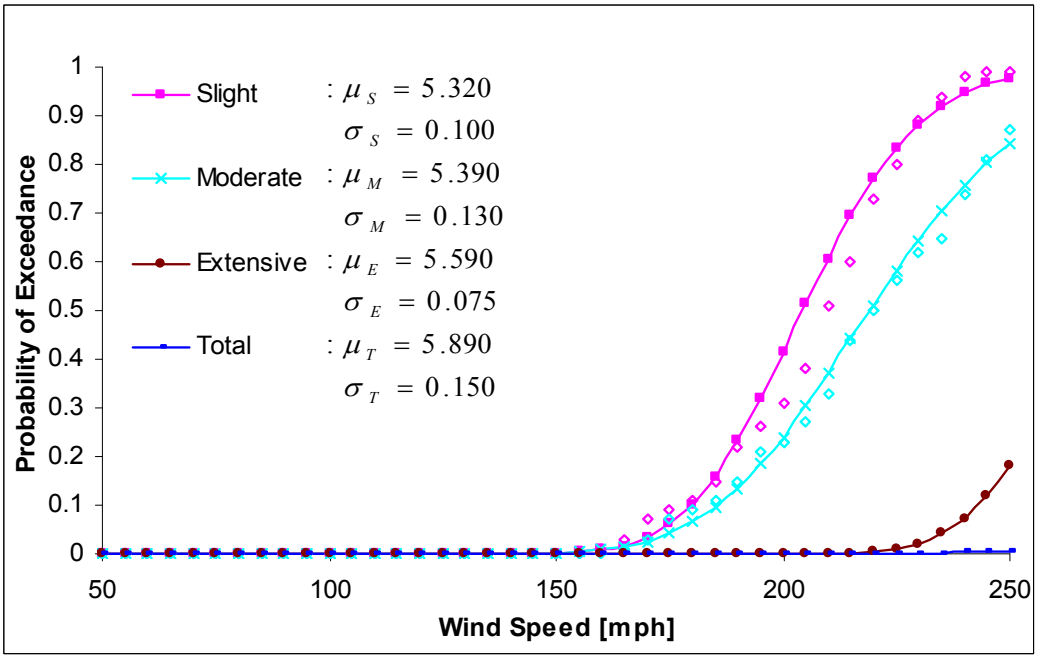

Figure 6.8 - Fragility curves for retrofitted system with 6-12-6 configuration

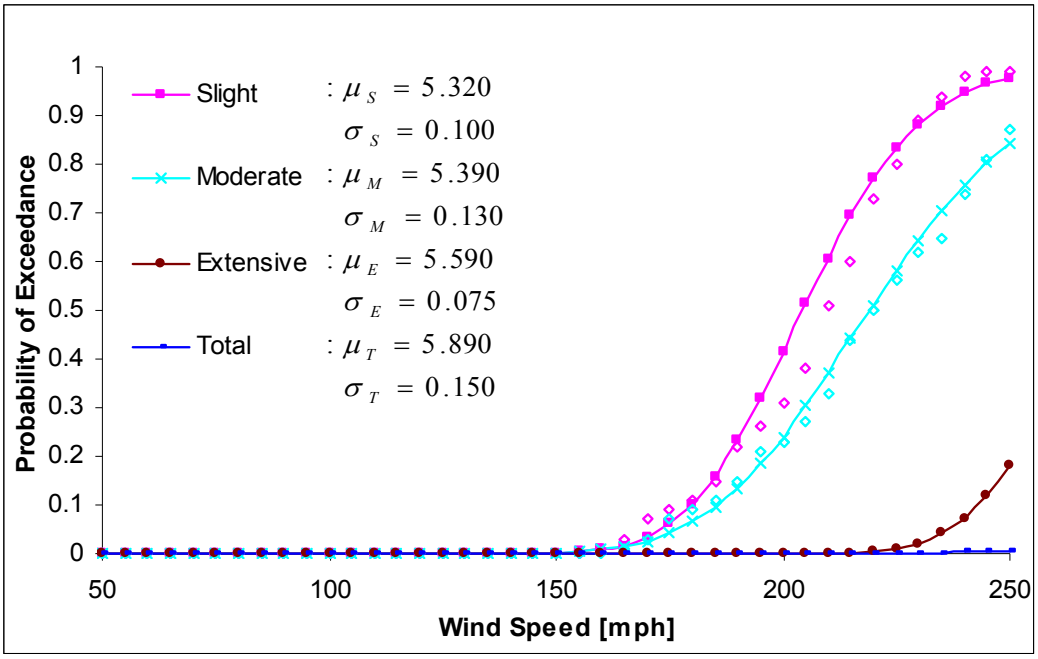

Figure 6.9 - Fragility curves for retrofitted system with 12-12-12 configuration

Table 6.3 – Summary of parameters for roof system fragilities

Prototypes		Slight	Moderate	Extensive	Total
6-6-6U	μ	5.250	5.330	5.530	5.800
	σ	0.105	0.120	0.090	0.150
6-12-6U	μ	5.005	5.105	5.350	5.520
	σ	0.105	0.130	0.070	0.090
12-12-12U	μ	4.885	5.030	5.210	5.360
	σ	0.085	0.090	0.080	0.080
6-6-6R	μ	5.320	5.390	5.590	5.890
	σ	0.100	0.130	0.075	0.150
6-12-6R	μ	5.290	5.380	5.540	5.760
	σ	0.090	0.120	0.070	0.100
12-12-12R	μ	5.290	5.380	5.540	5.760
	σ	0.090	0.120	0.070	0.100

CHAPTER 7

ROOF-TO-WALL CONNECTIONS

7.1 Introduction

In recent years, the use of metal straps in roof-to-wall connections has been heavily promoted in the Island. After all, transferring the uplift loading from the roof to the foundation is essential for maintaining the integrity of the structure. The campaign has been successful to the extent that almost all remodeled or newly built structures use these straps. However, very few studies have been done to evaluate their effectiveness. The study by Reed et al. (1997) is a noted exception. The reported capacities from that study are summarized in the next section and used during the simulations. However, that study does not cover the U-hangers widely used in the Island. Laboratory testing was used to obtain the data on those connectors. Also tested were steel cables used to temporarily tie down the roofs. All the acquired capacities are fed into the simulation engine to evaluate the performances of various roof-to-wall connection configurations.

7.2 Reported Capacities of Connectors

The roof-to-wall connections for wood-zinc houses may use toe-nails only, small straps, or U-hangers. The study by Reed et al. (1997) provides the capacities for two of these cases. The toe-nailed connections were shown to have an average capacity of 430 lbs and a *COV* of 0.23. Also evaluated in this work are the capacities of several other connection types and configurations such as large straps and double small straps from wall element or top plate to rafters with capacities as high as 3,220 lbs. The implementation of epoxy adhesives as a fastening tool, either as a retrofitting scheme or as the main binding system, was also presented. The epoxy performance proved comparable to some of the smaller mechanical connectors.

The results on small straps are of particular interest to this study. Adopted from Reed et al. (1997), Table 7.1 lists the capacities for toe-nails plus straps at every rafter and toe-nails plus straps at every other rafter. Interestingly enough, the reduction in the number of straps by half reduces the capacity by only 25 percent. These capacities were the direct inputs into the simulation engine, whereby the listed *COV* of 0.11 were used to adjust the values for different connectors.

Table 7.1 – Selected roof-to-wall connection capacities from Reed et al. 1997[1]

Description	No. of Specimens	Average Ultimate Uplift Force	Coefficient of Variation	Predominant Failure Modes
Toe nail only	16	430 lbs.	0.23	Nail pullout of top plate
Toe nail + small strap	19	1,640 lbs.	0.10	Strap tear, rafter split, nail pullout of rafter
Toe nail + small strap every other rafter	1	1,210 lbs.	0.11[a]	Not reported
[a] Assumed by the author in accordance with the values presented in the original work.				

7.3 Experimental Capacity of Connectors

The most common roof-to-wall connectors used in wood-zinc construction in Puerto Rico are the Simpson Strong-Tie® U-shaped hangers LU28 and LUS26. The reported uplift capacities of these hangers are 1,140 lbs for LU28 and 930 lbs for LUS26. Through personal communications with a Simpson factory representative, Cope set the factor of safety associated with these capacities at 3 (Cope, 2004). The experimental study discussed in this section was designed to verify her assumption.

7.3.1. Dynamic Tests

The connections between the roofing system and the walls was tested under cyclic uplift loading in a MTS© 810 Hydraulic Frame. A tee-shaped sample was used to model the connection with the web representing the rafter and the flange representing the wall element. Figure 7.1 shows one of the tested samples and the testing apparatus used. The

[1] Adopted from Reed et al. (1997)

average capacity was 500 lbs for the seven connectors tested. This was only half of the allowable loads reported by the manufacturer. The lower than expected capacity was due to lack of restrains on both ends of the sample, allowing high rotations not representative of field conditions. Nonetheless, the fact that the damages are caused by nails breaking through the end grain (Figure 7.2) demonstrated the means by which to improve these connectors. A better design will expand the nailing area and move it further away from the end grains. This will result in bulkier hangers and added cost, but in a hurricane prone region the benefit-to-cost ratio will be high.

Figure 7.1 – Dynamic load test set up for roof-to-wall connections

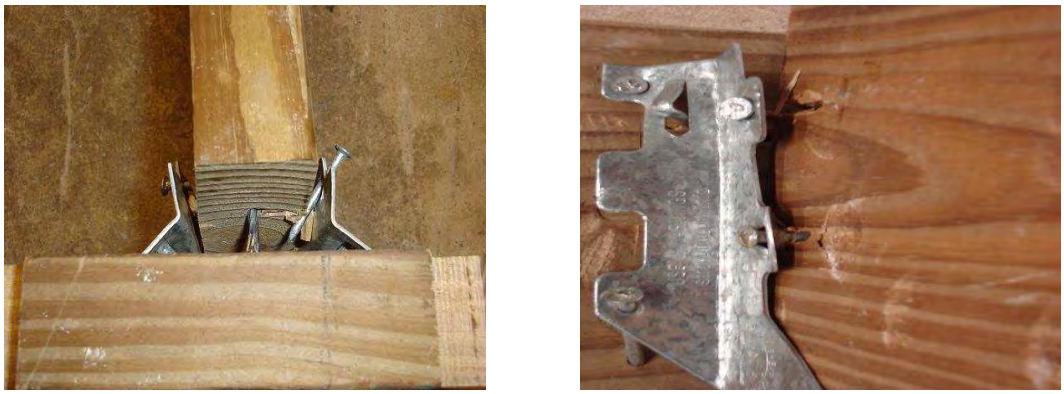

Figure 7.2 – Failure mode for roof-to-wall connections in dynamic load tests

7.3.2. Static Load Tests

In the first static load test, a full size rafter was subjected to two point loads equally spaced at one third the span length of 10-ft. The rafter failed in flexure before the connectors could reach their limits. The span length was reduced to 6-ft and the test was repeated. Displacements were monitored at three points, including the center of the beam. Notice that the test was intended for capturing the uplift behavior of the connector, which is why the connector in Figure 7.3 is placed upside down. The connector used for this test was the Simpson Strong-Tie® LUS26 connector.

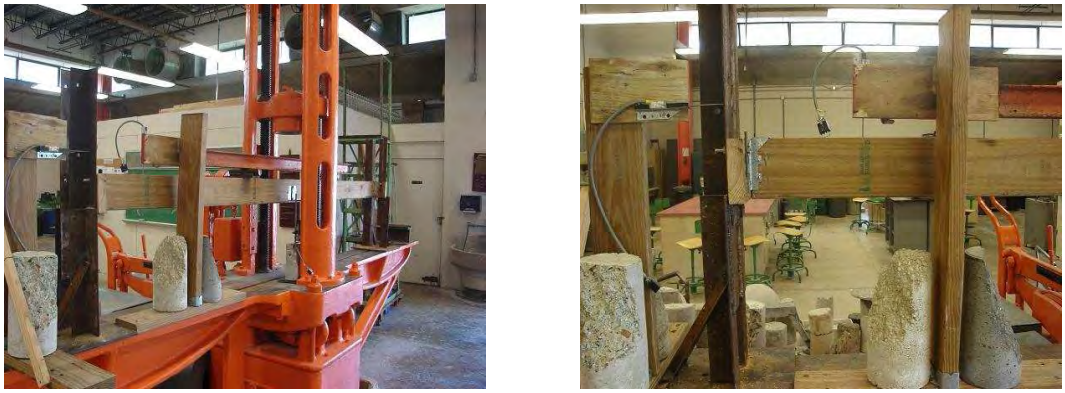

Figure 7.3 – Full-scale test setup

The recorded failure load was 4,980 lbs, or 2,490 lbs per connector. The failure mode was consistent with what was observed from the small scale dynamic load tests. The N8 1-1/2-in long nails used for fastening the U-hangers to the ensemble had cut through the end grains, separating the hanger from the rafter as illustrated in Figure 7.4. Comparing the test result with the reported allowable capacity of 930 lbs, a safety factor of 2.68 is obtained, which is less than the value suggested by Cope (2004). During the

simulation process, the mean capacity assigned to the U-hangers was 2,500 lbs per connector, randomly adjusted using a *COV* of 0.11. This ignores the slightly higher allowable capacity reported for LU28, and assumes that these hangers have similar characteristics to the connectors tested by Reed et. al (1997).

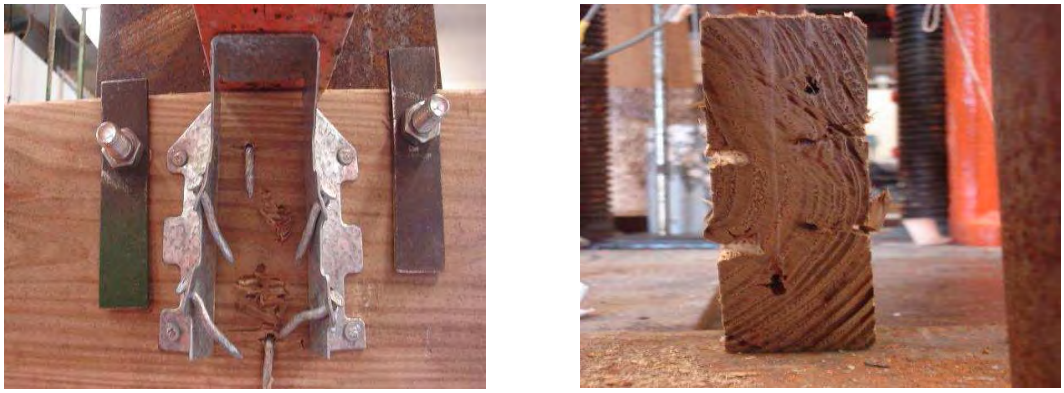

Figure 7.4 – Damages in full-scale test

7.4 Modeling Connection Demands

In simulating the performance of the roof-to-wall connections in any given system, prior knowledge of the loads transferred through the connectors is required. In order to evaluate these demands, a structural analysis model is formulated based on the actual field observations in Puerto Rico. Figure 7.5 depicts one such example where no interior joist was placed along the ridge line. Instead, the two rafters arrive at the center line of the house and are spliced together using a connection plate. This type of setup is sometimes supported by eccentrically placed columns or wall elements that provide

additional support to the roof system. Either one or two additional elements might be present, reducing the load demand on the roof-to-wall connections.

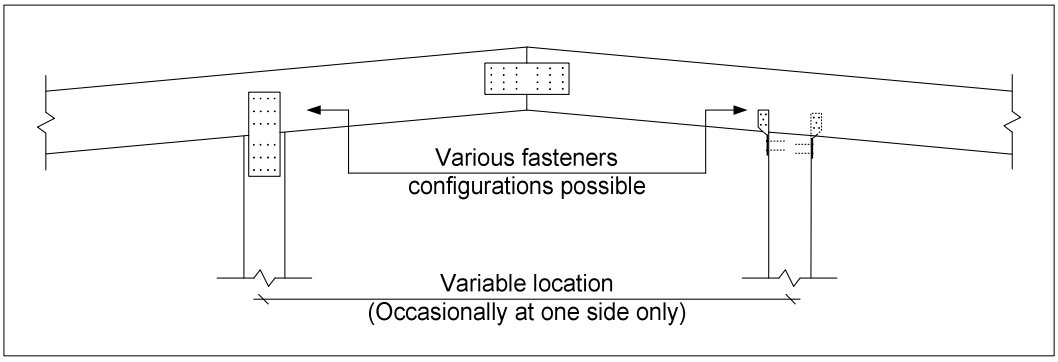

Figure 7.5 – Roof joist connected without top beam

A second example is the case where rafters converge in the apex of the roof and are connected to a supporting member or joist. The supporting member is constructed similar to a top plate, using a pair of sections typical to rafters. The member is supported along its length on several locations, behaving like a continuous beam with variable span lengths. This is shown in Figure 7.6.

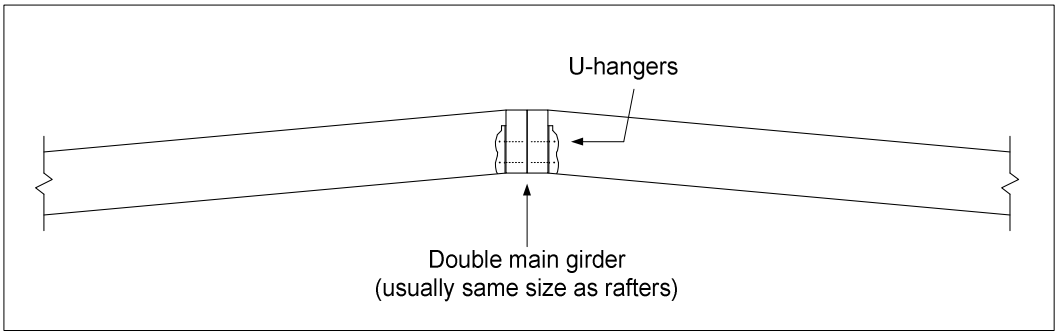

Figure 7.6 – Roof truss connected to top double beam

Both of the roof-to-wall connection cases discussed are conservatively modeled using the simple mechanism shown in Figure 7.7. The vertical reactions at the ends represent the total demand on the roof-to-wall connections on each side. The placement of an internal hinge between the rafters is more in line with the first example while the absence of intermediate supports is more consistent with the second. The parameters shown in the figure are defined in the beginning of each simulation, where L is the least side dimension of the structure, θ is the roof slope, and the distances a and b are defined as needed by the wind directionality in order to represent the appropriate demand zones, be it zone 2, 2E, 3, or 3E. Loads W_1 through W_4 represent the equivalent tributary loading throughout the whole roof per section of roof area. They are randomly generated according to aleatory wind velocities, structural sizes and orientations, and roof angles. Load demands on the connections for the pressure grid subject to the localized C&C external pressures are adjusted accordingly. The procedure is similar to one discussed in Chapter 6.

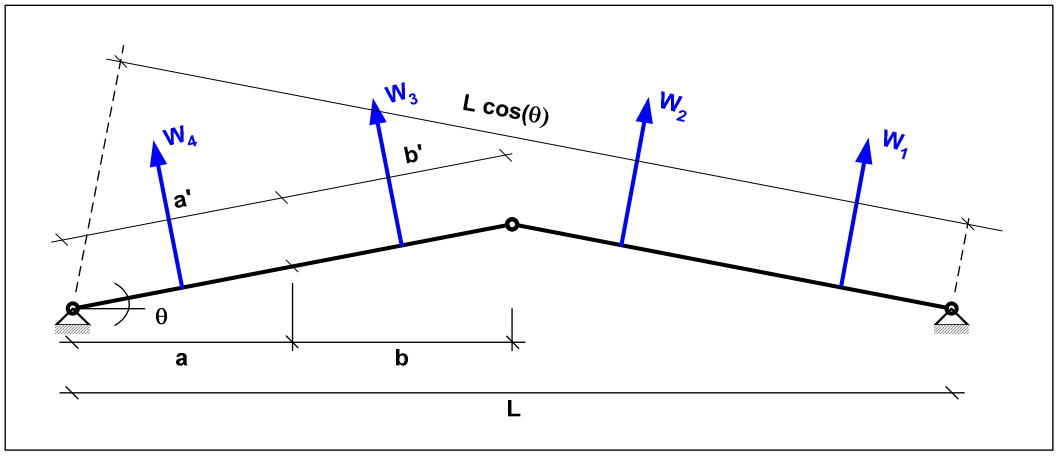

Figure 7.7 – Structural model used for obtaining roof-to-wall load

Once the analytical model is defined, the basic static equilibrium equations are used to obtain the reactions. Summing the moments about the left support:

$$R_R L = W_1\left(L\cos\theta - \frac{a'}{2}\right) + W_2\left(L\cos\theta - a' - \frac{b'}{2}\right) + W_3\left(a' + \frac{b'}{2}\right) + W_4\left(\frac{a'}{2}\right) \tag{7-1}$$

Summing the vertical forces:

$$R_L = (W_1 + W_2 + W_3 + W_4)\cos\theta - R_R \tag{7-2}$$

Note that the reactions obtained from Equations 7-1 and 7-2 are distributed between the connectors based on the different pressure zones on the roof. The process followed for achieving this goal is explained in the next section.

7.5 Modeling Fragility

In order for the roof-to-wall connections to affect the system fragilities, the wood-zinc roof system should be completely separated from the rest of the structure in which case a total damage state exists. This can be viewed as a yes or no proposition, meaning that some connector failures in isolated locations may be overlooked depending on how the stresses are redistributed beyond the effected areas. Using the connection demand model from Section 7.4, the total reactions on each side of the structure are assigned to two different pressure zones in proportion to their tributary areas. During the simulation runs, the size and orientation of each structure are known and so are the numbers of connectors per zone. The connector types are randomly selected from the four options

listed in Table 7.2. These are toe-nails only, toe-nails with small straps, toe-nails with small straps every other rafter, and toe-nails with U-hangers.

Table 7.2 – Summary of connectors used during the reliability analysis

Case	Description	Likelihood of Occurrence	Average Ultimate Uplift Force [lbs]	Coefficient of Variation
1	Toe-nail only	0.40	430	0.23
2	Toe-nail + small strap	0.20	1,640	0.10
3	Toe-nail + small strap every other rafter	0.20	1,210	0.11[a]
4	Toe-nail + Simpson Strong-Tie® LUS26 or LU28 U-Hanger	0.20	2,500	0.11[a]

[a] Assumed by the author in accordance with the values presented in the original work.

In recent years, there have been attempts to promote the use of metal straps in the Island. Almost all remodeled or newly built structures use these straps. However, in our field studies, a significant number of these straps were found to be improperly installed. Consequently, a likelihood of occurrence weight of 0.2 is assigned to each small straps or U-hanger case. The weight assigned to the toe-nail only case was 0.4. The fasteners are batch selected; meaning that only one out of the four possible configurations discussed is used for each particular building during the simulation. This is consistent with the usual practice in the field. Connector capacities are determined in accordance with the mean and the *COV* values listed in Table 7.2. The first three cases were discussed in Section 7.2 while the last case is from Section 7.3.2. The zone capacities are evaluated by adding the capacities of all the connectors in that zone.

Zone demands are compared to zone capacities and when the demand exceeds the capacity, a partial failure is recorded. Because zone 2E is the highest loaded zone

defined by the ASCE 7-02, the failure is first checked in that zone. Furthermore the demands on the first four connectors in that zone will be based on the C&C external pressure coefficient of -2.1. In the case that zone 2E fails, its share of the load will be redistributed to the contiguous zone sharing the same ridge side of the ensemble. This will mean zone 2 for perpendicular-to-ridge loading and zone 3 for parallel-to-ridge loading, as shown in Figure 7.8. In cases where the loads are redistributed, the next step would be to check the ridge sides for the failure. The simulation routine assigns 0 and 1 values to each structure at every wind speed, with 1 indicating the failure. Counting the number of 1's for all wind speeds and tabulating the results creates a data array that is fitted into a cumulative log-normal distribution using the 3-second gust wind speeds as the variable. When plotted, the distribution will give the fragility curve for total damage state. For further clarifications, the reader is referred to Section 1.6. The flowchart in Figure 7.9 depicts the process by which the fragility curve of the roof-to-wall connections is generated.

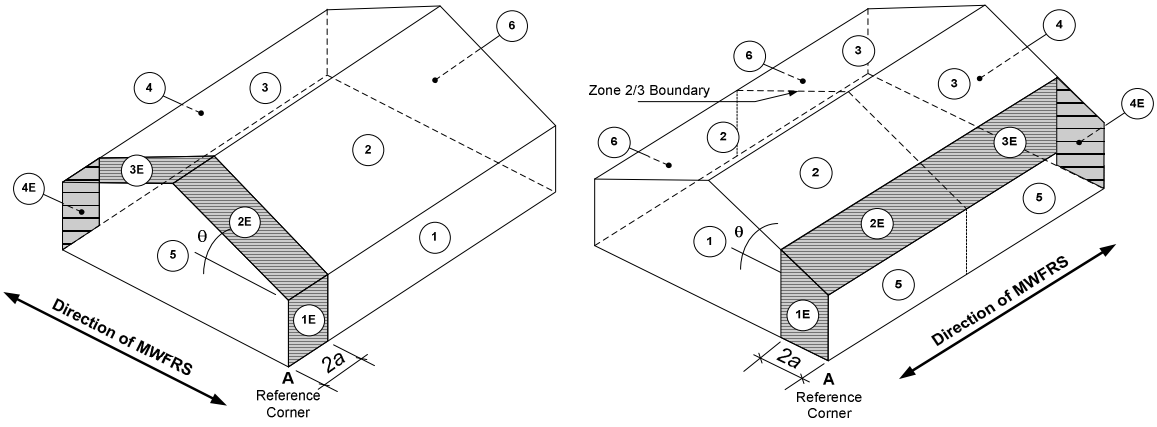

(a) Transverse load case **(b) Longitudinal load case**

Figure 7.8 – Principal load cases analyzed for the roof-to-wall connection modeling[2]

[2] Adapted from ASCE 7-02

The fragility curves developed during the simulations are shown in Figure 7.10. Each curve represents the total damage state for a different roof-to-wall connection configuration. Note the improvements when metal straps are used throughout. Specially striking is the effect the U-hangers have on the overall integrity of the system. It can also be concluded that the practice of only toe-nailing the roof-to-wall connections should be disallowed in hurricane prone regions.

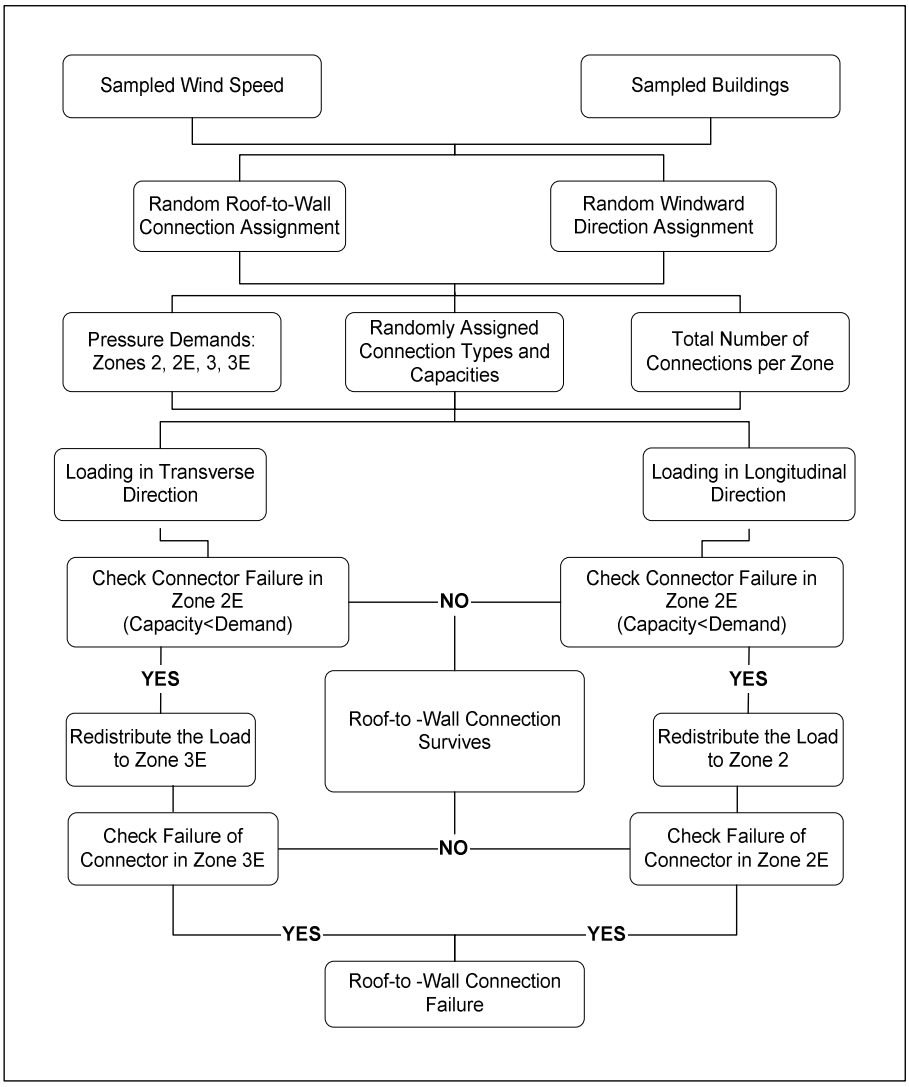

Figure 7.9 - Flowchart of roof-to-wall connection damage simulation

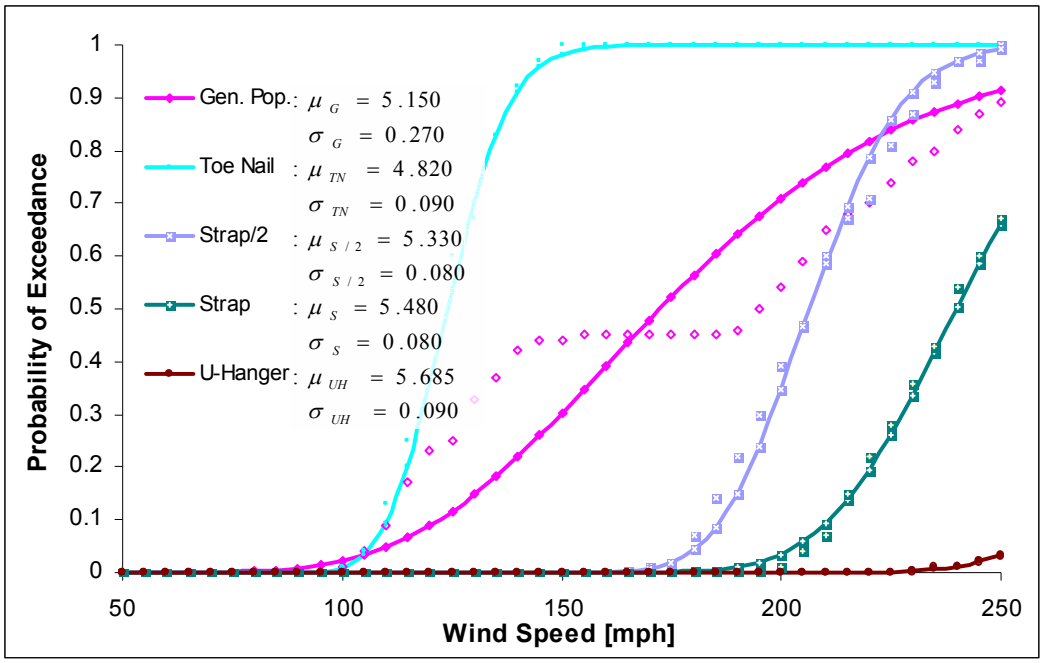

Figure 7.10 – Fragility curves for various roof-to-wall connectors

7.6 Implementation of Guys

The use of steel cables or guys to temporarily tie down a roof system during a hurricane is a common practice in Puerto Rico. In order to be effective, the guys need to be pre-tensioned and in contact with the roof structure. Turnbuckles are used at both ends, embedded to the foundation or to the sides of the structure. The guys are placed on the outside, over the roof and perpendicular to the roof ridge, as shown in Figure 7.11. They are usually spaced around 8-ft to 10-ft apart, resulting in three guys per residence, although more may be used. An informal survey by the author amongst both home owners and contractors found the most commonly used cables have plastic covering and are either 1/8-in or 1/4-in in diameter.

Figure 7.11 – Picture of guy implementation and turnbuckle

From our survey, less than 20 percent of houses use the guy setup. Given the difficulties with proper installation of the guys, it was assumed during simulations that only 10 percent of all houses use active guys. The safety factor used by manufacturers when reporting the maximum allowable loads for cables was obtained by testing samples from one cable in tension and comparing their ultimate loads to the allowable one. The selected samples were 3 ft long pieces cut from 1/8-in diameter cable. The tested capacity was 770 lbs, resulting in a safety factor of 2.25 when divided by the manufacturer capacity of 340 lbs. Assuming the same safety factor, the ultimate capacity of the 1/4-in diameter guy was estimated as 3,200 lbs. The *COV* for these cables is set at 0.2. Once the capacities of the cables were obtained, their contributions were inputted into the simulation engine. It was assumed that 60 percent of guys used are 1/8-in in

diameter and the rest are 1/4-in. The contributions of the guys are accounted for by subtracting their capacities from the demands on the roof-to-wall connections.

Figure 7.12 shows the fragility curves for the total damage states developed for the general population and assuming various guys setups. For comparison purposes, the general case without guys is also included. This is the first curve moving from top down. The second curve in the set was developed using the 1/8-in guys in 10 percent of the population. The third curve uses 1/8-in guys in 6 percent of the population and 1/4-in guys in 4 percent. The last curve uses 1/4-in guys in 10 percent of the population. The changes shown are slight, proving that guys can not be a substitute for properly designed roof-to-wall connections.

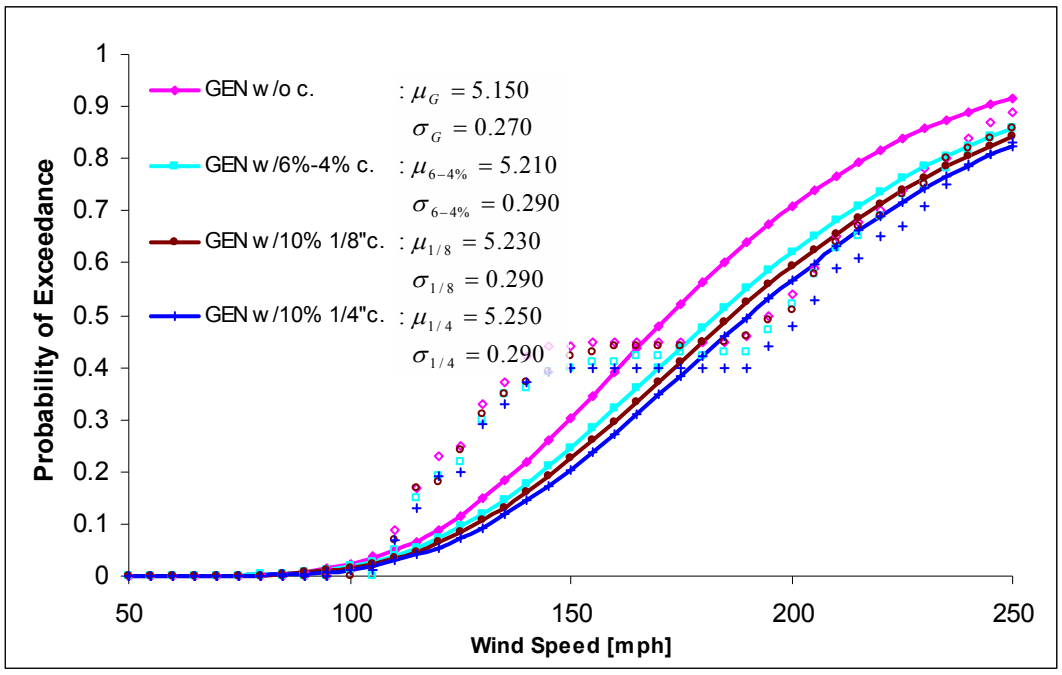

Figure 7.12 – Fragility curves considering guy interaction

CHAPTER 8

STUD WALL SYSTEMS AND SIDINGS

8.1 Introduction

Wall failures in wood houses are often a consequence of either damages to the roof system or the loss of connections securing wall to wall plates. The overall capacity dictated by wall studs and panel sheathings is generally more than adequate to resist uplift and transverse loading as well as the shear transferred from the roofing system.

The exterior wall sidings used in Puerto Rico are typically 1/2-in. or 5/8-in. thick plywood panels. Decorative panels or 3/8-in. plywood panels are used inside, although they are not always present. The standard size for all these panels is 4-ft x 8-ft. The wall studs are nominal 2-in x 4-in spaced 24-in on center. The heights of the wall elements are typically 8-ft, taking full advantage of the longer dimension of the panel.

Figure 8.1 shows examples of wood shear walls in Puerto Rico. The combinations of the elements along with the fasteners that hold the ensemble together are researched in this chapter. Also discussed is the mathematical PCM model for the wall that when combined with the stud connection capacities at wall plates should provide

wall system fragility. For wall sheathings, basic NDS shear capacities for the nails are tested against the load transfer demands from the roof.

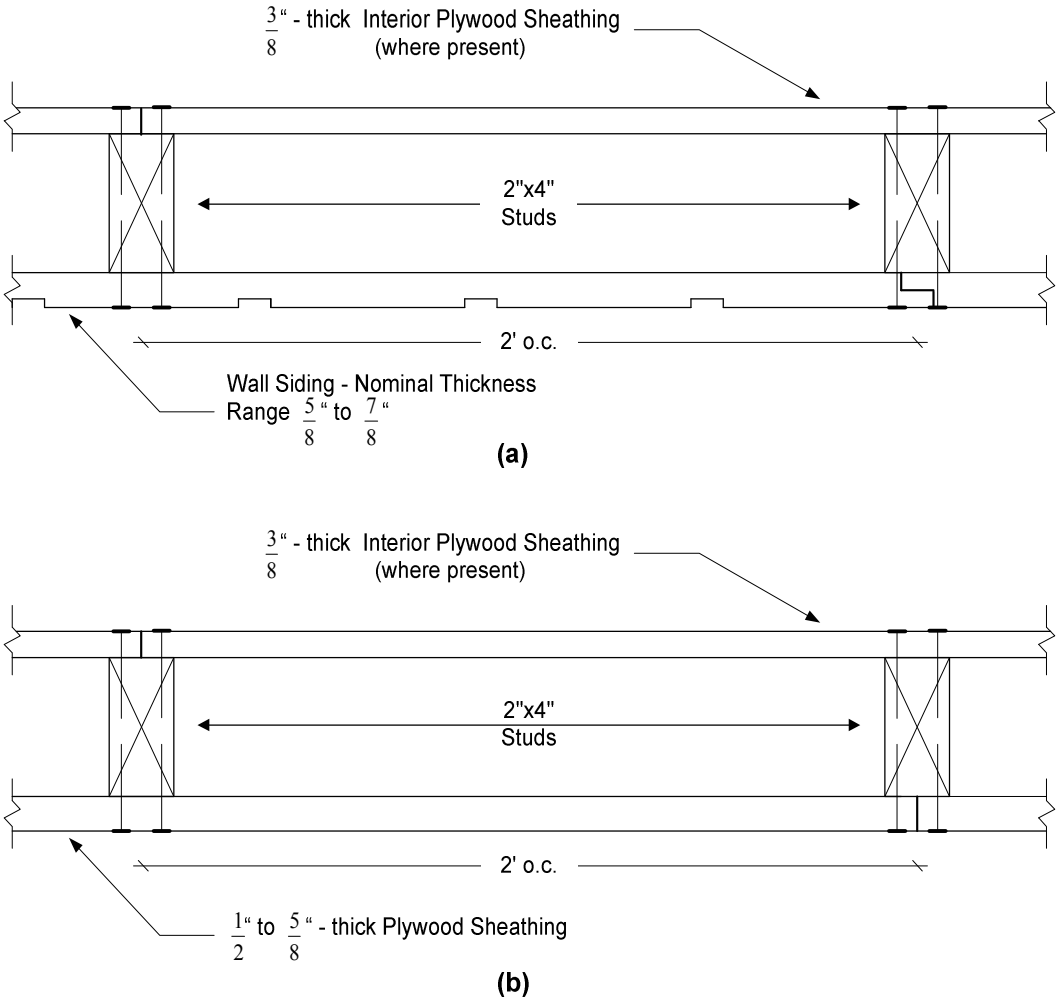

Figure 8.1 – Typical wooden wall construction

Table 8.1 lists material properties used during simulations to generate the fragility curves along with their statistics, with the source from which they were obtained.

Table 8.1 – Material properties used during the simulations

Geometric and Mechanical Properties of Members				
Property	**Value**		**COV**	**Source**
Wall Studs				
Elasticity Modulus, E [psi]	S.P.	1,500,000	0.25	APA
	D.F.	1,500,000	0.25	APA
Specific Gravity, S.G.	S.P.	0.55	0.10	APA
	D.F.	0.53	0.10	APA
Rupture Modulus, MoR [psi]	S.P.	7,984	0.38	Bulleit et.al. 2005
	D.F.	8,016	0.34	Bulleit et.al. 2005
Nails				
Diameter, D [in.]	6d	0.113	0.05	APA
	8d	0.131	0.05	APA
Bending Yield Strength, F_{yb} [psi]	100,000		0.10	NDS
External Sheathing				
Effective Thickness, t_{ext} [in.]	1/2	0.47	0.05	APA
	5/8	0.59	0.05	APA
Effective Area, A_{ext} [in^2]	1/2	9.17	0.05	APA
	5/8	9.32	0.05	APA
Moment of Inertia, I_{ext} [in^4]	1/2	0.27	0.05	APA
	5/8	0.48	0.05	APA
Elasticity Modulus, E [psi]	1/2	1,500,000	0.25	APA
	5/8	1,500,000	0.05	APA
Internal Sheathing				
Thickness, t_{int} [in.]	3/8	0.34	0.05	APA
Area, A_{int} [in^2]	3/8	5.228	0.05	APA
Moment of Inertia, I_{int} [in^4]	3/8	0.108	0.05	APA
Elasticity Modulus, E [psi]	3/8	1,500,000	0.25	APA

8.2 Analytical Wall Model

A methodology proposed by Bulleit et al. (2005) is used to asses the stability of the wall structure. The wall section is assumed to behave similarly to an I-beam resting on elastic supports. The analog beam-spring model is shown in Figure 8.2. The model provides tools for considering the rotational stiffness provided by the partial restraints at the top and bottom plates. The wall studs are the webs while the flanges are composed of

the sheathing panels. The section formed by sheathing, the stud, and the connectors is referred to as the partially composite member (PCM). Since the sheathing is nailed to the stud, absolute transferal of the shear flow between elements of the PCM cannot be assumed. Instead, an effective bending stiffness is calculated using the transformed area method and the parallel axis theorem.

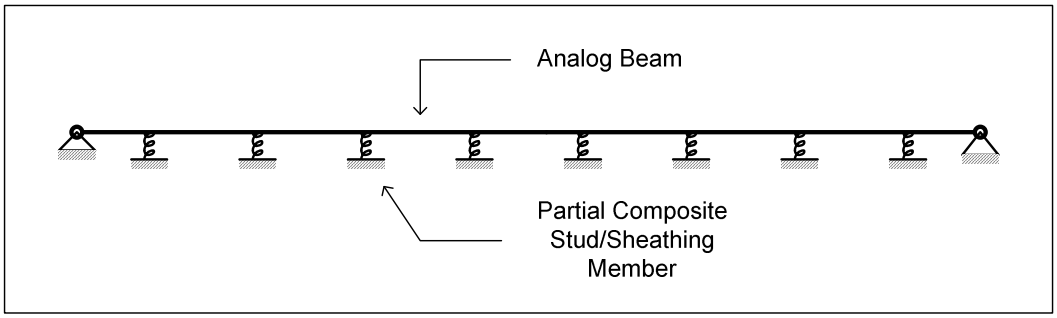

Figure 8.2 – Analog beam-spring model

The reduced axial stiffness of the sheathing members, $\overline{EA}_S$, can be determined using Equation 8-1:

$$\overline{EA}_{Si} = \frac{EA_{Si}}{1+10\dfrac{EA_{Si}}{\left(\dfrac{K_{ni}}{S_{ni}}\right)G_{psi}^2}} \tag{8-1}$$

where EA_{Si} is the axial stiffness of the panel, i=1 for external and i=2 for internal panels. K_{ni} is the load/slip ratio of the fastening nails, S_{ni} is the average spacing of the nails, and G_{psi} is the gap spacing of the sheathing along the length of the stud.

The load/slip ratio is calculated from:

$$K_{ni} = 96{,}000 G^{1.5} d^{0.8} \tag{8-2}$$

where G is the specific gravity of the wood member containing the nail tip and d is the dowel diameter, in inches. The equation is unit sensitive, returning the load/slip ratio in lbs/in. This equation is converted from the Eurocode-5 equation for dowels installed without pre-drilling. In its original form (Eurocode-5, 1994):

$$K_{ni} = \frac{\rho^{1.5} d^{0.8}}{25} \tag{8-3}$$

where ρ is the wood density in kg/m^3 and d is the diameter of the fastener in mm. The result of Equation 8-3 is in N/mm.

Once the reduced axial stiffness of the sheathing is calculated, the total transformed axial stiffness of the PCM can be calculated from Equation 8-4:

$$\overline{EA} = EA_{ST} + \overline{EA}_{S1} + \overline{EA}_{S2} \tag{8-4}$$

where EA_{ST} is the axial stiffness of the stud. Having the axial stiffness of all of the PCM components, the neutral axis of the newly formed section, $\bar{y}$, can be determined as follows:

$$\bar{y} = \frac{h_1 \overline{EA}_{S1} + h_2 \overline{EA}_{S2}}{\overline{EA}} \tag{8-5}$$

where h_1 and h_2 are the distances from the stud centroid to the external and internal panel centroids, respectively.

Once the PCM centroid is known, the parallel axis theorem can be applied for obtaining the effective bending stiffness of the composite section.

$$EI = EI_u + EA_{ST}(\bar{y})^2 + \overline{EA}_{S1}(h_1 - \bar{y})^2 + \overline{EA}_{S2}(h_2 - \bar{y})^2 \tag{8-6}$$

In Equation 8-6, EI_u represents the sum of the bending stiffness of the individual PCM

components (stud and sheathing). The effective moment of inertia of the PCM can then be obtained by dividing the flexural stiffness of the PCM by the elasticity modulus of the stud, E_{ST} :

$$I_{EFF} = \frac{EI}{E_{ST}} \tag{8-7}$$

Modeling the PCM element as beam supported at the ends by rotational springs of identical properties, one can calculate the maximum centerline deflection, Δ_{PCM}, and the maximum moment, M_{PCM}, from Equations 8-8 and 8-9, respectively.

$$\Delta_{PCM} = \frac{WL^4}{384EI}\left(\frac{10+B}{2+B}\right) \tag{8-8}$$

$$M_{PCM} = \left[\frac{EI}{L^2}\left(\frac{96+16B}{10+B}\right)\right]\Delta_{PCM} \tag{8-9}$$

In the above equations, W is the transverse uniform load on the PCM, generated by wind suction, per unit length. L is the wall height. B is a constant which considers the effects of the rotational restraints on the wall supports given by:

$$B = \frac{K_r L}{EI} \tag{8-10}$$

K_r is the rotational spring constant of the end supports, randomly selected during simulation from one of the six values (0, 6, 15, 50, 100, 150 kip-in/rad) given by Bulleit et al. (2005).

After calculating the maximum moment acting on the PCM, the maximum stress on the wall stud can be determined by adding both the axial stress and the flexural stress on the wall as follows:

$$\sigma = \frac{P_{ST}}{A_{ST}} + \frac{M_{PCM} C}{I_{EFF}} \tag{8-11}$$

In Equation 8-11, A_{ST} is the cross sectional area of the wall stud, C is the distance from the centroid of the I-beam to the extreme fiber of the stud, and P_{ST} is the load transferred from the roof-to-wall connection to the stud. This last component was previously calculated in Chapter 7. When the calculated stress in any given stud exceeds the modulus of rupture of that stud, the failure is assumed. The implementation of the mathematical model is explained in the next section.

8.3 PCM Model Evaluation

From sensitivity studies on the beam-spring wall model, Liu and Bulleit (1995) established the system failure criteria given in Table 8.2. The parameters in this table are defined based on the spring load-deformation curve presented in Figure 8.3. The yield and post-yield points for typical wood shear walls coincide and a value of θ equal to 1 is considered reasonable (Bulleit et al. 2005). One may recall that in the analysis of the wall structure, the failure is defined similar to that of roof-to-wall connections, making this a fail or safe proposition. Using the more relaxed deflection limits, the failure criteria will be based on four adjacent studs. A sensitivity study by the author on the failure criteria did not exhibit significant differences in the overall fragility when using failure limits of three and four adjacent studs.

Figure 8.4 depicts the process by which the PCM model was used during damage simulations. The material properties listed in Table 8.1 were used. The flowchart

assumes that the studs to wall plate connections are fully secured. It became evident following simulations that for a typical residence, wall system would not fail under these conditions. That is because the rupture modulus of the wood is high enough to endure the most demanding load combination applied during the simulation. A more realistic model combining the effects of studs to wall plates connections and the PCM model was then examined. The results are discussed in Section 8.4.

Table 8.2 – System failure criteria[1]

Hardening Parameter η	Ultimate Deflection Limit λ	Resistance Parameter θ	System Failure Criteria [1]
$0 \le \eta \le 0.1$	$2 \le \lambda \le 4$	$0 \le \theta \le 0.5$	Any two
$0 \le \eta \le 0.1$	$2 \le \lambda \le 4$	$0.5 < \theta \le 0.7$	Any three
$0 \le \eta \le 0.1$	$2 \le \lambda \le 4$	$0.7 < \theta \le 1$	Adjacent three [2]
$0 \le \eta \le 0.1$	$2 \le \lambda \le 4$	$0 < \theta \le 0.3$	Any two
$0.1 \le \eta \le 0.2$	$2 \le \lambda \le 4$	$0.3 < \theta \le 0.5$	Any three
$0.1 \le \eta \le 0.2$	$2 \le \lambda \le 4$	$0.5 < \theta \le 0.7$	Adjacent three
$0.1 \le \eta \le 0.2$	$2 \le \lambda \le 4$	$0.5 < \theta \le 1$	Adjacent four [3]

[1] System failure is based on yielded members.

[2] When $\theta = 1$ and $3 \le \lambda \le 4$, yielding of adjacent 4 members is system failure criterion.

[3] When $0.7 < \theta \le 1$ and $2 \le \lambda \le 3$, yielding of adjacent 4 members is system failure criterion.

[1] Adapted from Liu and Bulleit (2005)

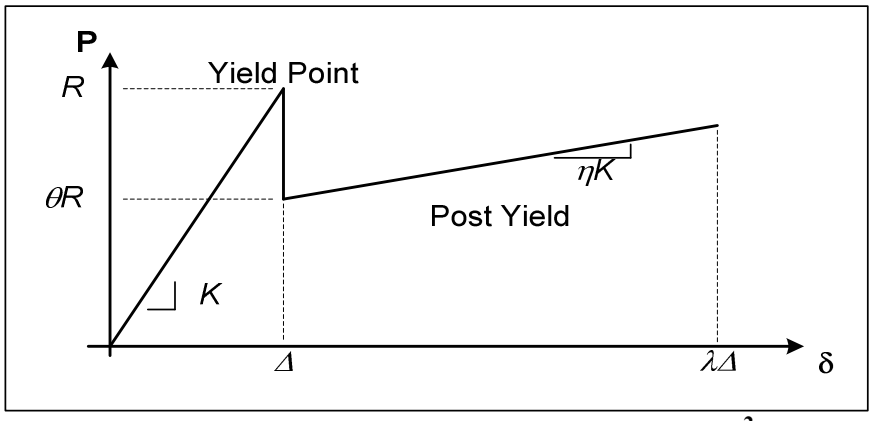

Figure 8.3 – Spring Load-Deformation Curve[2]

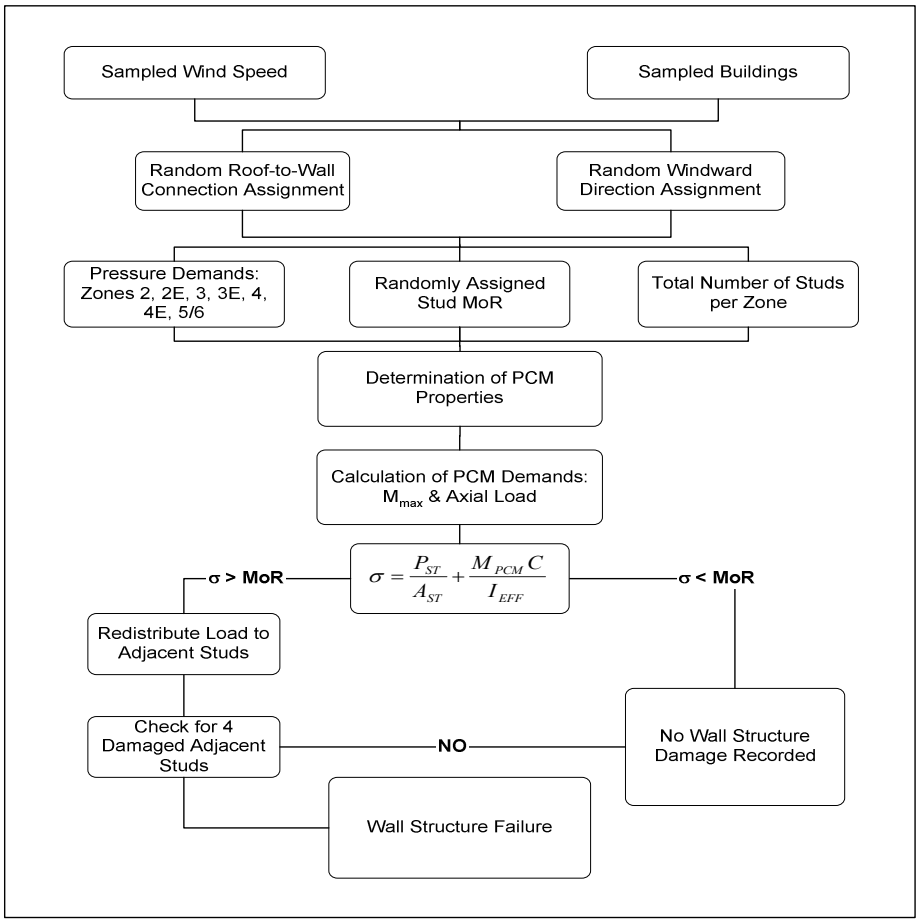

Figure 8.4 – Flowchart of PCM damage simulation

[2] Adapted from Liu and Bulleit (2005)

8.4 Wall Stability Model

In the PCM model evaluation of Section 8.3, it was implicitly assumed that the end-stud connections are resilient to all loads. As with any structural assembly, the connections between members are instrumental in transferring loads from the components down to the foundation. The connection of the wall stud to the wall plate and the sill beam needs to transfer both the axial load from the roof uplift and the transverse load generated by the suction load in the wall sheathing. From the field survey, it was observed that these connections are usually made using metal connectors, although in rare cases the joints may be simply toe-nailed. In unusual cases both the connector and three toe-nails are present, although at least one toe-nail is usually used.

The capacity of the metal connectors can be defined conservatively by the number of nails used for the fastening of the strap and the loading type, be it withdrawal or shear. Most of the connectors provide holes for using four nails per member connected. However, in many cases only three nails are used. The general case for the simulations is defined by having 40 percent of metal connectors fastened with 3 nails and 60 percent with 4 nails. Figure 8.5 shows various stud-to-sill beam configurations.

The withdrawal capacity of the nails is determined in accordance with the National Design Specifications for Wood Construction (NDS, 2003):

$$W' = 1380 G^{5/2} D\, l \tag{8-12}$$

G is the specific gravity of the main wood member, D is the dowel diameter, and l is the nail penetration into the main member. The statistics of parameters used were presented in Table 8.1.

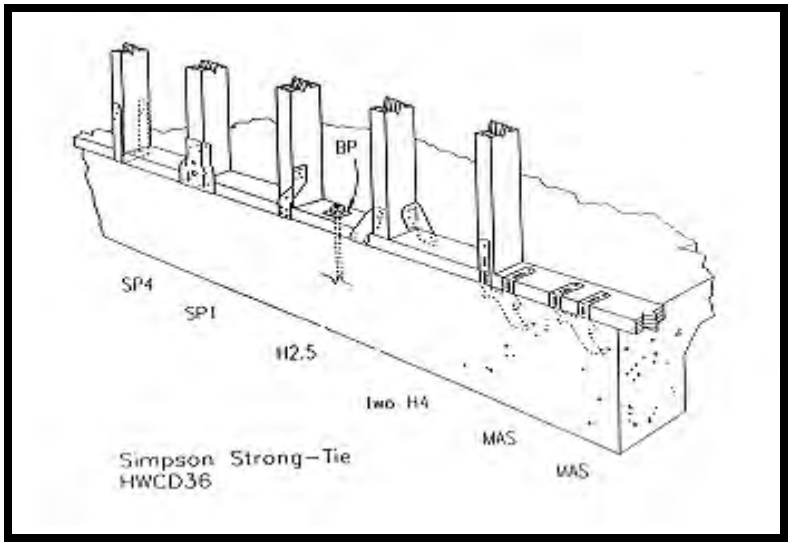

Figure 8.5 – Various stud-to-sill beam connectors[3]

The interaction between the fastener loading in shear and withdrawal is accounted for by using the following equation from the NDS (2001):

$$Z'_{\alpha} = \frac{(W'_p)Z'}{(W'_p)\cos(\alpha) + Z'\sin(\alpha)} \tag{8-13}$$

W'_p is the allowable withdrawal capacity of the fastener defined by Equation 8-12. Z' is the allowable shear capacity of the fastener calculated from the yield limit theory (Table 8.3). Parameter α is the angle between the stud and the vector additions of the loads acting on the connector. The results are multiplied by a safety factor of 3.5 (Cope 2004).

The simulation engine starts by calculating the demands on the connectors. The reactions from the roof-to-wall connections and the transverse loading generated by the suction of the wall elements are determined. Each stud is marked safe if neither the PCM model nor the connection model fail. Once again the failure of four adjacent studs will

[3] Adopted from FEMA (1999)

signify the wall loss. Figure 8.6 depicts the complete flowchart for wall stability analysis.

Table 8.3 – Yield limit equations for shear capacity of fasteners[4]

Yield Mode	Yield Limit Equation	Parameter Definition
I_m	$Z_{I_m} = \frac{D l_m F_{em}}{R_d}$	D = dowel diameter [in.]
I_s	$Z_{Is} = \frac{D l_s F_{es}}{R_d}$	F_{yb} = dowel bending yield stress [psi]
II	$Z_{II} = k_1 \frac{D l_s F_{es}}{R_d}$	R_d = reduction term (2.2)
III_m	$Z_{III_m} = k_2 \frac{D l_m F_{em}}{(1+2R_e)R_d}$	F_{em} = main member dowel bearing stress [psi]
III_s	$Z_{IIIs} = k_3 \frac{D l_s F_{em}}{(2+R_e)R_d}$	F_{es} = side member dowel bearing stress [psi]
IV	$Z_{IV} = \frac{D^2}{R_d}\sqrt{\frac{2F_{em}F_{yb}}{3(1+R_e)}}$	$R_e = F_{em}/F_{es}$
Auxiliary Parameters		l_m = main member dowel bearing length [in.]
$k_1 = \frac{\sqrt{R_e + 2R_e^2(1+R_t+R_t^2)+R_t^2R_e^3} - R_e(1+R_t)}{1+R_e}$		l_s = side member dowel bearing length [in.]
$k_2 = -1+\sqrt{2(1+R_e)+\frac{2F_{yb}(1+2R_e)D^2}{3F_{em}l_m^2}}$		$R_t = l_m/l_s$
$k_3 = -1+\sqrt{\frac{2(1+R_e)}{R_e}+\frac{2F_{yb}(1+2R_e)D^2}{3F_{em}l_s^2}}$		k_1, k_2, k_3 = auxiliary parameters

The simulation runs predicted losses for the general case starting at 150 mph 3-second gust wind speed which will roughly correspond to category 2 hurricanes (Section 3.1). As it was the case for the roof-to-wall connections, the fragility of the wall system

[4] Adopted from NDS for Wood Construction (2001)

is a yes or no proposition. The fragility curves for the total damage states in Figure 8.7 emphasize the importance of using metal straps at stud-to-wall plate connections. When only toe-nails are used, the losses start at 130 mph and all systems are lost after 180 mph. However, using both toe-nails and metal connectors, the fragility curve will shift to the right so much, that only a category 5 hurricane can damage the wall system.

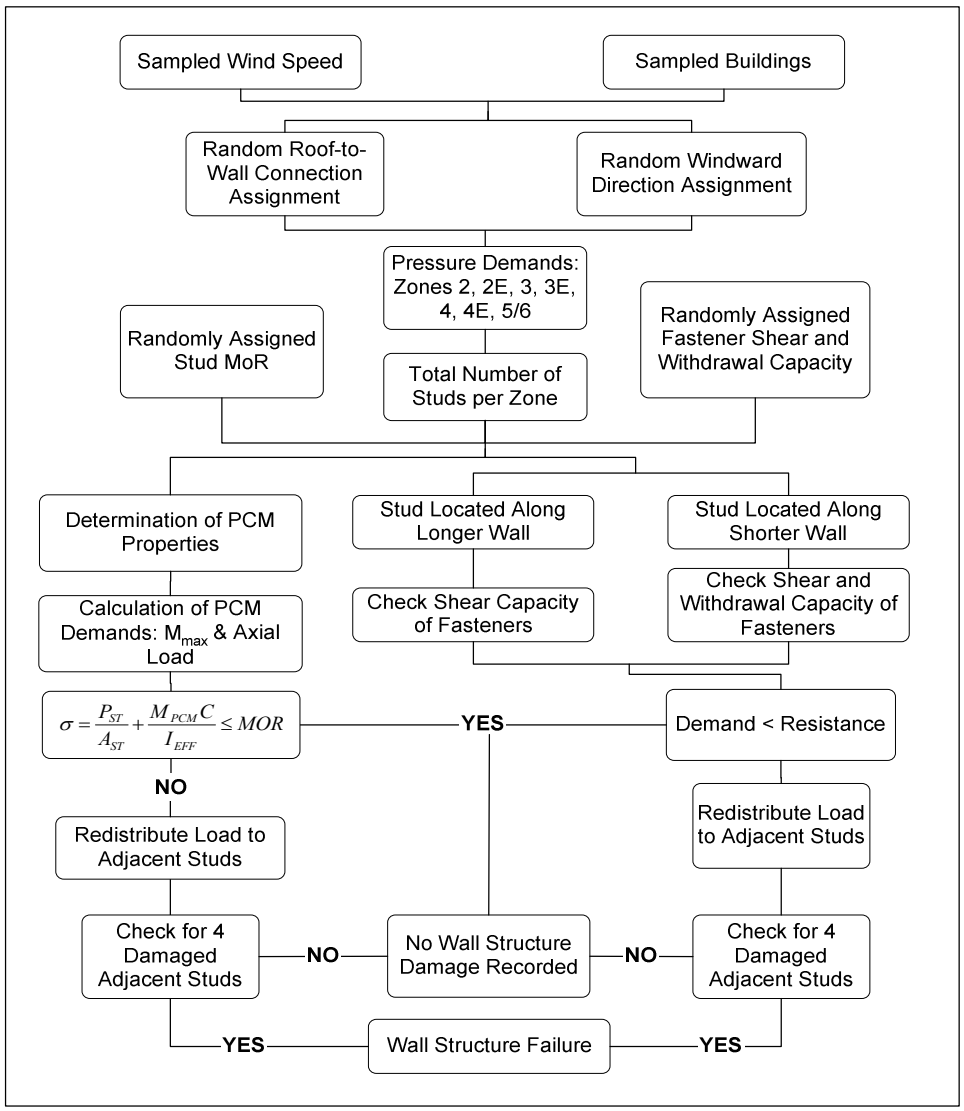

Figure 8.6 – Flowchart for simulating wall system fragility

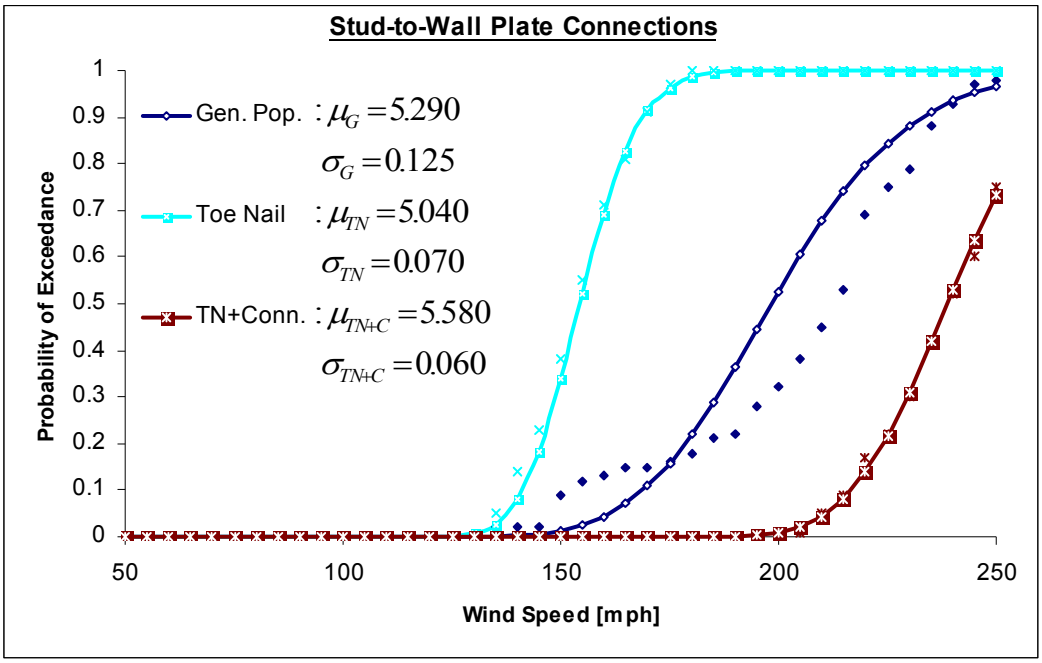

Figure 8.7 – Wall system fragilities

8.5 Wall Sheathing Fragility

The C&C external pressure coefficients are used to calculate shear demands on wall sheathings. The number of panels considered in the simulation is determined by subtracting the window width from the wall length and then dividing the result into an integer number of panels. The capacity for each panel is calculated by adding the shear capacities of the nails connecting that panel to wall studs. In equation form:

$$V = 3.5 n C_D Z \tag{8-14}$$

The factor 3.5 is the safety factor adopted from Cope (2004). The shear capacity of the nails, Z, was previously given in Table 8.3. C_D is the load duration factor taken as 1.6 for wind loads, and n is the total number of nails in the diaphragm. The framing factor, C_{fr}, and the diaphragm action factor, $C_{d,i}$, are assumed to cancel each other. All other

adjustment factors specified by the NDS are set equal to 1. The spacing of the nails is assumed to be 8-in on center. Figure 8.8 shows the steps followed in simulating the wall sheathing fragilities. No failures were recorded during these simulations.

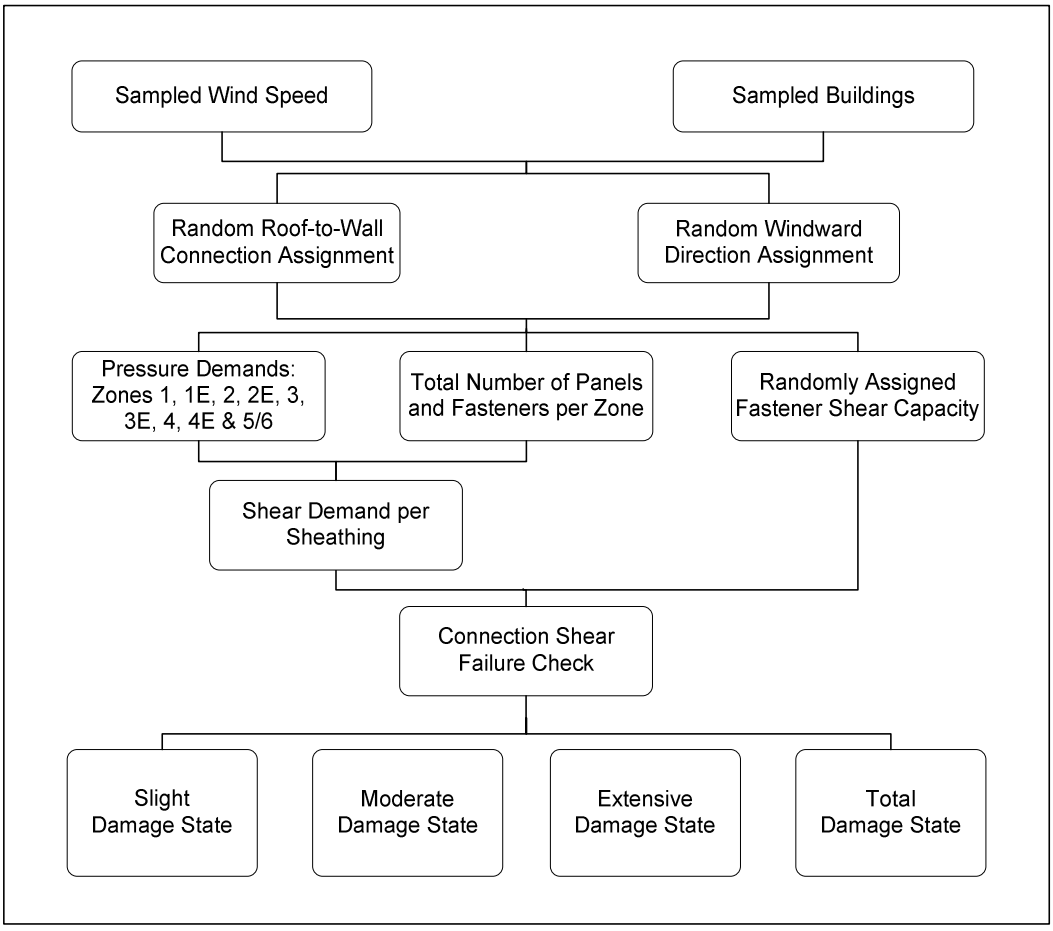

Figure 8.8 – Flowchart for simulating the fragilities of wall sheathings

CHAPTER 9

WALL OPENINGS

9.1 Introduction

Although windows are not structural components, indirect losses resulting from them could be quite severe. Examples include water damages to the inside walls and loss of contents. The windows used in all wood-zinc houses have similar characteristics. Glass louvered windows are used in the front entrance. Aluminum louvered windows are used in the sides and in the back. The placement of windows tends to be symmetric, counting the same number of windows in opposing walls.

In general, the uniform pressure demands on all wall openings are calculated based on the C&C external pressure coefficients. What sets windows apart is the damage caused by debris. Several key assumptions are made to complete the simulations. First, the type and number of screws used to install a window is batch selected for each house. Second, possible changes in internal pressure coefficients are ignored. Third, based on our field surveys and historical data, the doors are considered secured enough not to be pulled out at any loads. Fourth, the capacity of a window frame to resist uniform wind

pressures equals the shear capacities of the fasteners connecting it to the wall studs. Last, the effects of the debris are considered for the windows in the front wall and one of the side walls. This is a conservative assumption for covering the wind directions at an angle to the front wall.

9.2 Modeling Uniform Pressure Effects

The window frames are fastened to the wall studs using wood screws. The wood screws are typically supplied by the windows manufacturer. However, based on an informal survey conducted by the author, those screws are not used in all cases. Many small time contractors prefer the gypsum board or drywall screws because of their ease of application, even though their capacities are considerably lower.

The previously stated assumption that the capacity of the windows under uniform wind pressure is controlled by the shear capacity of the fasteners connecting the window frames to studs is consistent with the limited historical data available on the subject. Taking this into account, several tests were conducted in order to obtain upper and lower limits for the shear capacity of the commonly used fasteners. The specimens tested were similar to those shown in Figure 9.1. The drywall screws, which had a 1/8-in diameter, provided an average shear capacity of 800 lbs. The shear strength for the 3" long wood screws with a ¼-in diameter was 2,475 lbs. Consistent with all material properties, a *COV* of 0.2 is assumed. In our field survey, the number of fasteners used with each window frame varied between four and six, independent of the window size or the type of screws used.

(a) Dry Wall Screw (1/8" diameter) **(b) Wood Screw (1/4" diameter)**

Figure 9.1 – Types of screws used with window frames

During the simulations, the pressure demands on each window are calculated based on C&C external pressure coefficients listed in Table 3.4. The number of windows on each wall was obtained from the existing database on wood-zinc structures (Table 2.2). The number of connectors for window frames is randomly generated and it varies between 4 and 6 fasteners per window. At each wind speed, the number of failures are counted and combined with the results from the impact model, making sure that a window is not counted twice. The end results are compared against the limits in Table 1.1, and the corresponding damage state is identified.

9.3 Modeling Impacts from Debris

Airborne debris is the main cause of damages to both windows and window frames. A simple model used by Cope (2004) in her studies gives the likelihood of a window being struck and damaged by debris as:

$$p_D(w) = 1 - \exp\left(-A \cdot N_A \cdot B \cdot C \cdot D\right) \quad (9\text{-}1)$$

In the above equation, w is the 3-second gust wind at which the damage probability, $p_D(w)$, is evaluated. Parameters A and N_A are directly related to the number of potential missiles in the air during an extreme wind event. The parameter B is the percentage of the airborne debris that actually hit the house. The parameter C is the fraction of wall space covered by windows per wall. The parameter D indicates whether a successful window hit is strong enough to cause damages.

The parameter A is modeled using a normal cumulative density function, with an average 3-second wind gust velocity of 135 mph and a standard deviation of 15 mph. The function achieves its peak value of 1.0 around the 170 mph mark, meaning that at that time all potentially available missiles are airborne. The values taken by the A parameter as a function of the wind speed are depicted in Figure 9.2.

The values for the N_A parameter are related to the construction types and wind exposure categories. The louvered glass windows used in the Island are different from window types considered by Cope in that one impact can cause the loss of a few glass panels but not necessarily the entire window. In addition, for security reasons, metal cages are often installed in front of glass windows, further impeding the path of the debris. On these bases, the value assigned to the N_A parameter is lowered to 50 from the 100 suggested by Cope (2004). Because the number of potential missiles capable of damaging an aluminum window is much less than those able to destroy a glass window, the N_A parameter for aluminum windows is set at 3.

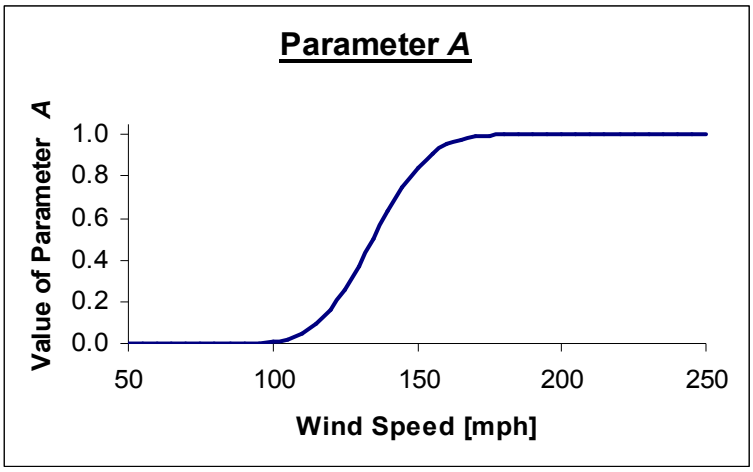

Figure 9.2 – Values of Parameter *A* used in the missile impact model

The parameter *B* in Equation 9-1 is modeled based on the premise that higher wind velocities would imply longer flight time and travel distance for the debris. Cope (2004) approximated the *B* parameter as a linear function of the wind speed, with values of 0 and 0.40 corresponding to 50 mph and 250 mph, respectively. The *C* parameter which is the fraction of wall space covered by windows is determined from our database on wood-zinc structures.

Recognizing that the momentum of the debris exceeds the impact capacity of the glass window by more than 37 times, Cope defined the D parameter as a normal cumulative distribution function with a mean of 70 mph and a standard deviation of 10 mph (Cope, 2004). The parameter is plotted in Figure 9.3.

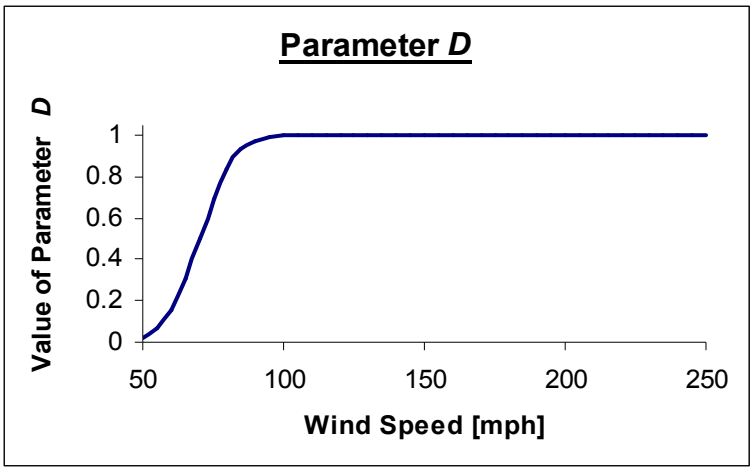

Figure 9.3 - Values of Parameter *D* used in the missile impact model

For the fragility analysis, the existing database on wood-zinc houses was utilized to calculate the average number of aluminum windows for the side walls at 3.0 windows with a *COV* of 0.2. The openings to wall areas have an average ratio of 0.19 with a *COV* of 0.37. The number of glass windows in the font wall was constant at 2. The openings to wall areas have an average ratio of 0.17 and a *COV* of 0.32. The sampled statistics for the back walls were taken the same as the front wall.

9.4 Windows Fragility

The fragility of the windows is determined by comparing random demands generated by 3-second gust speeds and the corresponding sampled limit states. The model combines uniform pressure effects and impacts from debris. The general procedure followed during the simulation is depicted in Figure 9.4. The windows fragility curves are shown in Figure 9.5.

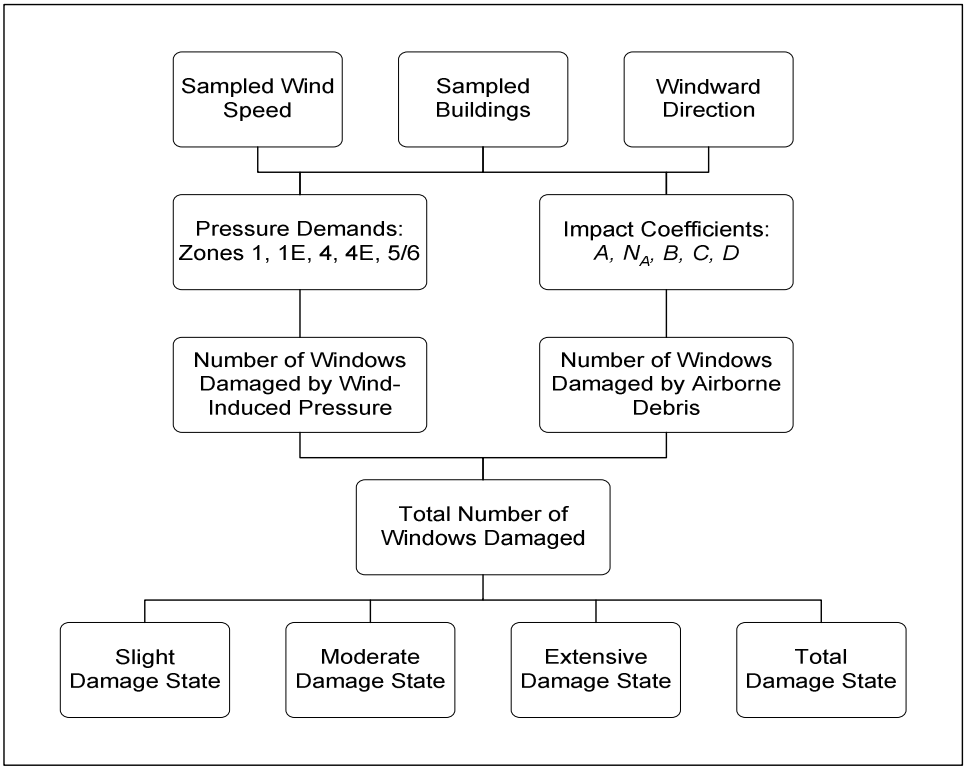

Figure 9.4 – Flowchart of window damage simulation

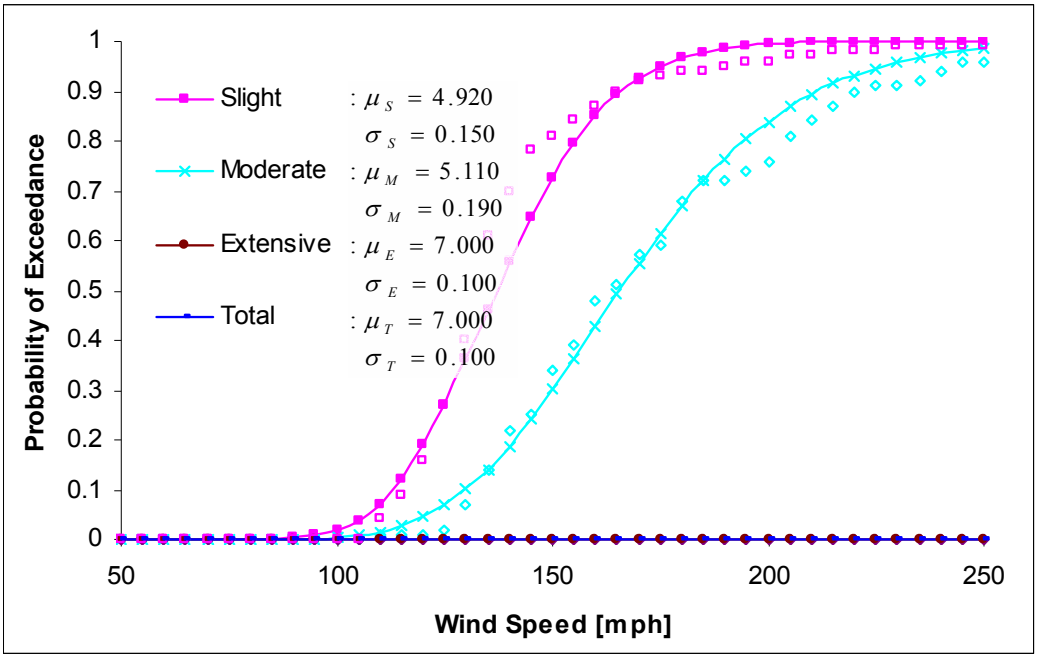

Figure 9.5 – Fragility curve for windows in wood-zinc houses

CHAPTER 10

RESIDENTIAL SYSTEM FRAGILITY

10.1 Introduction

The system fragility is obtained by assigning equal weight to each component defined in the damage matrix. Whichever component assumes the highest damage state, the structure is allocated under that same designation. Four distinct systems are considered when deriving fragilities for wood zinc houses. The weak W-system combines the worst practices in the field as it relates to the roof (12-12-12), roof to wall connections (no metal straps), and wall system (simple toe-nailing of studs to wall plates). The common C-system uses the default fragilities for all components. For zinc sheets on the roof, this will mean 6-in spacing at the edges and 12-in spacing elsewhere (6-12-6). For roof to wall connections and wall systems, random selections of metal straps and toe-nailing described in Chapters 7 and 8 are followed. The pre-engineered C2-systems use the same roof system as the C1-system, but it eliminates the possibility of the selection of weak components from the simulation. The strong S1-system improves on the C-systems by using the best metal straps for roof-to wall and stud-to-wall plate

connections along with the best unretrofitted roof ensemble (6-6-6). The strong S2-system uses the zinc-strap retrofit on the general roof configuration (6-12-6R). The ultimate U-system improves on the S-system by using the 6-6-6R assembly. All cases are evaluated with and without the contribution of window shutters. A sensitivity analysis is also performed for identifying critical components in the structural assembly.

10.2 Combination Algorithm

During the simulation, the damage progression for each component is recorded for all wind speed increments. A fragility identification number, I_{fc}, is assigned to each component having values ranging from 0 to 4. For each building at any given wind speed, I_{fc}, is read for each component and the highest value is recorded. The components for which no damage, slight, moderate, extensive, and total damage states exist can give a value of 0, 1, 2, 3, or 4, respectively. The components whose damage state is defined by a yes or no proposition give either 0 or 4 values. At each wind speed, all I_{fc} with values of 1 are counted towards the slight damage state. All I_{fc} values of 2 are counted towards the moderate and slight total damage state, and so forth. An I_{fc} value of 4 would account for every one of the damages states from total through slight. Figure 10.1 depicts a flowchart showing the selection process for the system fragility identification number, I_f. Note that the algorithm requires the wind speeds, the building selection, house orientation, and component capacities to be the same for each specific case during the simulation in order to be able to evaluate the system fragility correctly.

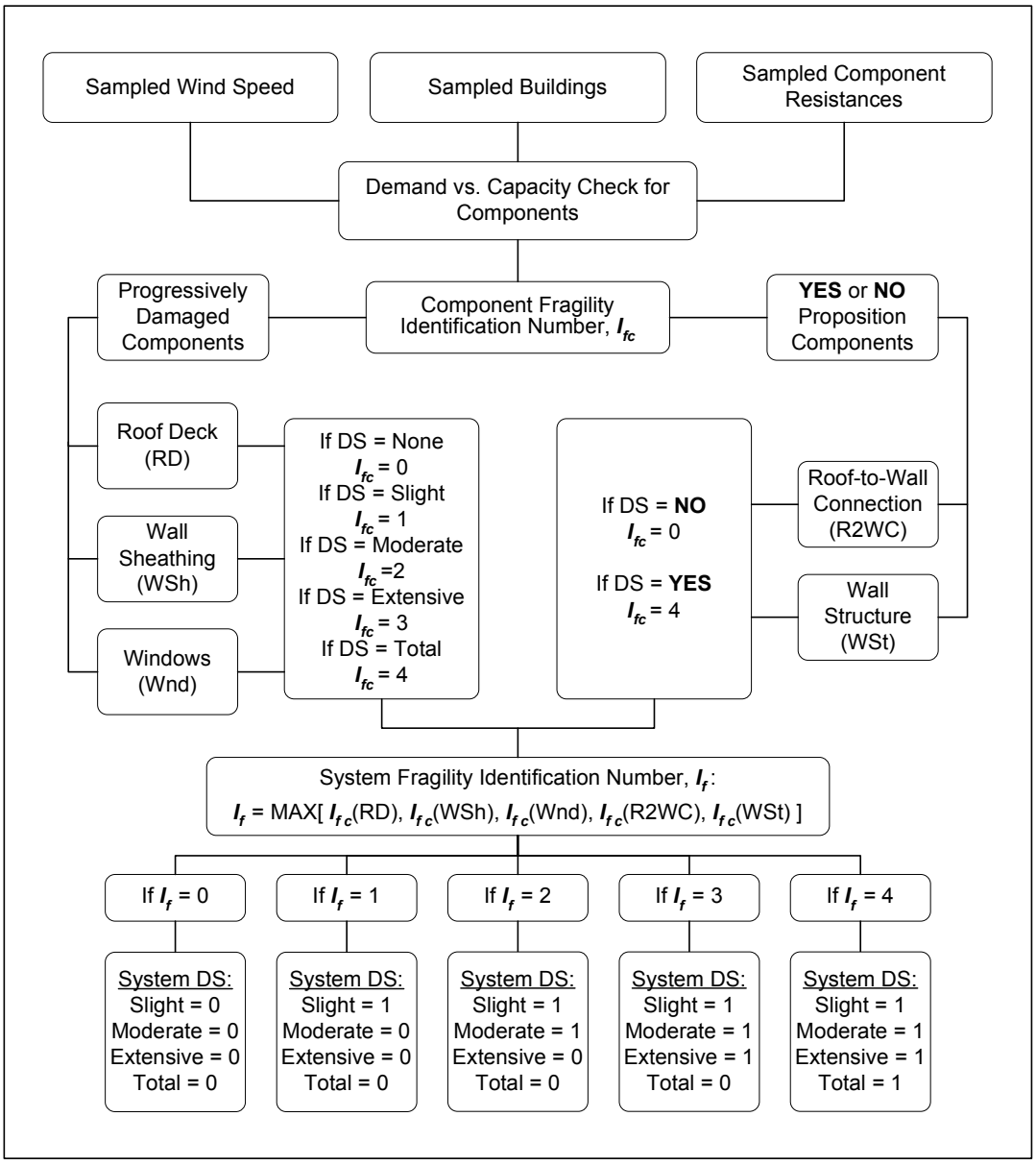

Figure 10.1 – Flowchart of system fragility evaluation

10.3 Weak System Fragility

The weak system is the worst possible case which could be found in a field survey. It incorporates the most fragile components (12-12-12 roof system and toe-nailed

connections between roof-to-wall connections and wall stud to wall plate). The slight damage state for the system fragility of the W-system is dominated by the roof system, with slight contributions of the roof-to-wall connections and the windows. The other remaining damage states are dominated overwhelmingly by the roof-to-wall connections. In fact, it is as if the damage state translates from minor to total, bypassing the moderate and extensive. This shows the inability of a toe-nailed only connection to secure the roof to wall structure. Since the reliability analysis is based on 3-second gusts, the W-system presents a high risk of being damaged under strong tropical storms and Category 1 hurricanes (as per the Saffir-Simpson scale). These results are consistent with historical data and observations in the Island.

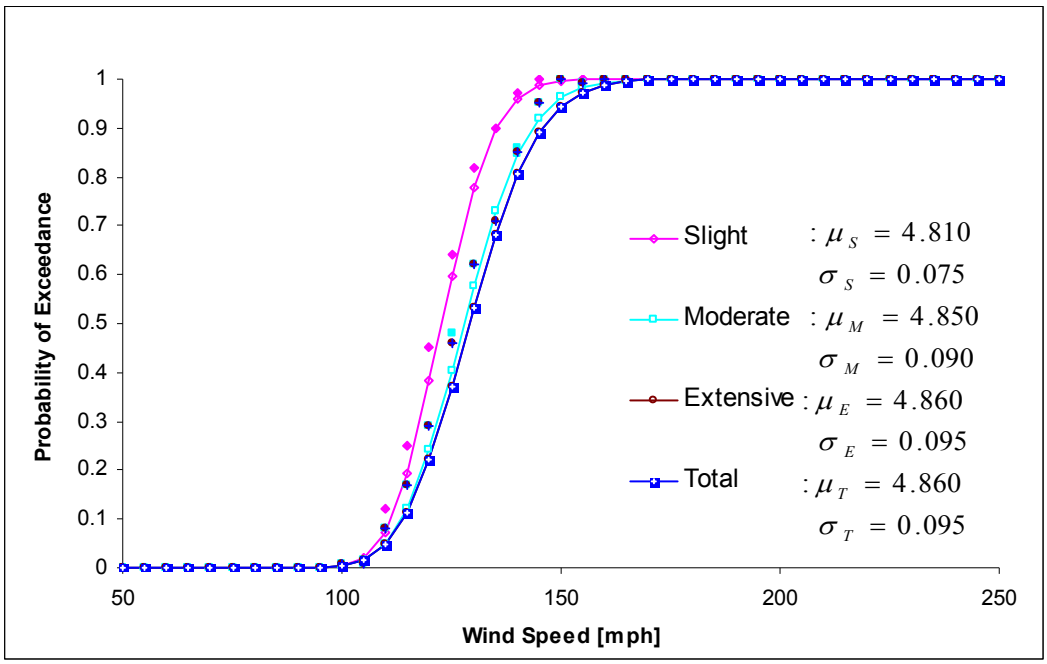

Figure 10.2 – W-system family of fragility curves

For assessing the effects of storm shutters or temporary blockings, the window component was removed from the system fragility analysis. The only appreciable difference between this simulation and the previous one was a slight shift at the slight damage state towards higher wind speeds. No noticeable differences are present in the higher damage states. Figure 10.3 shows the family of fragility functions for the W-system without the contribution of window damages. The small improvement over the original system proves that spending money on storm shutters is not a reasonable investment in such frail systems.

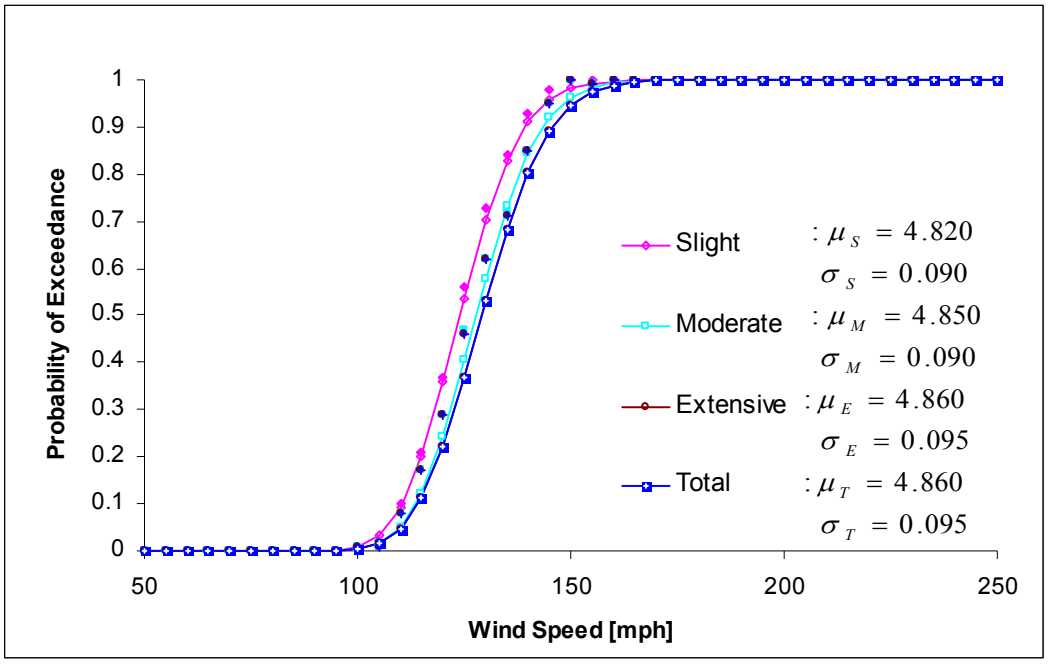

Figure 10.3 - W-system family of fragility curves with window shutters

10.4 Common System Fragility

The C-systems captures the general specimens one can expect to find throughout the Island. The C1-system uses the default 6-12-6 roof assembly, improving on the one used with the weak system. All other components are randomly selected from all available options with appropriate weights, as explained in the previous pertaining chapters. The slight damage state is controlled by the window component. The moderate damage state is dominated by the roof deck performance. The extensive and total damage states are defined by the roof-to-wall connection behavior. Although the C1-systems start recording damages at the same wind speeds as the W-system, the slope of the curves is less steep. This phenomenon is due to the presence of both weak and strong links in the selection pool of components; weaker components start recording early failures as stronger components tend to reduce the steepness of the curves. The curves for the C1-system are shown in Figure 10.4.

The C1-system with window protection showed a considerable improvement in performance over the one experienced by the W-system. The slight and moderate damage states are defined by the roof deck and the roof- to-wall connection performance. The extensive and total damage states are controlled again by the roof-to-wall connection capacity. The shift of the curves for the lower damage states, shown in Figure 10.5, demonstrates that the protection of windows in these systems can reduce greatly the damage expectancy during extreme wind events up to a Category 2 hurricane.

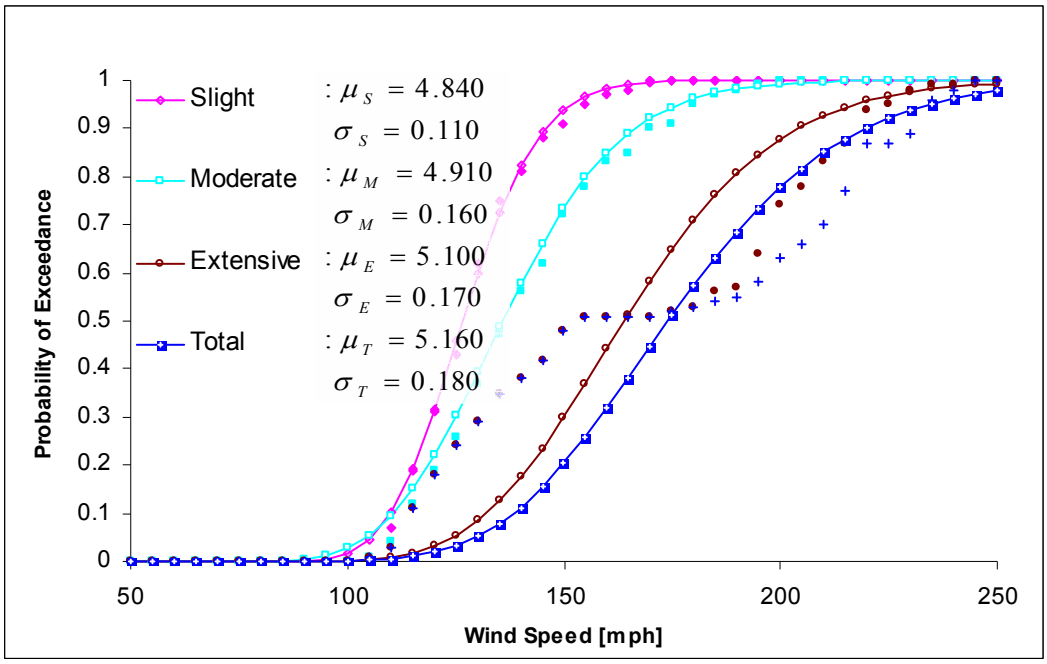

Figure 10.4 – C1-system family of fragility curves

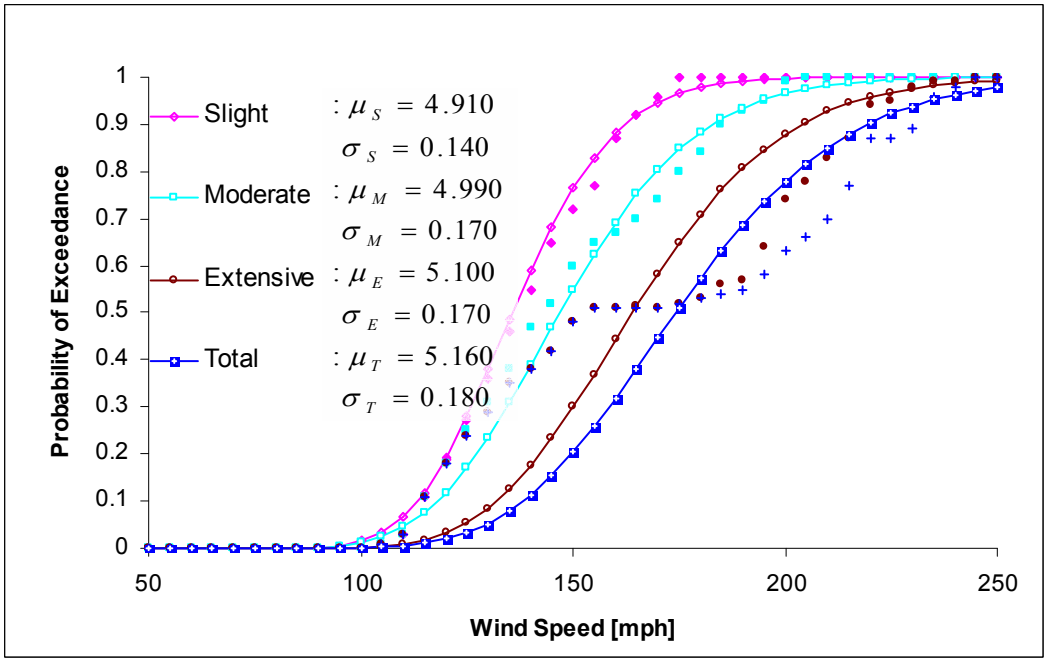

Figure 10.5 – C1-system family of fragility curves with window shutters

The C2-system represents the pre-engineered wood houses in Puerto Rico which exhibit higher construction standards. This is achieved by eliminating the selection of the toe-nailed connections for the roof-to-wall and stud-to-wall plate connections during the simulation. The other components in the simulation are selected as per the C1-system criteria. The slight damage state is controlled by the window damages. The remaining damage states are controlled by the roof deck execution. The performance of these systems is commendable, as no extensive or total failures are predicted by the simulation for hurricanes as high as Category 3. Also, the fact that the roof deck is the controlling component, the retrofitting schemes proposed in Avilés (2006) could prove to be instrumental in optimizing the performance of these wood-box systems. The fragility functions for the C2-system are shown in Figure 10.6.

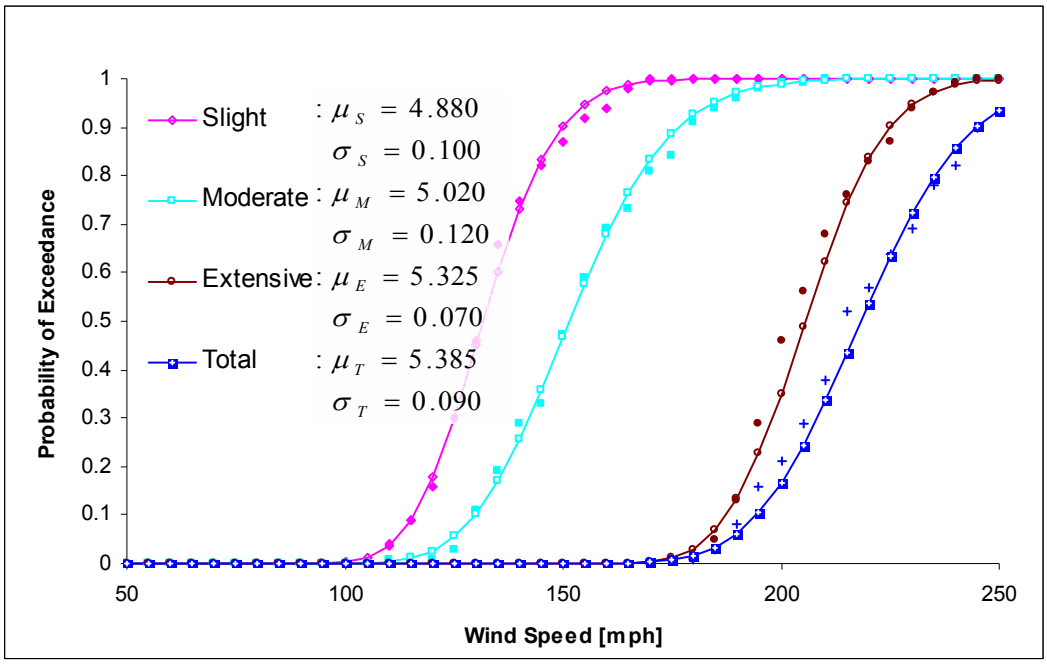

Figure 10.6 – C2-system family of fragility curves

The exclusion of the window component in the C2-systems yields an improvement in the performance on lower wind speeds. All four damage states were defined by the roof system behavior. The reliability analysis shows that with the elimination of the weak components from the structural system and the protecting of windows, only 25 percent of the residences would suffer slight damages and 5 percent moderate damages for wind speeds of 140 mph, which is the design wind speed specified by the UBC-97 for the Island. No extensive or total damages are recorded. Figure 10.7 shows the fragility curves for this system.

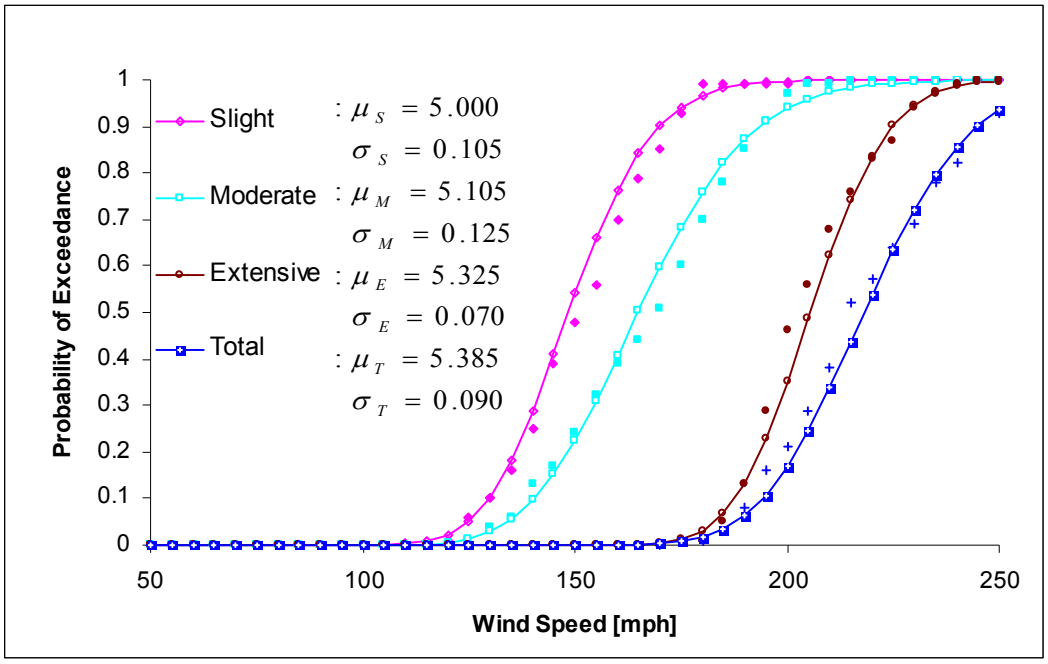

Figure 10.7 – C2-system family of fragility curves with window shutters

10.5 Strong System Fragility

The S1-system represents the case on which all the best connectors and straps are used between various structural components. The roofing is also improved on, as the best unretrofitted system is used during the simulation (6-6-6). As expected, the system fragility for the S1-system is controlled by the window damages in the slight and moderate damage states, with the roof deck controlling over 220 mph. The extensive damages state is defined by roof deck performance. The total damage state limiting component is the stud-to-wall plate connection. There is a substantial improvement from the C2-system, particularly in the higher damage states, as no damages of their type are expected for hurricanes of less than Category 5. Figure 10.8 shows the damage functions for the S1-system.

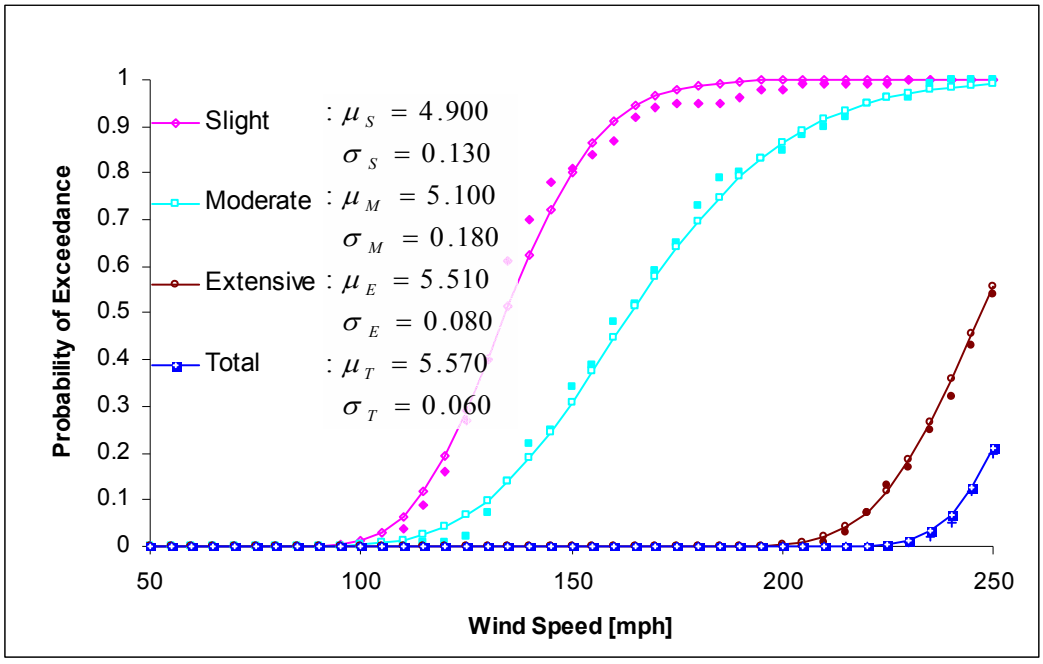

Figure 10.8 – S1-system family of fragility curves

The higher quality systems, similar to the C2-system, receive a considerable improvement in performance whenever the window damages are mitigated. All but the total damage state are being defined by the roof system behavior. The last damage state is again controlled by the stud-to-wall plate connection. The behavior of the system is shown in Figure 10.9.

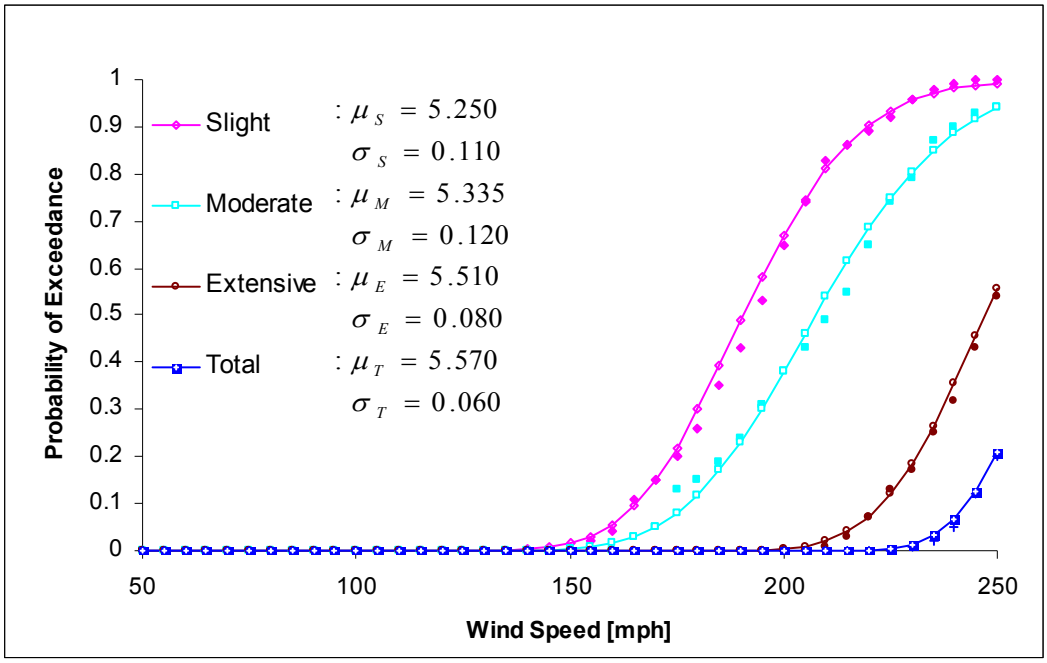

Figure 10.9 – S1-system family of fragility curves with window shutters

Recognizing the dominance of the roof system damage state on the previous systems, the S2-system introduces the retrofitted 6-12-6R assembly. The same component dominance observed for the S1-system is present for this system. The S2-system presents a slight improvement over the S1-system, most noticeable in the

extensive and total damage states. Figure 10.10 shows the family of fragility curves for the S2-system. Figure 10.11 shows the fragility functions for the S2-system with window protection. Notice the improvement on the slight and moderate damage states.

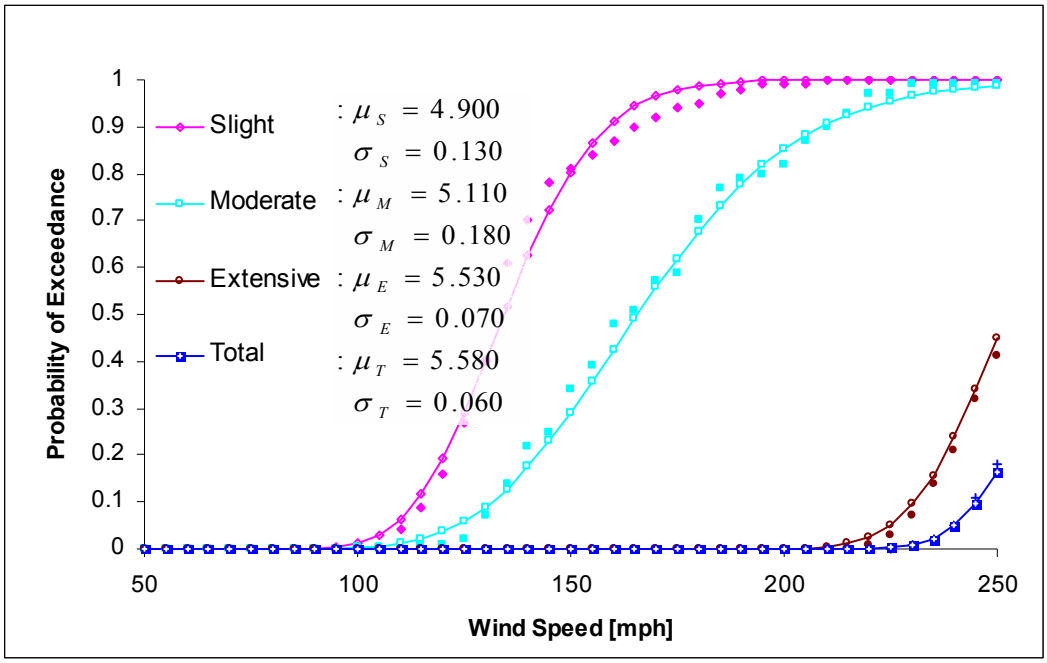

Figure 10.10 – S2-system family of fragility curves

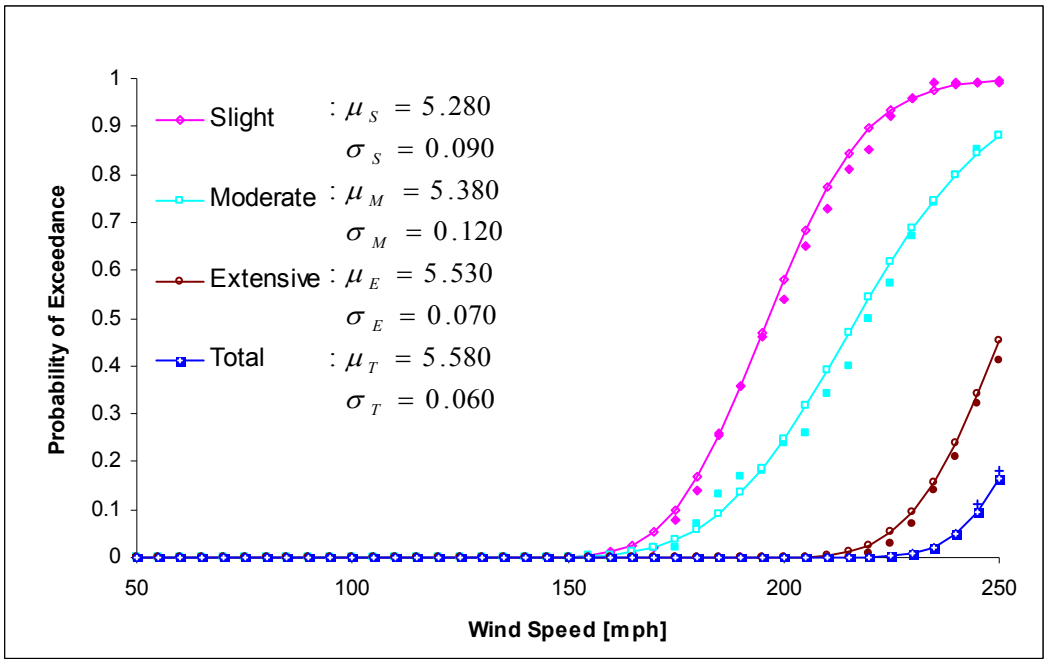

Figure 10.11 – S2-system family of fragility curves with window shutters

10.6 Ultimate System Fragility

The U-system evaluates the performance of a hypothetical ultimate system which includes not only the best connectors considered between components but also the best possible roof assembly (6-6-6R). As with both S-systems, the behavior of the U-system is defined in both slight and total damage states are controlled by the window component performance. The Extensive damage state is defined by the roof deck and the total damage state is controlled by the stud-to-wall plate connection. No extensive or total damages are recorded before 190 mph wind gusts. As with the S-systems, the U-system benefits greatly from window protection. Figure 10.12 shows the behavior of the U-system without window protection.

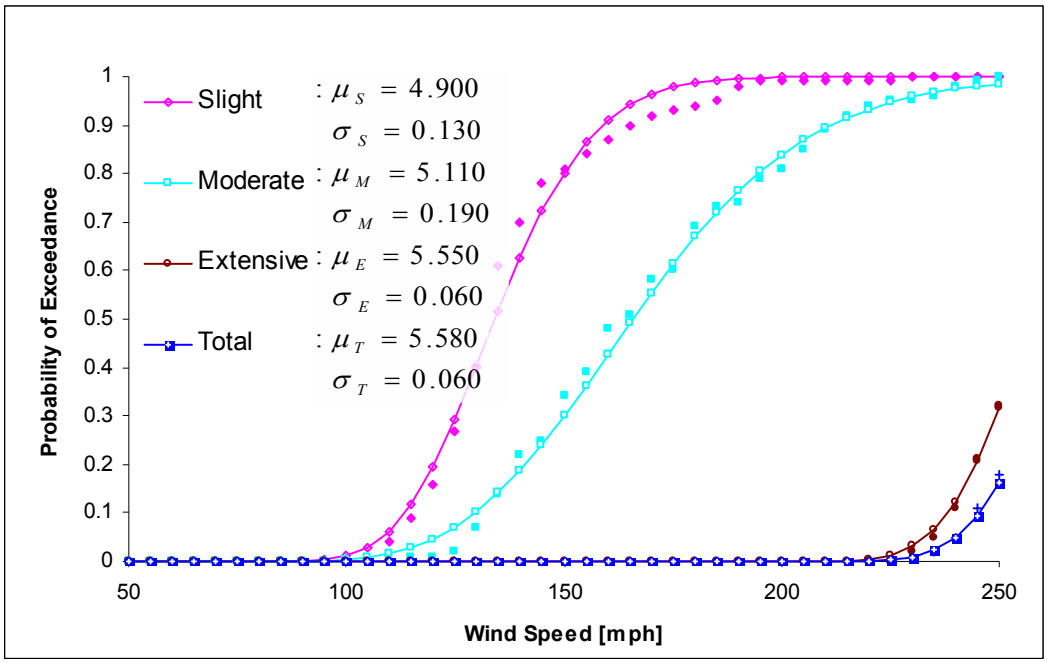

Figure 10.12 – U-system family of fragility curves

With window protection in place, the behavior of the U-system surpasses all other systems. The damage states are controlled by the roof assembly performance except for the last one, which is defined by the stud-to-wall plate connections. The fragility curves for the U-system without the window component are shown in Figure 10.13.

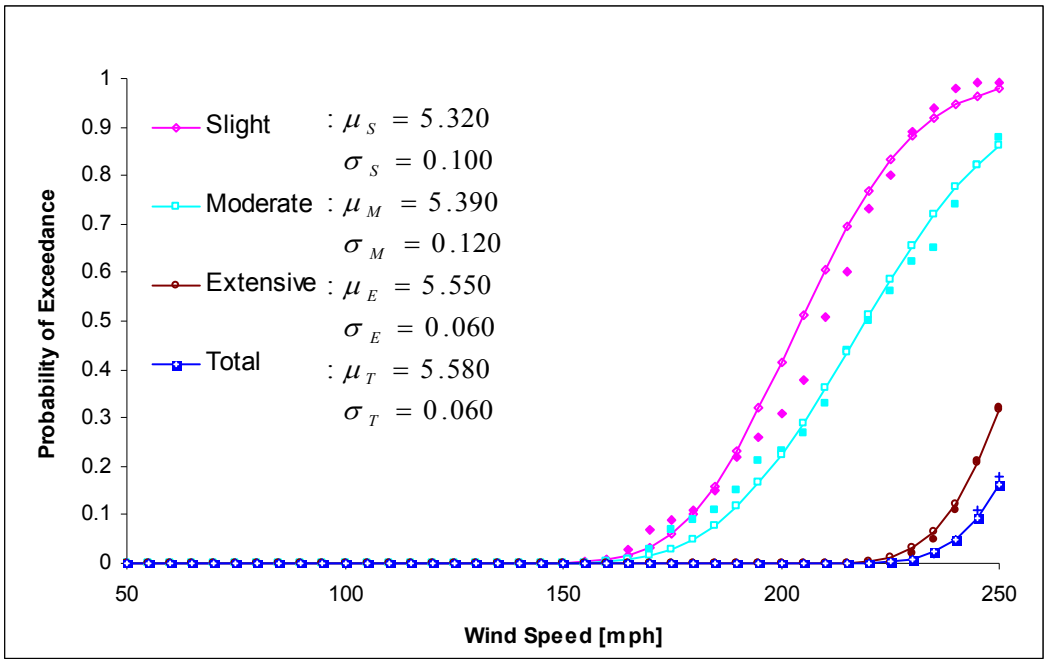

Figure 10.13 - U-system family of fragility curves with window shutters

10.7 Sensitivity Study

In previous sections, we examined the performance of several existing systems (W, C1, C2, and S1) as well as two proposed systems (S2 and U). Table 10.1 presents a summary of statistical parameters for defining the behavior of those systems. In this section, we shall briefly examine the effects of various connection types and retrofitting schemes on the overall performance of the S1-system. With its clearly defined design parameters and inherent strength, S1-system is easily adaptable to this kind of study. Vary the roof-to-wall connection types, for example, and proceed with simulations without worrying about other components to fail prematurely. Only the extensive and total damage states will be examined.

Table 10.1 – Statistical parameters for structural systems

System		Damage State			
		Slight	Moderate	Extensive	Total
W	μ	4.810	4.850	4.860	4.860
	σ	0.075	0.090	0.095	0.095
W w/o Wnd	μ	4.820	4.850	4.860	4.860
	σ	0.090	0.090	0.095	0.095
C1	μ	4.840	4.910	5.100	5.160
	σ	0.110	0.160	0.170	0.180
C1 w/o Wnd	μ	4.910	4.990	5.100	5.160
	σ	0.140	0.170	0.170	0.180
C2	μ	4.880	5.020	5.325	5.385
	σ	0.100	0.120	0.070	0.090
C2 w/o Wnd	μ	5.000	5.105	5.325	5.385
	σ	0.105	0.125	0.070	0.090
S1	μ	4.900	5.100	5.510	5.570
	σ	0.130	0.180	0.080	0.060
S1 w/o Wnd	μ	5.250	5.335	5.510	5.570
	σ	0.110	0.120	0.080	0.060
S2	μ	4.900	5.110	5.530	5.580
	σ	0.130	0.180	0.070	0.060
S2 w/o Wnd	μ	5.280	5.380	5.530	5.580
	σ	0.090	0.120	0.070	0.060
U	μ	4.900	5.110	5.550	5.580
	σ	0.130	0.190	0.060	0.060
U w/o Wnd	μ	5.320	5.390	5.550	5.580
	σ	0.100	0.120	0.060	0.060

10.7.1. Roof System Retrofitting

The effects of roof retrofitting are best exemplified by comparing the performances of the S1 with the different roof systems. Figure 10.14 shows the fragility curves for all six roof configurations. The extensive and total damage states are represented by dashed and solid lines, respectively. Notice how the 12-12-12R and 6-12-6R systems coincide. This occurs because they both share the same capacity and thus return a similar result. The statistical parameters that define each different system along

with the parameters of the sole components in are presented in Table 10.2. The parameters for the system are almost identical to those of the roof system, showing how a weak component in an assembly can shift the fragility of the system towards lower wind speeds. Since the S1-system uses the best connector types, the best roof system configurations should be used in order to maximize the performance of the structure. The performance of the conventional 6-6-6 system is noteworthy, as it as competent as that of the retrofitted systems.

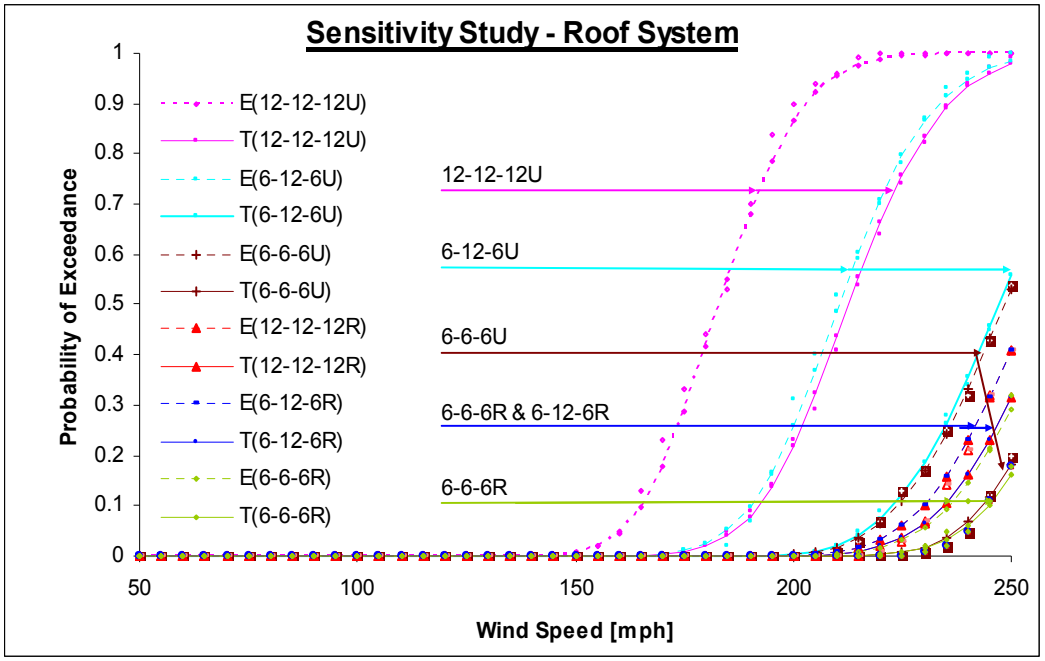

Figure 10.14 – Sensitivity of roof system on S1-system in extensive and total damage states

Table 10.2 – Comparison of roof sensitivity and roof component parameters on the extensive and total damage states

Roof Type on S1-System		System Damage State		Component Damage State	
		Extensive	Total	Extensive	Total
6-6-6U	μ	5.515	5.585	5.530	5.800
	σ	0.080	0.070	0.090	0.150
6-12-6U	μ	5.350	5.510	5.350	5.520
	σ	0.080	0.080	0.070	0.090
12-12-12U	μ	5.210	5.360	5.210	5.360
	σ	0.080	0.080	0.080	0.080
6-6-6R	μ	5.565	5.590	5.590	5.890
	σ	0.080	0.070	0.075	0.150
6-12-6R	μ	5.540	5.560	5.540	5.760
	σ	0.080	0.080	0.070	0.100
12-12-12R	μ	5.540	5.560	5.540	5.760
	σ	0.080	0.080	0.070	0.100

10.7.2. Roof-to-Wall Connection Retrofitting

In order to show the effects of roof-to-wall connections, one can start with S1-systems and vary the connection type from U hangers to small straps to small straps every other rafter to toenail only. Since the roof-to-wall connection failure is a yes or no proposition, the total damage state is the one being evaluated. Figure 10.15 shows the effect of the various roof-to-wall connections on the studied system. As it can be observed from Table 10.3, the parameters that define toe-nailed, small strap every other rafter, and small strap every rafter connections are almost the same as the component themselves. Since the U-hanger did not register any damages during the simulation, the total damage state is controlled by the stud-to-wall plate connection. The expected damages obtained by these analyses suggest that in order to take full advantage of the S1-

system, the U-hanger should be utilized, knowing that the damages are being pushed towards the wall structure.

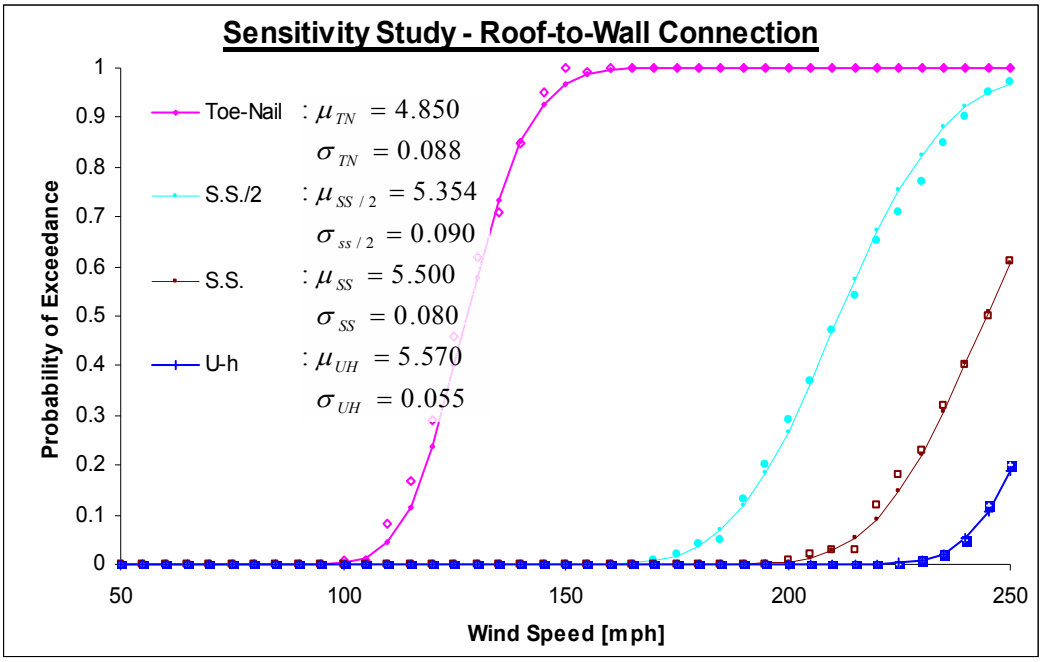

Figure 10.15 - Sensitivity of roof-to-wall connection in S1-system on the total damage state

Table 10.3 - Comparison of roof-to-wall connection sensitivity and roof-to-wall connection component parameters on the total damage state

Roof-to-Wall Connection on S1-System		Total Damage State	
		System	Component
Toe-Nail	μ	4.850	4.820
	σ	0.088	0.090
Small Strap every 2 Rafters	μ	5.354	5.380
	σ	0.090	0.100
Small Strap	μ	5.500	5.480
	σ	0.080	0.100
U-hanger	μ	5.570	*7.0*
	σ	0.055	*0.1*

10.7.3. Roof-to-Wall Plate Retrofitting

The effects of roof-to-wall plate connections are studied in a similar manner to roof-to-wall connections. Start with S1 model and vary the roof to wall plate connections from properly installed brackets plus toe-nails to properly installed brackets only to brackets installed with some deficiencies to toe-nails only. Similar to the previous sensitivity studies, the weak components tend to control the behavior of the total damage state of the ensemble, as seen in Figure 10.15. Besides the strong connector plus toe-nail connection, the system performance was controlled by the stud-to-wall plate connection. Table 10.4 shows the component reliability coinciding with the system reliability for the first three connector types. The best connection did not control the simulation, with effects of the roof system and window components recording additional damages.

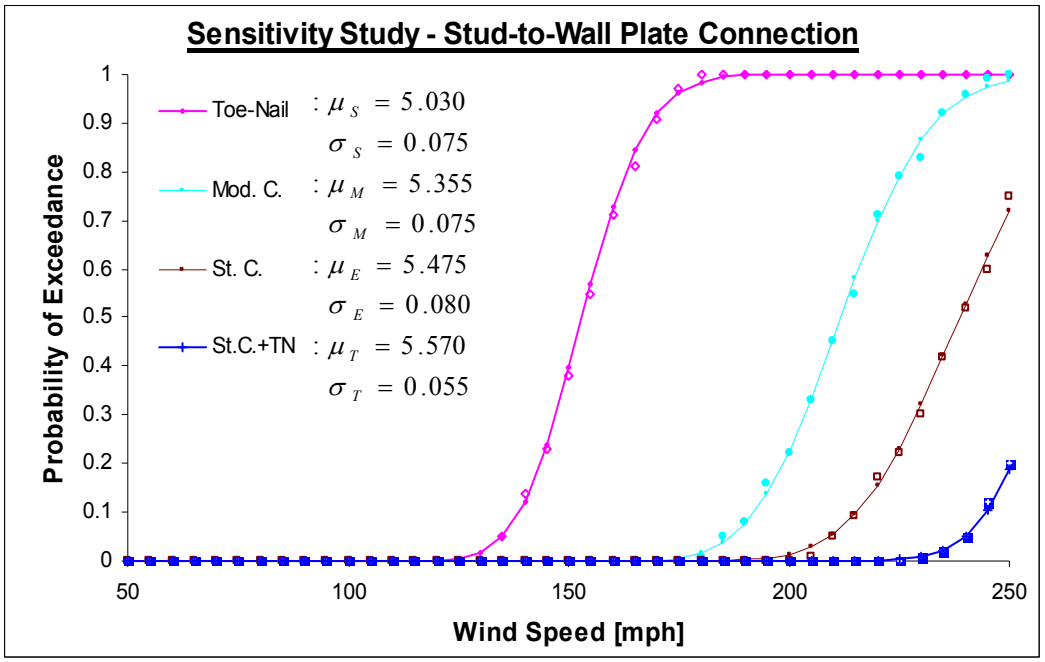

Figure 10.16 - Sensitivity of stud-to-wall plate connection in S1-system on the total damage state

Table 10.4 - Comparison of roof-to-wall plate connections sensitivity and roof-to-wall plate connections component parameters on the total damage state

Stud-to-Wall Plate Connection on S1-System		Total Damage State	
		System	Component
Toe-Nail	μ	5.030	5.040
	σ	0.075	0.070
Moderate Connector	μ	5.355	5.360
	σ	0.075	0.075
Strong Connector	μ	5.475	5.475
	σ	0.080	0.075
Strong Connector plus Toe-Nail	μ	5.570	5.580
	σ	0.055	0.060

CHAPTER 11

ADDITIONS AND INSTITUTIONAL BUILDINGS

11.1 Introduction

Although the majority of wood-zinc structures in Puerto Rico are the houses discussed in Chapter 10, certain additions and institutional buildings still utilize these systems. Historically, many Island schools and other institutions have undergone gradual changes over their life spans. In most cases that had meant making additions, often as temporary structures and generally on small budgets, once the original building could not carry the full load of the institution. These additions have often ended up being used as permanent structures. Many were constructed using wood-zinc roof systems. Some older institutional buildings were also constructed in wood-zinc because of budgetary reasons and were maintained for many years before being upgraded. The upgrade is often in the form of replacing wood-zinc roofs with all steel deck systems. Additions to residential buildings were also constructed using these systems for similar reasons. In fact, the Puerto Rico building code for many years specified two alternative roof live loads in design, allowing both 20 psf and 40 psf. It was assumed that those houses that

the owner plans a later addition will use the higher value. The basic methodology presented for wood houses in Chapter 10 is extended to additions and institutions with some modifications.

11.2 Small Institutional Buildings

The small wood-zinc institutional buildings have similar sizes to wood houses studied in the previous chapter. Because of the government insurance requirements, the construction of institutional buildings follow high code standards. For simulation purposes, the improvements are accounted for by assuming a minimum C2-system rating. Figure 11.1 show the fragilities of the C2-system in all wood-zinc construction. Table 11.1 lists the parameters for defining the system fragilities for C2 , S1, S2 and U systems. The simulation predicts no extensive and total damages resulting from Category 2 hurricanes.

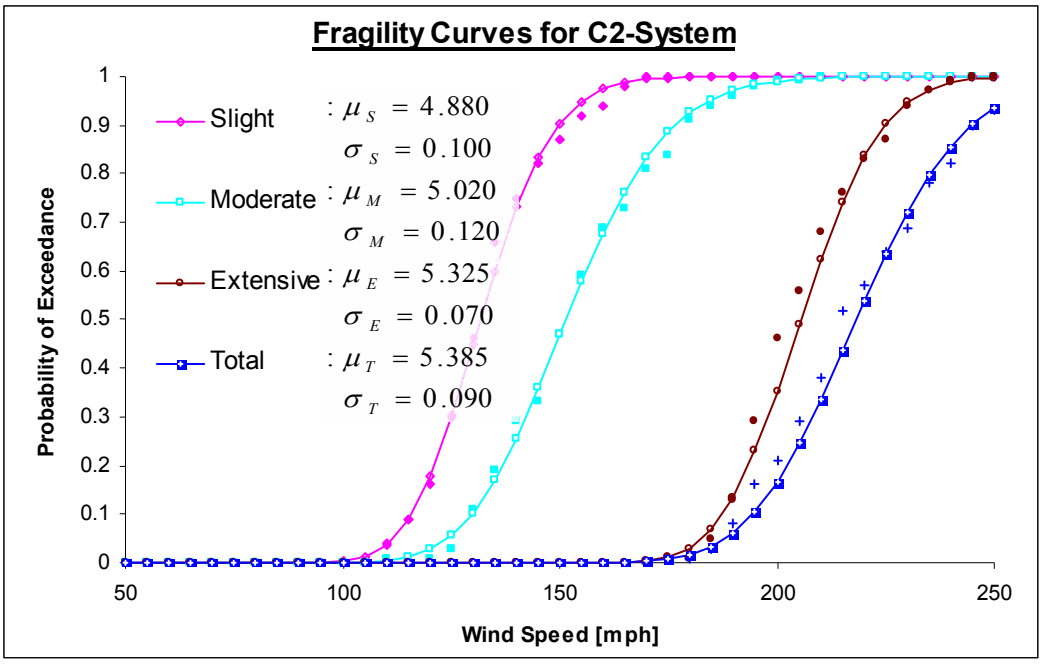

Figure 11.1 – Fragility curves for the C2-system wood-zinc institutional buildings

Table 11.1 – Statistical fragility parameters for wood-zinc institutional buildings

System		Damage State			
		Slight	Moderate	Extensive	Total
C2	μ	4.880	5.020	5.325	5.385
	σ	0.100	0.120	0.070	0.090
C2 w/o Wnd	μ	5.000	5.105	5.325	5.385
	σ	0.105	0.125	0.070	0.090
S1	μ	4.900	5.100	5.510	5.570
	σ	0.130	0.180	0.080	0.060
S1 w/o Wnd	μ	5.250	5.335	5.510	5.570
	σ	0.110	0.120	0.080	0.060
S2	μ	4.900	5.110	5.530	5.580
	σ	0.130	0.180	0.070	0.060
S2 w/o Wnd	μ	5.280	5.380	5.530	5.580
	σ	0.090	0.120	0.070	0.060
U	μ	4.900	5.110	5.550	5.580
	σ	0.130	0.190	0.060	0.060
U w/o Wnd	μ	5.320	5.390	5.550	5.580
	σ	0.100	0.120	0.060	0.060

11.2.1. Mixed Construction

Many small institutional buildings use a combination of reinforced concrete or masonry walls with wood-zinc roof systems. Historical data from past hurricanes have shown that wall stability do not influence the system fragilities in such cases. From a modeling perspective, this will be accounted for by removing the stud wall and sheathing damages from the simulation engine, leaving only the roof system, roof-to-wall connection and window damages. Figure 11.2 show the fragilities of the C2-system in these mixed systems. Table 11.2 lists the parameters for defining the system fragilities for C2, S1, S2 and U systems.

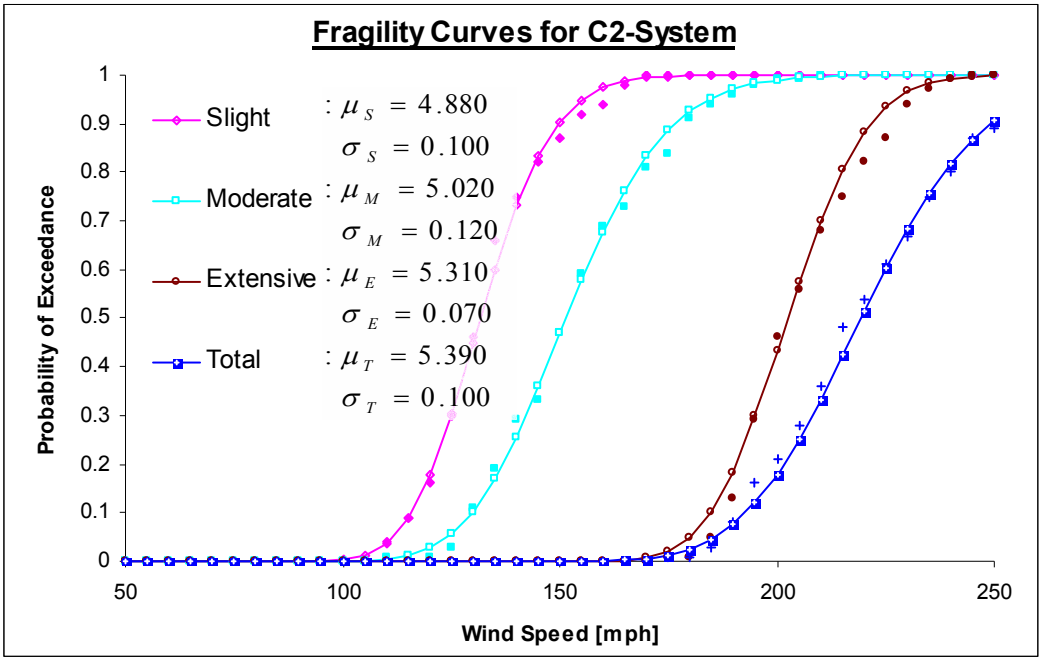

Figure 11.2 – Fragility curves for the C2-system wood-zinc mixed walled institutional buildings

Table 11.2 – Statistical fragility parameters for mixed wood-zinc institutional buildings

System		Damage State			
		Slight	Moderate	Extensive	Total
C2	μ	4.880	5.020	5.310	5.390
	σ	0.100	0.120	0.070	0.100
C2 w/o Wnd	μ	5.000	5.105	5.310	5.390
	σ	0.105	0.125	0.070	0.100
S1	μ	4.900	5.100	5.525	5.630
	σ	0.130	0.180	0.090	0.060
S1 w/o Wnd	μ	5.250	5.335	5.525	5.630
	σ	0.110	0.120	0.090	0.060
S2	μ	4.900	5.110	5.545	5.630
	σ	0.130	0.180	0.070	0.060
S2 w/o Wnd	μ	5.280	5.380	5.545	5.630
	σ	0.090	0.120	0.070	0.060
U	μ	4.900	5.110	5.570	5.640
	σ	0.130	0.190	0.060	0.060
U w/o Wnd	μ	5.320	5.390	5.570	5.640
	σ	0.100	0.120	0.060	0.060

The fact that the wall stability criteria was excluded in generating fragilities for mixed wood-zinc structures will not affect the performances up to S1-system level. Only then minor changes were observed at extensive and total damage states. Figure 11.3 shows the slight shifts in the curves for S1-sytems.

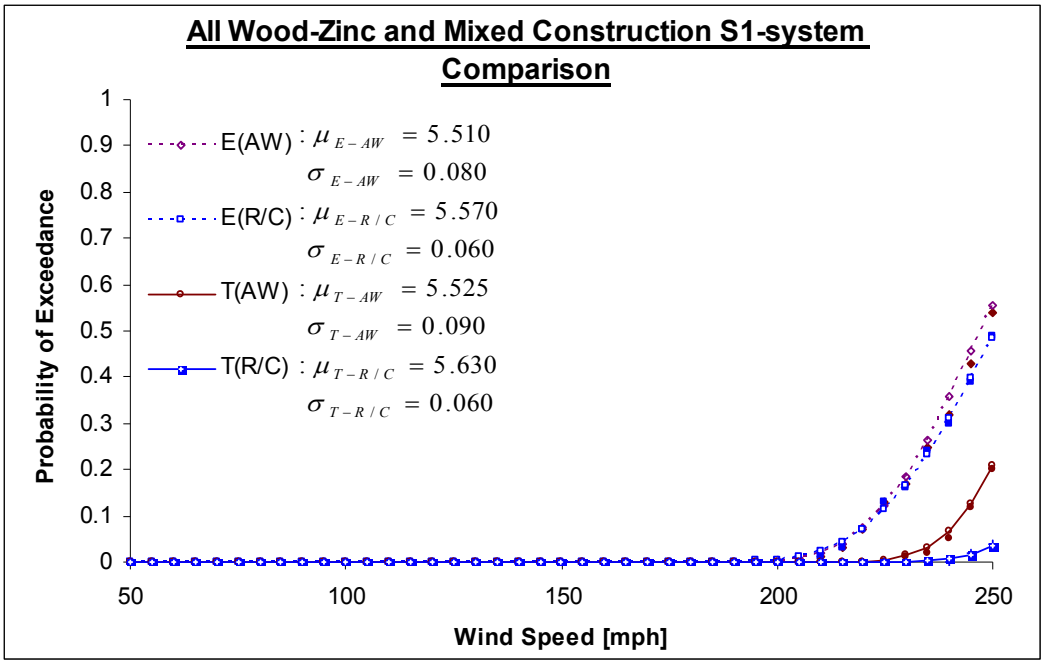

Figure 11.3 – Comparison between extreme and total damage states for all wood-zinc and mixed construction S1-systems

11.3 Large Institutional Buildings

Large institutional buildings are subjected to similar rules and regulations as small institutional buildings are. The building sizes included in this category cover footprint areas of more than 1,000 squared feet. Figure 11.4 shows an example of a large institutional building with wood-zinc roof system located in the Mayagüez Campus of the University of Puerto Rico. All large institutional buildings surveyed are with reinforced concrete shear walls, so the approach outlined in Section 11.2.1 is used. Figure 11.5 presents the C2-system fragility for large institutional buildings, while the statistical parameters for the system fragilities are listed in Table 11.3.

Figure 11.4 – Large institutional building with light-framed roofing system

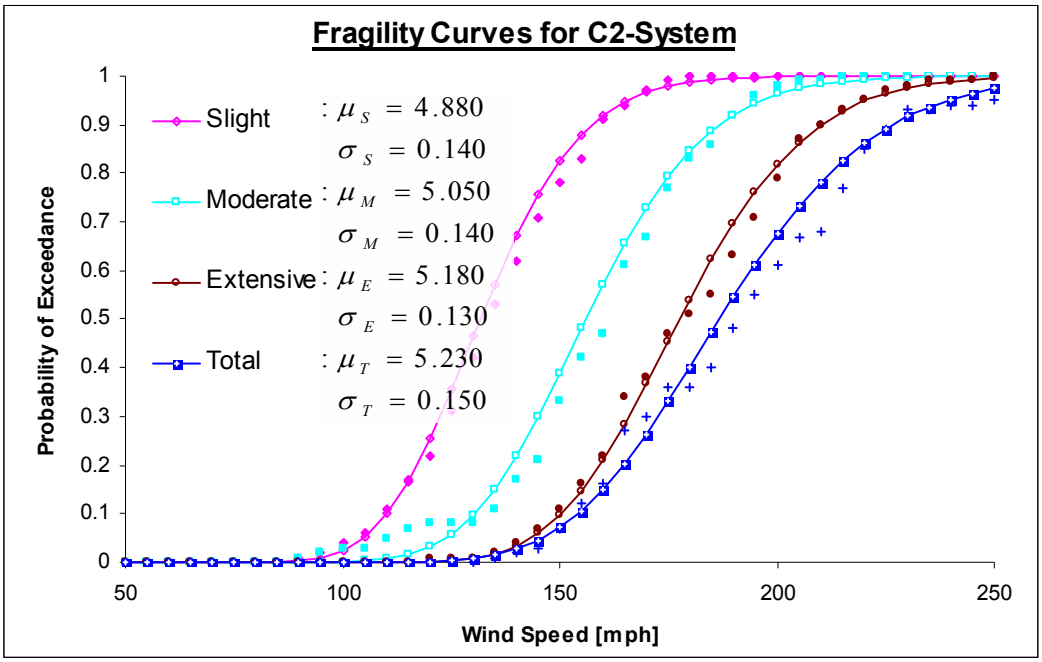

Figure 11.5 Fragility curves for the C2-system large institutional buildings

Table 11.3 - Statistical fragility parameters for large institutional buildings

System		Damage State			
		Slight	Moderate	Extensive	Total
C2	μ	4.880	5.050	5.180	5.230
	σ	0.140	0.140	0.130	0.150
C2 w/o Wnd	μ	5.000	5.105	5.220	5.240
	σ	0.105	0.125	0.140	0.150
S1	μ	4.940	5.180	5.300	5.540
	σ	0.160	0.180	0.140	0.130
S1 w/o Wnd	μ	5.250	5.335	5.475	5.525
	σ	0.110	0.120	0.090	0.110
S2	μ	4.940	5.180	5.300	5.540
	σ	0.160	0.180	0.140	0.130
S2 w/o Wnd	μ	5.280	5.390	5.500	5.530
	σ	0.100	0.110	0.110	0.120
U	μ	4.940	5.180	5.300	5.540
	σ	0.160	0.180	0.140	0.130
U w/o Wnd	μ	5.310	5.400	5.510	5.540
	σ	0.090	0.100	0.110	0.120

11.4 Second Story Residential Additions

Residential additions are usually built on the roof of an existing reinforced concrete frame or shear wall structure. Figure 11.6 shows a typical case of a second story wood-zinc house addition. Although of similar size to typical wood-zinc houses, these additions are subject to higher wind demands because of the increased height. The average eave heights are taken as 20-ft in the simulations. The second story addition may be all wood-zinc or mixed construction.

Figure 11.6 - Second story all-wood residential addition

The fragilities are evaluated similar to small institutional, however high code can not be assumed. They are sometimes constructed with reinforced concrete or masonry walls, meaning that wall stability and sheathing issues are not included during the fragility modeling. Since many of these structures are built without following any regulations, the construction quality corresponding to these structures is highly variable. The same critical components, which are the roof system and the roof to wall connections, are present in both systems. These two possible cases are presented in the following sections, with their respective fragilities. Figure 11.7 shows the performance of the second story addition with C2-system rating. Table 11.4 and 11.5 list the statistical parameters for system fragilities for all wood-zinc and mixed construction.

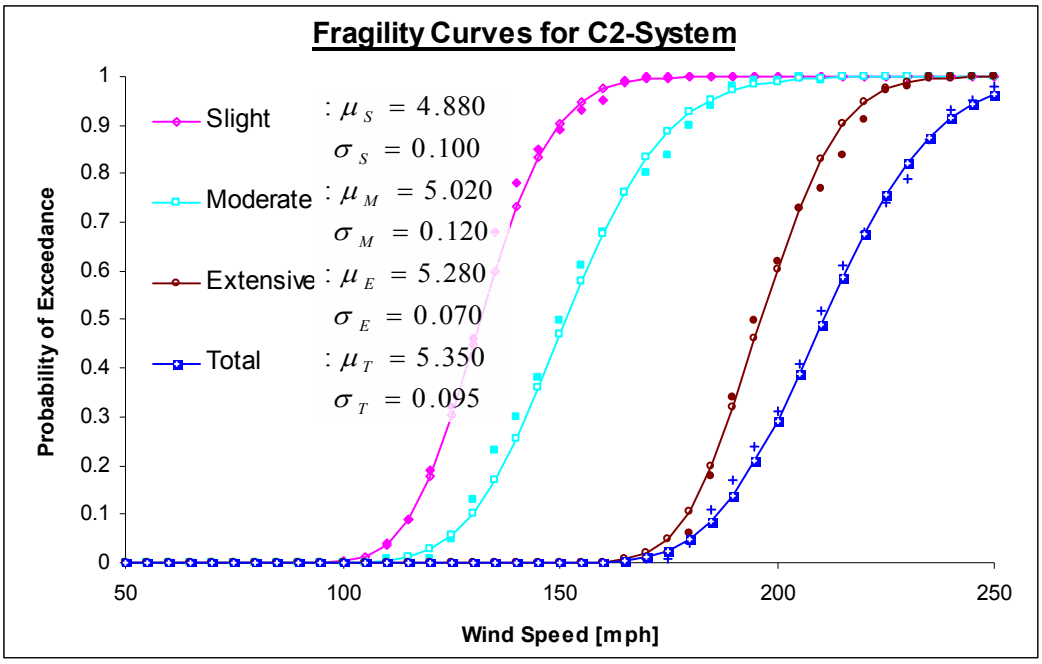

Figure 11.7 – Fragility curves for the all wood C2-sytem addition

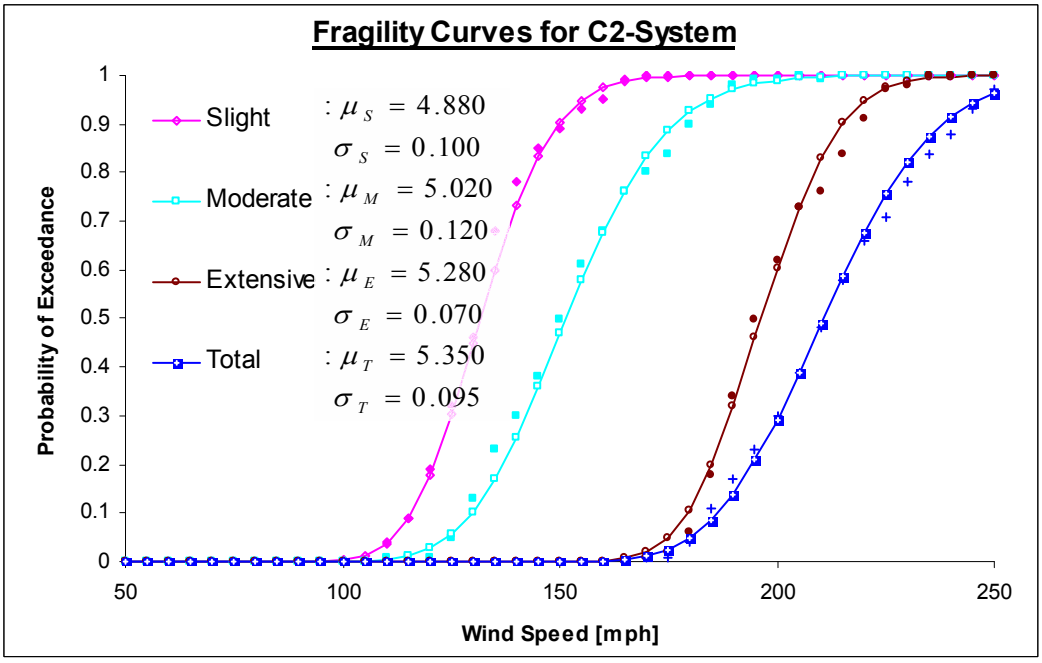

Figure 11.8 – Fragility curves for the C2-system wood-zinc mixed walled addition

Table 11.4 – Statistical fragility parameters for all wood additions

System		Damage State			
		Slight	Moderate	Extensive	Total
W	μ	4.810	4.850	4.860	4.860
	σ	0.075	0.090	0.095	0.095
W w/o Wnd	μ	4.820	4.850	4.860	4.860
	σ	0.090	0.090	0.095	0.095
C1	μ	4.840	4.910	5.100	5.160
	σ	0.110	0.160	0.170	0.180
C1 w/o Wnd	μ	4.910	4.990	5.100	5.160
	σ	0.140	0.170	0.170	0.180
C2	μ	4.880	5.020	5.325	5.385
	σ	0.100	0.120	0.070	0.090
C2 w/o Wnd	μ	5.000	5.105	5.325	5.385
	σ	0.105	0.125	0.070	0.090
S1	μ	4.900	5.100	5.510	5.570
	σ	0.130	0.180	0.080	0.060
S1 w/o Wnd	μ	5.250	5.335	5.510	5.570
	σ	0.110	0.120	0.080	0.060
S2	μ	4.900	5.110	5.530	5.580
	σ	0.130	0.180	0.070	0.060
S2 w/o Wnd	μ	5.280	5.380	5.530	5.580
	σ	0.090	0.120	0.070	0.060
U	μ	4.900	5.110	5.550	5.580
	σ	0.130	0.190	0.060	0.060
U w/o Wnd	μ	5.320	5.390	5.550	5.580
	σ	0.100	0.120	0.060	0.060

Table 11.5 – Statistical fragility parameters for wood-zinc mixed additions

System		Damage State			
		Slight	Moderate	Extensive	Total
W	μ	4.780	4.810	4.810	4.810
	σ	0.075	0.090	0.090	0.090
W w/o Wnd	μ	4.780	4.810	4.810	4.810
	σ	0.075	0.090	0.090	0.090
C1	μ	4.840	4.910	5.100	5.150
	σ	0.110	0.160	0.170	0.180
C1 w/o Wnd	μ	4.890	4.950	5.100	5.150
	σ	0.140	0.160	0.170	0.180
C2	μ	4.880	5.020	5.280	5.350
	σ	0.100	0.120	0.070	0.095
C2 w/o Wnd	μ	4.990	5.070	5.280	5.349
	σ	0.100	0.120	0.070	0.090
S1	μ	4.900	5.100	5.500	5.615
	σ	0.130	0.180	0.100	0.070
S1 w/o Wnd	μ	5.220	5.290	5.500	5.615
	σ	0.110	0.120	0.100	0.070
S2	μ	4.900	5.110	5.525	5.640
	σ	0.130	0.180	0.080	0.070
S2 w/o Wnd	μ	5.250	5.340	5.525	5.640
	σ	0.090	0.120	0.080	0.070
U	μ	4.900	5.110	5.550	5.640
	σ	0.130	0.200	0.070	0.070
U w/o Wnd	μ	5.290	5.350	5.550	5.640
	σ	0.100	0.120	0.070	0.070

11.5 Third Story Additions

Third story additions are not very common in the Island, although they can be seen from time to time. Because of the dead load considerations, they are all wood-zinc constructions. The sizes and basic characteristics are similar to wood-zinc houses. Except for the increased eave heights of about 30-ft, the simulation runs are analogous to houses and second story additions. Figure 11.9 shows the fragility curves for the third

story addition C2-system. The statistical parameters for system fragilities are listed in Table 11.6.

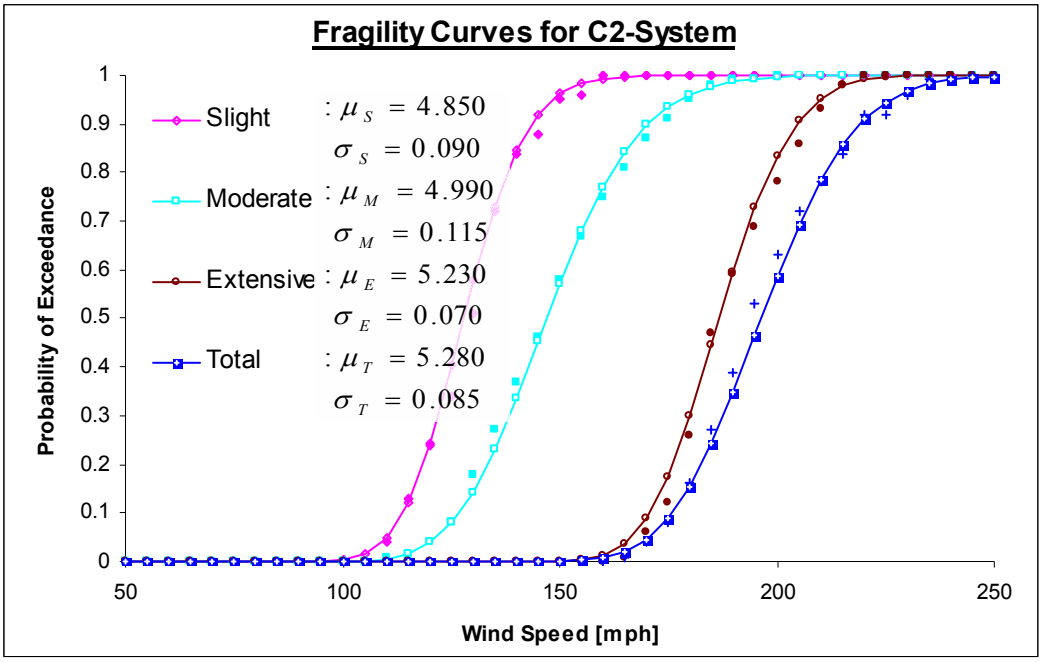

Figure 11.9 – Fragility curves for the C2 system third story addition

Table 11.6 - Statistical fragility parameters for third story additions

System		Damage State			
		Slight	Moderate	Extensive	Total
W	μ	4.740	4.770	4.770	4.770
	σ	0.075	0.090	0.090	0.090
W w/o Wnd	μ	4.740	4.770	4.770	4.770
	σ	0.075	0.090	0.090	0.090
C1	μ	4.800	4.890	5.020	5.080
	σ	0.110	0.160	0.170	0.180
C1 w/o Wnd	μ	4.830	4.910	5.020	5.080
	σ	0.130	0.170	0.170	0.180
C2	μ	4.850	4.990	5.230	5.280
	σ	0.090	0.115	0.070	0.085
C2 w/o Wnd	μ	4.930	5.030	5.230	5.280
	σ	0.100	0.120	0.070	0.085
S1	μ	4.900	5.100	5.380	5.410
	σ	0.130	0.180	0.100	0.110
S1 w/o Wnd	μ	5.170	5.240	5.380	5.410
	σ	0.110	0.110	0.100	0.110
S2	μ	4.900	5.110	5.390	5.410
	σ	0.130	0.180	0.105	0.110
S2 w/o Wnd	μ	5.210	5.290	5.390	5.410
	σ	0.090	0.120	0.105	0.110
U	μ	4.900	5.110	5.390	5.410
	σ	0.130	0.200	0.110	0.110
U w/o Wnd	μ	5.240	5.290	5.390	5.410
	σ	0.100	0.120	0.110	0.110

CHAPTER 12

DISCUSSIONS AND CONCLUSIONS

12.1 Summary

This research was started as an attempt by the MAE Center to examine the portability of the Consequence Based Engineering beyond the Mid-America region, and to test a loss visualization module developed for earthquakes in a well-defined wind hazards environment. It was also the continuation of an earlier effort at the UPRM that sought to improve on the wind performance of light frame structures in general and wood-zinc houses in particular.

Starting with the basic experimental setup and the retrofitting recommendations of Aviles (2006), the study grew into collection and archiving of wood-zinc system inventories in Puerto Rico and formulating fragility functions to predict hurricane damages to those inventories. The component based fragility approach was used.

Mathematical models for the openings, wall structure, and wall sidings are well known. Minor adjustments based on the system inventory were carried out in this research and produced results that are consistent with the field observations from past

hurricanes. Experimental data on roof-to-wall connections were used to evaluate that component by simply adding the capacities of the connectors and redistributing the loads whenever necessary.

The roof system itself required a novel approach. First, a modified SIGDERS dynamic protocol was used to rate the full-scale laboratory specimens of various nailing configurations with and without retrofitting zinc straps. Second, a procedure was established in which the entire roof system for a given building may be divided into a number of grids inside four pressure zones. Third, the experimental results were used to define three grid damage indices for each specimen types that may be assigned depending on the pressure demands on a grid. Fourth, the zone damage index was defined for each pressure zone as the average damage indices for grids in that zone. Finally, the roof performance indices were defined as the sums of damage indices from the four pressure zones. These indices would directly correspond to various roof fragility states.

The fragilities associated with various building components are combined in the usual manner to analyze all types of buildings with wood-zinc roof systems. This included houses, additions, schools and mass halls. The effects of using different nailing schedules on the roof, zinc straps, metal straps at roof to wall, connection plates at stud to wall plates, opening types, as well as the quality of construction, were considered.

12.2 Discussion of Results

The use of wood-zinc roof systems is not limited to residential buildings. In fact, the discussions in Chapter 11 were focused on institutional buildings including those with

masonry walls. Nevertheless, the wood-zinc houses provide a valuable insight into how changes in various system components influence the overall system fragility.

Depending on how well a wood-zinc house is constructed, it may be classified in an increasing order of performance as W, C1, C2, S1, S2, and U. The W-class represents poor construction practices while buildings in the U-class provide ultimate system performance. The basic requirements for each building class and the associated parameters for fragility curves were discussed in Chapter 10. Figure 12.1 shows examples of system performances at 200 mph wind speed. It was constructed using the fragility relationships developed in this thesis.

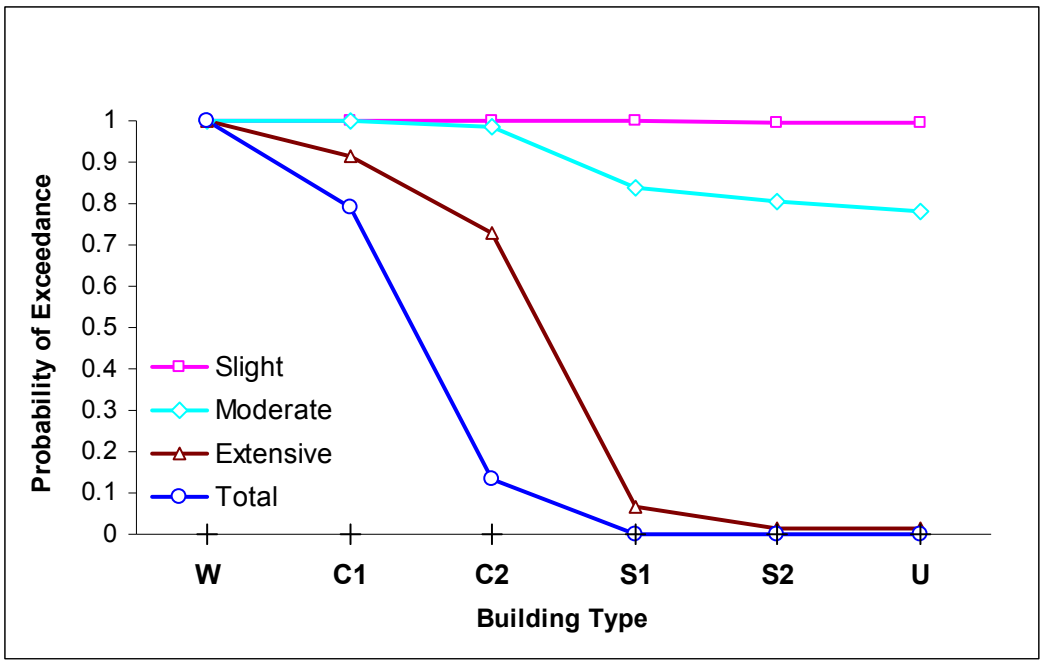

Figure 12.1 - System performance at 200 mph winds

As shown in Figure 12.1, none of the U-class buildings would collapse, compared to 100 percent of W-class. For every 100,000 units considered, the overall improvements

in terms of units saved from total collapse are 22,111 units from W-class to C1-class, 61,115 units from C1-class to C2-class, 16,774 units from C2-class to S1-class, and no improvements from S1-class to S2-class and S2-class to U-class. Similar comparisons for extensive damage states will result in 12,169 to 52,677 to 34,746 to 361 to 45 unit improvements. The effects are not as severe for other damage states, with values ranging from 761 to 258 to 12,509 to 1,245 to 1,308 for moderate and no considerable improvements for minor damage states. Table 12.1 lists a summary of improvements in matrix form.

Table 12.1 - Comparison of system performances for 100,000 units at 200 mph

Building Class	W	C1	C2	S1	S2	U	W	C1	C2	S1	S2	U
	Total Damage States						Extensive Damage States					
W	0	22111	83226	1E5	1E5	1E5	0	12169	64846	99593	99953	99998
C1		0	61115	77888	77888	77888		0	52677	87424	87784	87829
C2			0	16774	16774	16774			0	34746	35107	35152
S1				0	0	0				0	361	406
S2					0	0					0	45
U						0						0
	Moderate Damage States						Slight Damage States					
W	0	761	1019	13528	14773	16081	0	0	0	109	109	109
C1		0	258	12767	14012	15320		0	0	109	109	109
C2			0	12509	13754	15062			0	109	109	109
S1				0	1245	2553				0	0	0
S2					0	1308					0	0
U						0						0

The performance improvements are also a function of wind speeds. Figure 12.2 gives some examples of collapse resistance at various wind speeds. Similar relationships are shown in Figure 12.3 and Figure 12.4 for extensive and moderate damage states, respectively.

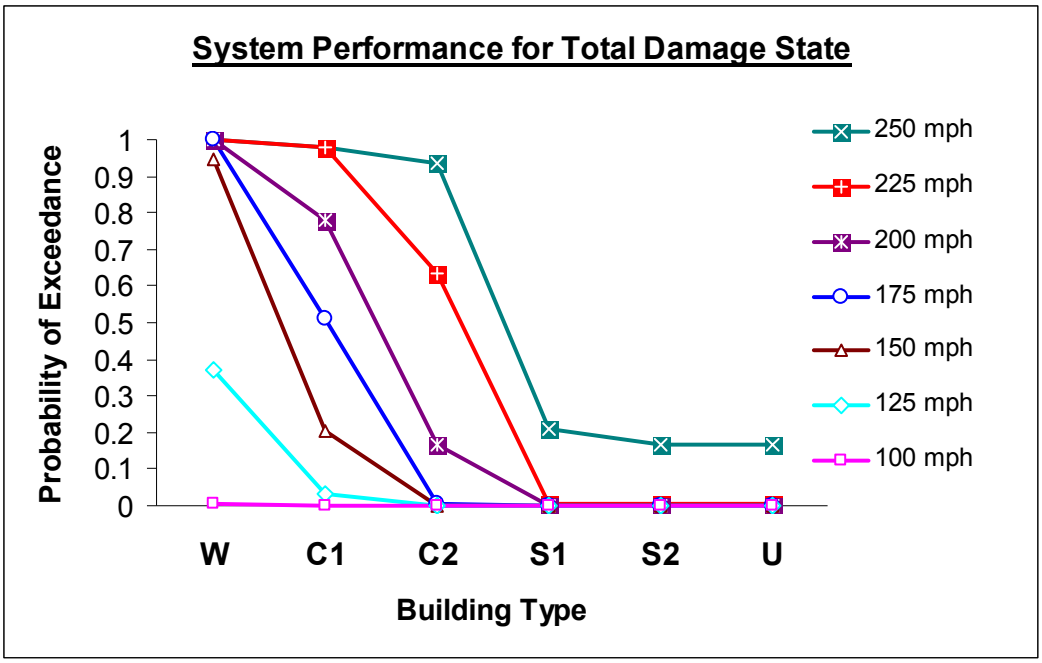

Figure 12.2 - Performance improvement as function of wind speed – total damage state

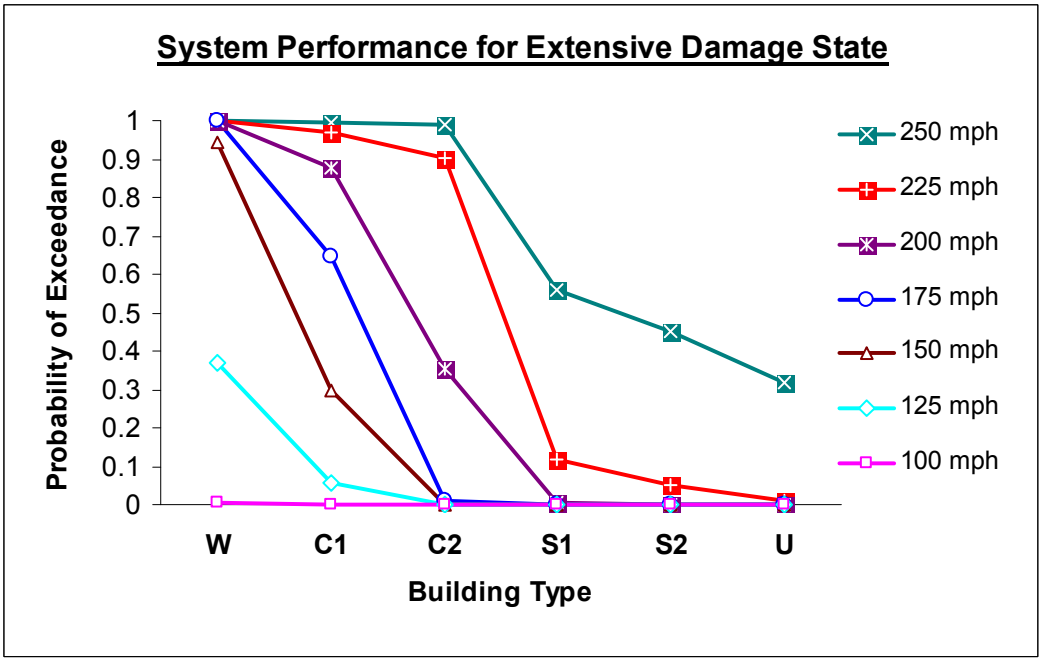

Figure 12.3 - Performance improvement as function of wind speed – extreme damage state

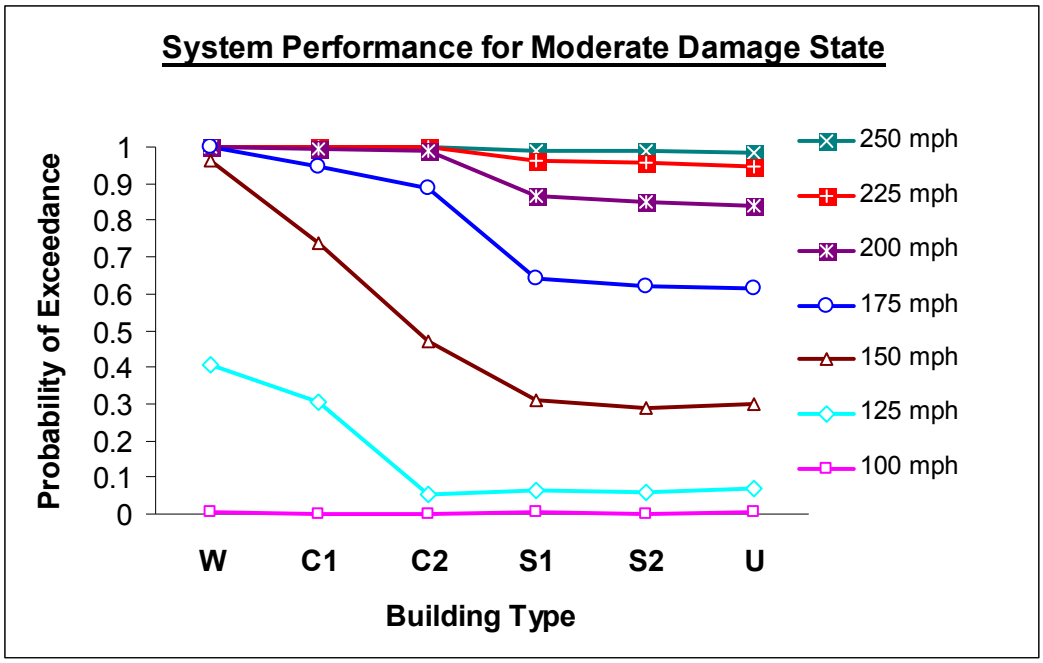

Figure 12.4 - Performance improvement as function of wind speed – moderate damage state

To bring some perspective to all these, some cost calculations were carried out for model 3 from Table 2.2. Assuming the W-class to represent the base value, the cost for all other building classes are presented as the percentages above base. This is shown in Figure 12.5. Given the mere 10 percent increase in cost to go from W-class to S2-class, and the almost 98-percent reduction in collapse and extensive damage numbers at 150 mph (Figure 12.1), the upgrade decision seems completely justified. The design recommendations in Section 12.3 assume S1-class as the lowest permissible. An upcoming report by Gerbaudo (2007) presents detailed cost-benefit ratio analysis of these systems under hurricane loading.

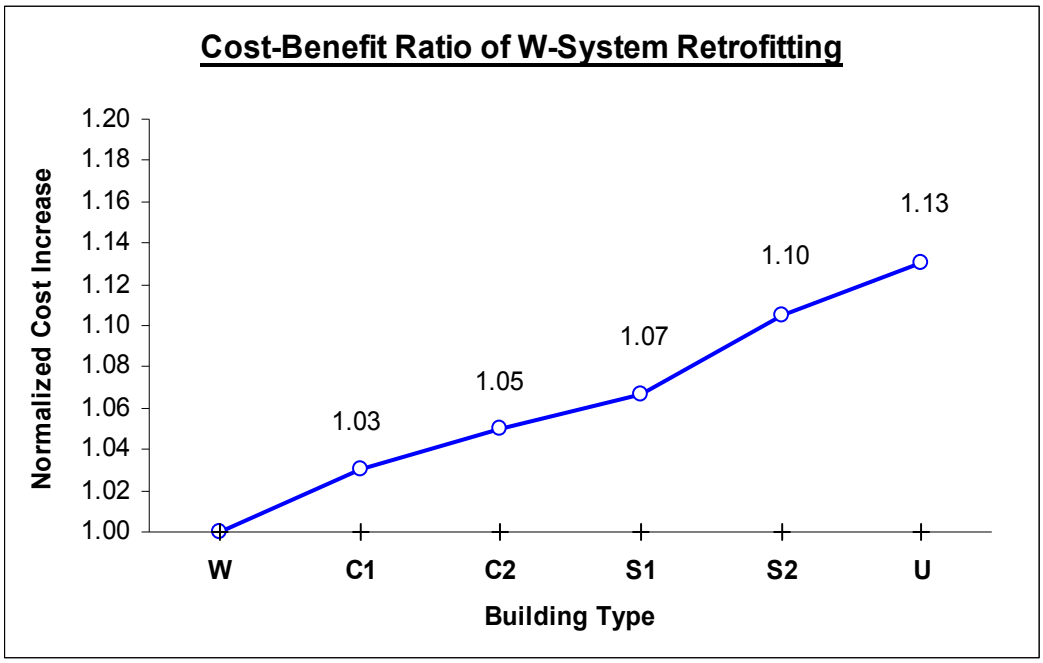

Figure 12.5 - Cost-benefit ratio of retrofitting the W-system

12.3 Conclusions

The common perception that wood-zinc structures are not functional in a hurricane environment was proven to be invalid. In fact, the performance issues associated with these structures were shown to be a function of construction practices and not the system design. Many existing wood-zinc houses on the Island will be designated as W by our rating system and are likely to suffer substantial damages under even the moderate hurricane wind loads. However, the added expense of upgrading a W-system to a S1 or S2-system is less than 10 percent of the total building cost.

In terms of individual components, the following conclusions can be drawn. The best conventional roof system can be easily constructed by adding the additional nails necessary to the 12-12-12 or 6-12-6 configurations. The bending of the roofing nails is

necessary for taking full advantage of the nailing schedule. These additional nails would take the roof performance to the levels comparable to the retrofitted systems. The use of toe-nails only connections in the roof-to-wall and stud-to-wall plate connections resulted in failures at very low wind speeds. Consequently, this connection mechanism should not be used in hurricane prone regions. Consistent with historical data, wall sidings performed adequately with only minor damages for the second and third level additions.

In terms of system behavior, the inclusion of any weak component can have a dominating effect. This was discussed in the context of the sensitivity analysis of Section 10.7. Easy to apply retrofitting measures are readily available for improving the performance of more common W and C1-systems. For example, the use of zinc straps on the roof, which is usually the controlling component, will result in substantial improvements to the system fragility. Another cost-effective option is the use of metal connectors at the roof-to-wall and stud-to-wall plate connections. The potential benefits of window shutters were shown to be limited to C2-system and better. Their installation does not improve the overall performance for W and C1-systems.

12.4 Recommendations

It was a stated objective of this research to clarify certain aspects of construction practices that apply to wood-zinc houses. Component fragility data clearly indicates the need to use metal straps in roof to wall and stud to wall plate connections. On the roof system itself, the practice of bending the nails at the back of spacers and connecting spacers to rafters with metal straps were proven invaluable. In what follows we shall

present a set of recommendation that should help alleviate some of the problems associated with this type of construction. The buildings complying with these will have an S1 rating which can further be improved by using zinc straps:

- Roof nailing schedule of 6-in minimum spacing on edges and 12-in maximum spacing elsewhere should be followed. Nails shall be umbrella-headed spiral-shanked nails 3-in long. Bending of all nails perpendicular to spacer longitudinal direction as per FEMA/CIAPR specifications is required.
- Use of 26-gage or better corrugated zinc sheets meeting or exceeding ASTM653/ASTM653M standards, overlapping by 6-in minimum in every direction is required.
- Use of 20-gage minimum metal connectors for spacer-to-rafter connections at every grid intersection (Simpson Strong-Tie® 2-H2.5/H2.5A, HRS/HST straps or equivalent) with all nail holes filled.
- Use of 20-gage minimum metal straps for roof-to-wall connections at every joist (Simpson Strong-Tie® H1, LUS, LU, HUS28, 2-H2.5/H2.5A or equivalent) with all nail holes filled.
- Use of 20-gage minimum metal for straps stud-to-wall/sill plate at every stud (Simpson Strong-Tie® SP1, SP4, DSP, TSP or equivalent) with all nail holes filled.
- Use of 20-gage minimum column-to-beam/floor connector (Simpson Strong-Tie® AC, CC, EPB/EPC series or equivalent) with all nail holes filled.

- Use of 5/8-in minimum thickness exterior wall sheathing, with a nailing schedule of 6-in o.c. at edge panels and 8-in o.c. elsewhere. Blocking shall be provided where needed.
- Window framing shall be fastened with 6 lag screws minimum to the wall studs that form the window framing, with a screw diameter ¼-in minimum.

References

Abdullah, M.M. and Norton, T.R. (2004). "Combined Hurricane and Earthquake Hazard Component Vulnerability Analysis". < http://mceer.buffalo.edu/outreach/intActivity/ ANCER/ Activities/2004/norton_t_mceer.pdf > (August 2005).

Abrams, D.P., Elnashai, A.S., and Beavers, J.E. (2001) "A New Engineering Paradigm: Consequence-Based Engineering." Mid-America Earthquake Center, University of Illinois, Urbana-Champaign. < http://mae.ce.uiuc.edu/Research/CBE/cbepaper.pdf > (September 2006)

ATC-13. (1985). "Earthquake Damage Evaluation Data for California". ATC-13, Applied Technology Council.

Avilés, D. (2006). "On Improving the Performance of Wood-Zinc Roof Systems." Ph.D. Thesis. Department of Civil Engineering, University of Puerto Rico at Mayagüez.

Baskaran, B.A., Chen, Y., and Vilaipornsawai, U. (1999). "A New dynamic wind load cycle to evaluate flexible membrane roofs". *Journal of Testing and Evaluation*. 27(4). 249-265.

Boose, E.R., Serrano, M.I., and Foster, D.R. (2004). "Landscape and Regional Impacts of Huricanes in Puerto Rico." *Ecological Monographs.* 74(2). 335-352

Bulleit, W.M. and Yates, J.L. (1991). "Probabilistic Analysis of Wood Trusses." *Journal of Structural Engineering*, 117(10). 3008-3025.

Bulleit, W.M. and Liu, W.F. (1995). "First-Order Reliability Analysis of Wood Structural Systems." *Journal of Structural Engineering,* ASCE. 121(3). 517-529.

Bulleit, W.M., Pang, W.C., and Rosowsky, D.V. (2005). "Modeling Wood Walls Subjected to Combined Transverse and Axial Loads." *Journal of Structural Engineering*, ASCE. 131(5). 781-793.

Committee on Earthquake Engineering (CoEE). (1989). "Estimating Losses from Future Earthquakes. Panel Report. On Earthquake Loss Estimation Methodology". National Academy Press. Washington, D.C.

Cope, A.D. (2004). "Predicting the Vulnerability of Typical residential Buildings to Hurricane Damage." Ph.D. Thesis. Department of Civil Engineering, University of Florida

Davidson, R.A., Zhao, H., and Kumar, V. (2003). "Quantitative Model to Forecast Changes in Hurricane Vulnerability of Regional Building Inventory". *J. Infra. Systems*, 9(2). 55-64,

Ellingwood B.R.; Rosowsky, D.V.; Li, Y., and Jun H.K. (2004). "Fragility Assessment of Light-Frame Wood Construction Subjected to Wind and Earthquake Hazards". *Journal of Structural Engineering*, ASCE. 130(12). 1921-1930.

European Committee for Standardization (CEN). (1994). "DD ENV 1995-1-1: Design of timber structures—Part 1-1 General rules and rules for buildings (together with United Kingdom National Application Document." *Eurocode 5*, London.

Federal Emergency Management Agency (FEMA). (2003). "Multi-hazard Loss Estimation Methodology, Hurricane Model". *HAZUS - MH MR1 Technical Manual.* Washington, D.C.

Federal Emergency Management Agency (1989). "Protegiendo su casa: Mitigación de riesgos en Puerto Rico después del huracán Hugo, Las conexiones son lo más importante." October 5, 1989.

Federal Emergency Management Agency (1999). "Construction Guide for One and Two Family Dwellingin Hhurricane and Seismic Zones". January 4, 1999.

Figueroa, V. (1996). "Performance of Steel Roof Decks Subjected to Repeated Wind Loading." Master Thesis. Department of Civil Engineering, University of Puerto Rico at Mayagüez.

Filliben, J.J., Gurley, K., Pinelli, J.P., Simiu, E., and Subramanian, C. (2002). "Fragility curves, damage matrices, and wind induced loss estimation". *Proceedings from the Third International Conference on Computer Simulation in Risk Analysis and Hazard Mitigation.* Sintra, Portugal. 119-126.

Gerbaudo, G. (2007). "Developing Insurance Solutions Software for Natural Hazard Loss Estimation." Ph.D. Thesis (to be defended). Department of Civil Engineering, University of Puerto Rico at Mayagüez.

Hart, G.C. (1976). "Estimation of Structural Damage due to Tornados". *Proceedings of the Symposium on Tornadoes: Assessment of Knowledge and Implications for Man in Lubbock*. Texas, 645-665.

Hsu, S.A. (2003). "Estimating Overwater Friction Velocity and Exponent of Power-Law Wind Profile from Gust Factor during Storms." *Journal of Waterway, Port, Coastal, and Ocean Engineering*. 129(4). 174-177.

Khanduri, A.C. and Morrow, G.C. (2003). "Vulnerability of Buildings to Windstorms and Insurance Loss Estimation". *J. Wind Engrg. and Indst. Aerodynamics*. Vol. 91. 455-467.

Leicester, R.H., Bubb, C.T.J., Dorman, C., and Beresford, F.D. (1979). "An Assessment of Potential Cyclone Damage to Dwellings in Australia". *Proceedings of the 5th International Conference on Wind Engineering*, Fort Collins, CO.

Liu, W.F and Bulleit, W.M. (1995). "Overload Behavior of Sheathed Lumber Systems." *Journal of Structural Engineering*, ASCE. 121(7). 1110-1118.

Mahendran M. (1993). "Simulation of Cyclonic Wind Forces on Roof Claddings by Random Block Load Testing." James Cook CSTS, Technical Report No. 38.

Melbourne W. (1977). "Loading cycles for simulation of wind loading." EBS Workshop. Sydney, Australia.

''Minimum design loads for buildings and other structures.'' (2002). *ASCE 7-02*, ASCE, Reston, Va.

Morgan, J. and Beck, V. (1977). "*Failure of sheet metal roofing under repeated wind loading*". Civil Engineering Transactions, Institute of Engineers, Australia, Vol. CB19. 1-5.

"National Design Specifications for Wood Construction" (2001) ANSI/AF&PA NDS-2001. American Forest & Paper Association. Washinigton, DC.

National Institute of Building Sciences (NIBS). (2000). "HAZUS Wind Loss Estimation Methodology". *Draft Technical Manual*. Washington, D.C.

Reed, T. D., Rosowsky, D. V., and Schiff, S. D. (1997). ''Roof rafter to top-plate connections in coastal residential construction.'' *Proc., International Wood Engineering Conference*, New Orleans, La. 4, 458-465.

Rosowsky, D. V., and Cheng, N. (1999). ''Reliability of light-frame roof systems in hurricane-prone regions, Part I: Wind loads.'' *Journal of Structural Engineering*, ASCE. 125(7), 725–733.

Rosowsky, D. V., and Cheng, N. (1999). ''Reliability of Light-Frame Roofs in High-Wind Regions. II: Reliability Analysis" *Journal of Structural Engineering*, ASCE. 125(7). 734-739.

Rosowsky, D.V. and Ellingwood, B.R. (2002). "Performance-Based Engineering of Wood Frame Housing: Fragility Analysis Methodology". *Journal of Structural Engineering*, ASCE. 128(1). 32-38.

Rosowsky, D.V. and Lee, K.H. (2004). "Fragility assessment for roof sheathing failure in high wind regions". *Journal of Structural Engineering*, ASCE. 27. 857 - 868.

Saffar, A., Ramos, R., Avilés, D., and García, R. (2003). "On Improving the Building Code Requirements for Wood Zinc Housing". *Final Report*. FEMA HMGP PR-0060-D.

Schiff, A.J. and Newsom, D.E. (1979). "Fragility of Electrical Power Equipment". *J. of Tech. Councils* ASCE. 105(2). 451-465.

Simpson Strong-Tie. (2002). "Connectors for Factory Built Homes." Technical Bulletin T-FBS02, Simpson Strong-Tie. < http://www.strongtie.com/ftp/bulletins/T-FBS02.pdf > (September 2006).

Shinozuka, M., Feng, M. Q., Lee, J., and Naganuma, T. (2000). "Statistical Analysis of Fragility Curves". *J. Struct. Mech*. 126(12). 1224–1231.

TR 440 (1978). "Guidelines for Testing and Evaluation of products for Cyclone prone areas." Experimental Building Station (EBS). Sydney, Australia.

Unanwa, C.O. and McDonald, J.R. (2000). "Building Wind Damage Prediction and Mitigation Using Damage Bands). *Natural Hazards Review*. Vol. 1, No. 4, November, 197 – 203.

Zhao, H. (2002). "A Quantitative Model Forecasting Changes in the Hurricane Vulnerability of Residential Wood-Frame Structures in North Carolina". M.S.C.E. Thesis, School of Civil and Environmental Engineering, Cornell University. Ithaca, NY.

APPENDIX A

Statistical Parameters for Components and Systems Fragilities

A.1. Wood-Zinc Houses

Table A.1 - Component parameters for wood-zinc houses

Component	Description		Damage State			
			Slight	Moderate	Extensive	Total
Roof Deck	6-6-6U	μ	5.250	5.330	5.530	5.800
		σ	0.105	0.120	0.090	0.150
	6-12-6U	μ	5.005	5.105	5.350	5.520
		σ	0.105	0.130	0.070	0.090
	12-12-12U	μ	4.885	5.030	5.210	5.360
		σ	0.085	0.090	0.080	0.080
	6-6-6R	μ	5.320	5.390	5.590	5.890
		σ	0.100	0.130	0.075	0.150
	6-12-6R	μ	5.290	5.380	5.540	5.760
		σ	0.090	0.120	0.070	0.100
	12-12-12R	μ	5.290	5.380	5.540	5.760
		σ	0.090	0.120	0.070	0.100
Roof-to-Wall Connection	Gen. Pop.	μ	-	-	-	5.150
		σ	-	-	-	0.270
	Toe Nail	μ	-	-	-	4.820
		σ	-	-	-	0.090
	S. Strap per 2 joists	μ	-	-	-	5.380
		σ	-	-	-	0.100
	S. Strap	μ	-	-	-	5.480
		σ	-	-	-	0.100
	U-hanger	μ	-	-	-	*7.0*
		σ	-	-	-	*0.1*
Wall Structure	Gen. Pop.	μ	-	-	-	5.290
		σ	-	-	-	0.125
	Toe Nail	μ	-	-	-	5.040
		σ	-	-	-	0.070
	T.N. + Conn.	μ	-	-	-	5.580
		σ	-	-	-	0.060
Wall Sheathing	Gen. Pop.	μ	*7.0*	*7.0*	*7.0*	*7.0*
		σ	*0.1*	*0.1*	*0.1*	*0.1*
Windows	Gen. Pop.	μ	4.920	5.110	*7.0*	*7.0*
		σ	0.150	0.190	*0.1*	*0.1*

Table A.2 - Statistical fragility parameters for wood-zinc houses

System		Damage State			
		Slight	Moderate	Extensive	Total
W	μ	4.810	4.850	4.860	4.860
	σ	0.075	0.090	0.095	0.095
W w/o Wnd	μ	4.820	4.850	4.860	4.860
	σ	0.090	0.090	0.095	0.095
C1	μ	4.840	4.910	5.100	5.160
	σ	0.110	0.160	0.170	0.180
C1 w/o Wnd	μ	4.910	4.990	5.100	5.160
	σ	0.140	0.170	0.170	0.180
C2	μ	4.880	5.020	5.325	5.385
	σ	0.100	0.120	0.070	0.090
C2 w/o Wnd	μ	5.000	5.105	5.325	5.385
	σ	0.105	0.125	0.070	0.090
S1	μ	4.900	5.100	5.510	5.570
	σ	0.130	0.180	0.080	0.060
S1 w/o Wnd	μ	5.250	5.335	5.510	5.570
	σ	0.110	0.120	0.080	0.060
S2	μ	4.900	5.110	5.530	5.580
	σ	0.130	0.180	0.070	0.060
S2 w/o Wnd	μ	5.280	5.380	5.530	5.580
	σ	0.090	0.120	0.070	0.060
U	μ	4.900	5.110	5.550	5.580
	σ	0.130	0.190	0.060	0.060
U w/o Wnd	μ	5.320	5.390	5.550	5.580
	σ	0.100	0.120	0.060	0.060

A.2. Second Story Additions

A.2.1. All Wood Systems

Table A.3 - Component parameters for second story all wood construction additions

Component	Description		Damage State			
			Slight	Moderate	Extensive	Total
Roof Deck	6-6-6U	μ	5.220	5.290	5.500	5.770
		σ	0.105	0.120	0.090	0.150
	6-12-6U	μ	4.980	5.070	5.320	5.490
		σ	0.105	0.130	0.075	0.090
	12-12-12U	μ	4.850	4.980	5.170	5.330
		σ	0.085	0.090	0.080	0.080
	6-6-6R	μ	5.290	5.350	5.555	5.820
		σ	0.100	0.120	0.075	0.140
	6-12-6R	μ	5.260	5.350	5.525	5.730
		σ	0.090	0.120	0.080	0.100
	12-12-12R	μ	5.260	5.350	5.525	5.730
		σ	0.090	0.120	0.080	0.100
Roof-to-Wall Connection	Gen. Pop.	μ	-	-	-	5.140
		σ	-	-	-	0.280
	Toe Nail	μ	-	-	-	4.820
		σ	-	-	-	0.090
	S. Strap per 2 joists	μ	-	-	-	5.320
		σ	-	-	-	0.095
	S. Strap	μ	-	-	-	5.480
		σ	-	-	-	0.100
	U-hanger	μ	-	-	-	*5.7*
		σ	-	-	-	*0.1*
Wall Structure	Gen. Pop.	μ	-	-	-	5.260
		σ	-	-	-	0.140
	Toe Nail	μ	-	-	-	5.000
		σ	-	-	-	0.080
	T.N. + Conn.	μ	-	-	-	5.590
		σ	-	-	-	0.090
Wall Sheathing	Gen. Pop.	μ	5.580	5.590	5.620	5.620
		σ	0.100	0.100	0.100	0.100
Windows	Gen. Pop.	μ	4.920	5.200	*7.0*	*7.0*
		σ	0.140	0.220	*0.1*	*0.1*

Table A.4 - Statistical fragility parameters for second story all-wood construction additions

System		Damage State			
		Slight	Moderate	Extensive	Total
W	μ	4.780	4.810	4.810	4.810
	σ	0.075	0.090	0.090	0.090
W w/o Wnd	μ	4.780	4.810	4.810	4.810
	σ	0.075	0.090	0.090	0.090
C1	μ	4.840	4.910	5.050	5.100
	σ	0.110	0.160	0.170	0.180
C1 w/o Wnd	μ	4.890	4.950	5.050	5.100
	σ	0.140	0.160	0.170	0.180
C2	μ	4.880	5.020	5.280	5.350
	σ	0.100	0.120	0.070	0.095
C2 w/o Wnd	μ	4.990	5.070	5.280	5.349
	σ	0.100	0.120	0.070	0.090
S1	μ	4.900	5.120	5.480	5.540
	σ	0.130	0.180	0.080	0.080
S1 w/o Wnd	μ	5.220	5.290	5.490	5.540
	σ	0.110	0.120	0.090	0.075
S2	μ	4.900	5.100	5.500	5.545
	σ	0.130	0.180	0.075	0.080
S2 w/o Wnd	μ	5.250	5.340	5.504	5.545
	σ	0.090	0.120	0.075	0.080
U	μ	4.900	5.110	5.520	5.540
	σ	0.130	0.200	0.070	0.075
U w/o Wnd	μ	5.290	5.350	5.520	5.540
	σ	0.100	0.120	0.070	0.075

A.2.2. Mixed Systems

Table A.5 - Component parameters for mixed additions

Component	Description		Damage State			
			Slight	Moderate	Extensive	Total
Roof Deck	6-6-6U	μ	5.220	5.290	5.500	5.770
		σ	0.105	0.120	0.090	0.150
	6-12-6U	μ	4.980	5.070	5.320	5.490
		σ	0.105	0.130	0.075	0.090
	12-12-12U	μ	4.850	4.980	5.170	5.330
		σ	0.085	0.090	0.080	0.080
	6-6-6R	μ	5.290	5.350	5.555	5.820
		σ	0.100	0.120	0.075	0.140
	6-12-6R	μ	5.260	5.350	5.525	5.730
		σ	0.090	0.120	0.080	0.100
	12-12-12R	μ	5.260	5.350	5.525	5.730
		σ	0.090	0.120	0.080	0.100
Roof-to-Wall Connection	Gen. Pop.	μ	-	-	-	5.140
		σ	-	-	-	0.280
	Toe Nail	μ	-	-	-	4.820
		σ	-	-	-	0.090
	S. Strap per 2 joists	μ	-	-	-	5.320
		σ	-	-	-	0.095
	S. Strap	μ	-	-	-	5.480
		σ	-	-	-	0.100
	U-hanger	μ	-	-	-	*5.7*
		σ	-	-	-	*0.1*
Windows	Gen. Pop.	μ	-	-	-	5.260
		σ	-	-	-	0.140

Table A.6 - Statistical fragility parameters for mixed additions

System		Damage State			
		Slight	Moderate	Extensive	Total
W	μ	4.780	4.810	4.810	4.810
	σ	0.075	0.090	0.090	0.090
W w/o Wnd	μ	4.780	4.810	4.810	4.810
	σ	0.075	0.090	0.090	0.090
C1	μ	4.840	4.910	5.100	5.150
	σ	0.110	0.160	0.170	0.180
C1 w/o Wnd	μ	4.890	4.950	5.100	5.150
	σ	0.140	0.160	0.170	0.180
C2	μ	4.880	5.020	5.280	5.350
	σ	0.100	0.120	0.070	0.095
C2 w/o Wnd	μ	4.990	5.070	5.280	5.349
	σ	0.100	0.120	0.070	0.090
S1	μ	4.900	5.120	5.500	5.615
	σ	0.130	0.180	0.100	0.070
S1 w/o Wnd	μ	5.220	5.290	5.500	5.615
	σ	0.110	0.120	0.100	0.070
S2	μ	4.900	5.100	5.525	5.640
	σ	0.130	0.180	0.080	0.070
S2 w/o Wnd	μ	5.250	5.340	5.525	5.640
	σ	0.090	0.120	0.080	0.070
U	μ	4.900	5.110	5.550	5.640
	σ	0.130	0.200	0.070	0.070
U w/o Wnd	μ	5.290	5.350	5.550	5.640
	σ	0.100	0.120	0.070	0.070

A.3. Third Story Additions

Table A.7 - Component parameters for third story additions

Component	Description		Damage State			
			Slight	Moderate	Extensive	Total
Roof Deck	6-6-6U	μ	5.190	5.250	5.455	5.570
		σ	0.105	0.120	0.090	0.060
	6-12-6U	μ	4.940	5.030	5.275	5.445
		σ	0.105	0.120	0.075	0.090
	12-12-12U	μ	4.810	4.940	5.130	5.290
		σ	0.085	0.090	0.080	0.080
	6-6-6R	μ	5.240	5.320	5.517	5.750
		σ	0.100	0.120	0.075	0.130
	6-12-6R	μ	5.210	5.310	5.485	5.630
		σ	0.090	0.110	0.080	0.070
	12-12-12R	μ	5.210	5.310	5.485	5.630
		σ	0.090	0.110	0.080	0.070
Roof-to-Wall Connection	Gen. Pop.	μ	-	-	-	5.110
		σ	-	-	-	0.280
	Toe Nail	μ	-	-	-	4.770
		σ	-	-	-	0.090
	S. Strap per 2 joists	μ	-	-	-	5.290
		σ	-	-	-	0.095
	S. Strap	μ	-	-	-	5.440
		σ	-	-	-	0.100
	U-hanger	μ	-	-	-	5.650
		σ	-	-	-	0.090
Wall Structure	Gen. Pop.	μ	-	-	-	5.220
		σ	-	-	-	0.120
	Toe Nail	μ	-	-	-	4.960
		σ	-	-	-	0.080
	T.N. + Conn.	μ	-	-	-	5.535
		σ	-	-	-	0.080
Wall Sheathing	Gen. Pop.	μ	5.420	5.420	5.430	5.430
		σ	0.150	0.150	0.150	0.150
Windows	Gen. Pop.	μ	4.900	5.180	5.640	5.740
		σ	0.130	0.220	0.080	0.100

Table A.8 - Statistical fragility parameters for third story additions

System		Damage State			
		Slight	Moderate	Extensive	Total
W	μ	4.740	4.770	4.770	4.770
	σ	0.075	0.090	0.090	0.090
W w/o Wnd	μ	4.740	4.770	4.770	4.770
	σ	0.075	0.090	0.090	0.090
C1	μ	4.800	4.890	5.020	5.080
	σ	0.110	0.160	0.170	0.180
C1 w/o Wnd	μ	4.830	4.910	5.020	5.080
	σ	0.130	0.170	0.170	0.180
C2	μ	4.850	4.990	5.230	5.280
	σ	0.090	0.115	0.070	0.085
C2 w/o Wnd	μ	4.930	5.030	5.230	5.280
	σ	0.100	0.120	0.070	0.085
S1	μ	4.900	5.120	5.380	5.410
	σ	0.130	0.180	0.100	0.110
S1 w/o Wnd	μ	5.170	5.240	5.380	5.410
	σ	0.110	0.110	0.100	0.110
S2	μ	4.900	5.100	5.390	5.410
	σ	0.130	0.180	0.105	0.110
S2 w/o Wnd	μ	5.210	5.290	5.390	5.410
	σ	0.090	0.120	0.105	0.110
U	μ	4.900	5.110	5.390	5.410
	σ	0.130	0.200	0.110	0.110
U w/o Wnd	μ	5.240	5.290	5.390	5.410
	σ	0.100	0.120	0.110	0.110

A.4. Small Institutional Buildings

A.4.1. Buildings with Stud Walls

Table A.9 - Component parameters for stud wall institutional buildings

Component	Description		Damage State			
			Slight	Moderate	Extensive	Total
Roof Deck	6-6-6U	μ	5.250	5.330	5.530	5.800
		σ	0.105	0.120	0.090	0.150
	6-12-6U	μ	5.005	5.105	5.350	5.520
		σ	0.105	0.130	0.070	0.090
	6-6-6R	μ	5.320	5.390	5.590	5.890
		σ	0.100	0.130	0.075	0.150
	6-12-6R	μ	5.290	5.380	5.540	5.760
		σ	0.090	0.120	0.070	0.100
Roof-to-Wall Connection	Gen. Pop.	μ	-	-	-	5.150
		σ	-	-	-	0.270
	S. Strap per 2 joists	μ	-	-	-	5.380
		σ	-	-	-	0.100
	S. Strap	μ	-	-	-	5.480
		σ	-	-	-	0.100
	U-hanger	μ	-	-	-	*7.0*
		σ	-	-	-	*0.1*
Wall Structure	Gen. Pop.	μ	-	-	-	5.290
		σ	-	-	-	0.125
	T.N. + Conn.	μ	-	-	-	5.580
		σ	-	-	-	0.060
Wall Sheathing	Gen. Pop.	μ	*7.0*	*7.0*	*7.0*	*7.0*
		σ	*0.1*	*0.1*	*0.1*	*0.1*
Windows	Gen. Pop.	μ	4.920	5.110	*7.0*	*7.0*
		σ	0.150	0.190	*0.1*	*0.1*

Table A.10 - Statistical fragility parameters for stud wall institutional buildings

System		Damage State			
		Slight	Moderate	Extensive	Total
C2	μ	4.880	5.020	5.325	5.385
	σ	0.100	0.120	0.070	0.090
C2 w/o Wnd	μ	5.000	5.105	5.325	5.385
	σ	0.105	0.125	0.070	0.090
S1	μ	4.900	5.120	5.510	5.570
	σ	0.130	0.180	0.080	0.060
S1 w/o Wnd	μ	5.250	5.335	5.510	5.570
	σ	0.110	0.120	0.080	0.060
S2	μ	4.900	5.100	5.530	5.580
	σ	0.130	0.180	0.070	0.060
S2 w/o Wnd	μ	5.280	5.380	5.530	5.580
	σ	0.090	0.120	0.070	0.060
U	μ	4.900	5.110	5.550	5.580
	σ	0.130	0.190	0.060	0.060
U w/o Wnd	μ	5.320	5.390	5.550	5.580
	σ	0.100	0.120	0.060	0.060

A.4.2. Mixed Constructions

Table A.11 - Component parameters for mixed institutional buildings

Component	Description		Damage State			
			Slight	Moderate	Extensive	Total
Roof Deck	6-6-6U	μ	5.250	5.330	5.530	5.800
		σ	0.105	0.120	0.090	0.150
	6-12-6U	μ	5.005	5.105	5.350	5.520
		σ	0.105	0.130	0.070	0.090
	6-6-6R	μ	5.320	5.390	5.590	5.890
		σ	0.100	0.130	0.075	0.150
	6-12-6R	μ	5.290	5.380	5.540	5.760
		σ	0.090	0.120	0.070	0.100
Roof-to-Wall Connection	Gen. Pop.	μ	-	-	-	5.150
		σ	-	-	-	0.270
	U-hanger	μ	-	-	-	*7.0*
		σ	-	-	-	*0.1*
Windows	Gen. Pop.	μ	4.920	5.110	*7.0*	*7.0*
		σ	0.150	0.190	*0.1*	*0.1*

Table A.12 - Statistical fragility parameters for institutional buildings

System		Damage State			
		Slight	Moderate	Extensive	Total
C2	μ	4.880	5.020	5.310	5.390
	σ	0.100	0.120	0.070	0.100
C2 w/o Wnd	μ	5.000	5.105	5.310	5.390
	σ	0.105	0.125	0.070	0.100
S1	μ	4.900	5.100	5.525	5.630
	σ	0.130	0.180	0.090	0.060
S1 w/o Wnd	μ	5.250	5.335	5.525	5.630
	σ	0.110	0.120	0.090	0.060
S2	μ	4.900	5.100	5.545	5.630
	σ	0.130	0.180	0.070	0.060
S2 w/o Wnd	μ	5.280	5.380	5.545	5.630
	σ	0.090	0.120	0.070	0.060
U	μ	4.900	5.110	5.570	5.640
	σ	0.130	0.190	0.060	0.060
U w/o Wnd	μ	5.320	5.390	5.570	5.640
	σ	0.100	0.120	0.060	0.060

A.5. Large Institutional Buildings

Table A.13 - Component parameters for large institutional buildings

Component	Description		Damage State			
			Slight	Moderate	Extensive	Total
Roof Deck	6-6-6U	μ	5.250	5.350	5.530	5.740
		σ	0.100	0.105	0.070	0.090
	6-6-6R	μ	5.320	5.430	5.590	5.740
		σ	0.080	0.090	0.060	0.090
	6-12-6R	μ	5.290	5.410	5.560	5.710
		σ	0.090	0.090	0.060	0.090
Roof-to-Wall Connection	Gen. Pop.	μ	-	-	-	5.250
		σ	-	-	-	0.260
	U-hanger	μ	-	-	-	5.540
		σ	-	-	-	0.120
Windows	Gen. Pop.	μ	4.950	5.200	5.330	*7.0*
		σ	0.140	0.190	0.170	*0.1*

Table A.14 - Statistical fragility parameters for large institutional buildings

System		Damage State			
		Slight	Moderate	Extensive	Total
C2	μ	4.880	5.050	5.180	5.230
	σ	0.140	0.140	0.130	0.150
C2 w/o Wnd	μ	5.000	5.105	5.220	5.240
	σ	0.105	0.125	0.140	0.150
S1	μ	4.940	5.180	5.300	5.540
	σ	0.160	0.180	0.140	0.130
S1 w/o Wnd	μ	5.250	5.335	5.475	5.525
	σ	0.110	0.120	0.090	0.110
S2	μ	4.940	5.180	5.300	5.540
	σ	0.160	0.180	0.140	0.130
S2 w/o Wnd	μ	5.280	5.390	5.500	5.530
	σ	0.100	0.110	0.110	0.120
U	μ	4.940	5.180	5.300	5.540
	σ	0.160	0.180	0.140	0.130
U w/o Wnd	μ	5.310	5.400	5.510	5.540
	σ	0.090	0.100	0.110	0.120

APPENDIX B

ROOF TESTS SUMMARY

B.1. Specimen 30

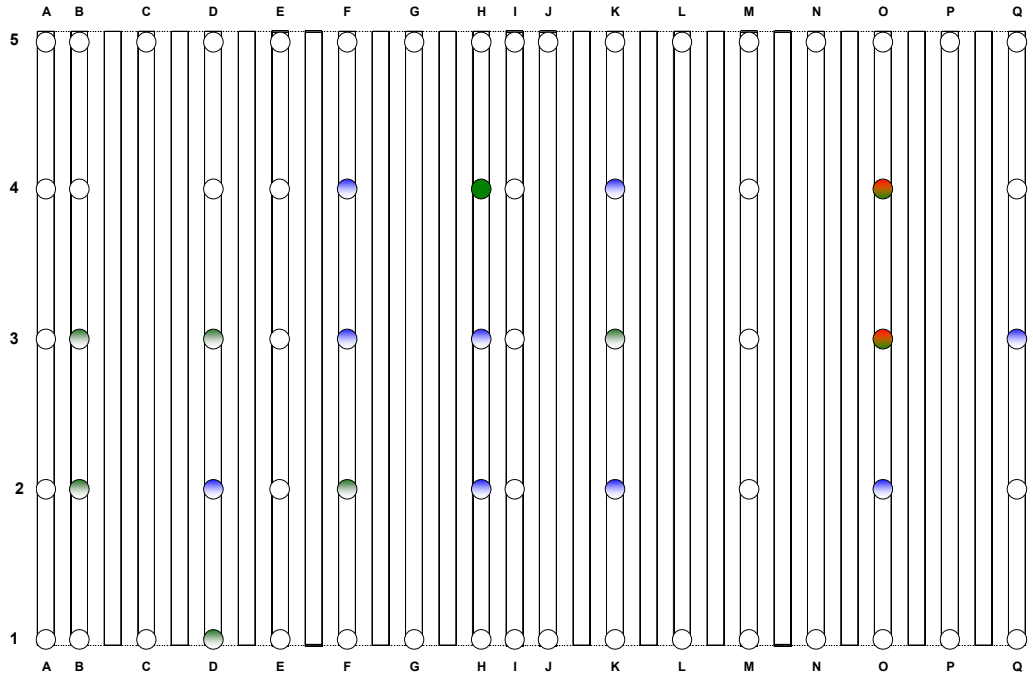

Figure B.1 - Schematic drawing of Specimen 30

Table B.1 - Damage summary of Specimen 30

Failures, in order of appearance: 10.5. Total number of fasteners: 67.

Lv.	Set	Comments
A	4	Fatigue crack around fastener in O4.
A	5	Fatigue crack around fastener in O3.
B	2	Fatigue crack around fastener in H2, H3.
B	3	Fatigue crack around fastener in F3, F4, K4.
B	6	Fatigue crack around fastener in K2, O2, D2.
B	8	Fatigue crack around fastener in Q3.
C	2	Fatigue crack around fastener in H4.
C	3	Connector head lost in H4. Fatigue crack around fastener in B2, B3, F2.
C	4	Connector separated from sheathing in O3.
C	5	Connector separated from sheathing in O4.
C	8	Fatigue crack around fastener in D1, D3, K3. Test finished.

Level A Index: 1.0
Level B Index: 5.5
Level C Index: 10.5

B.2. Specimen 31

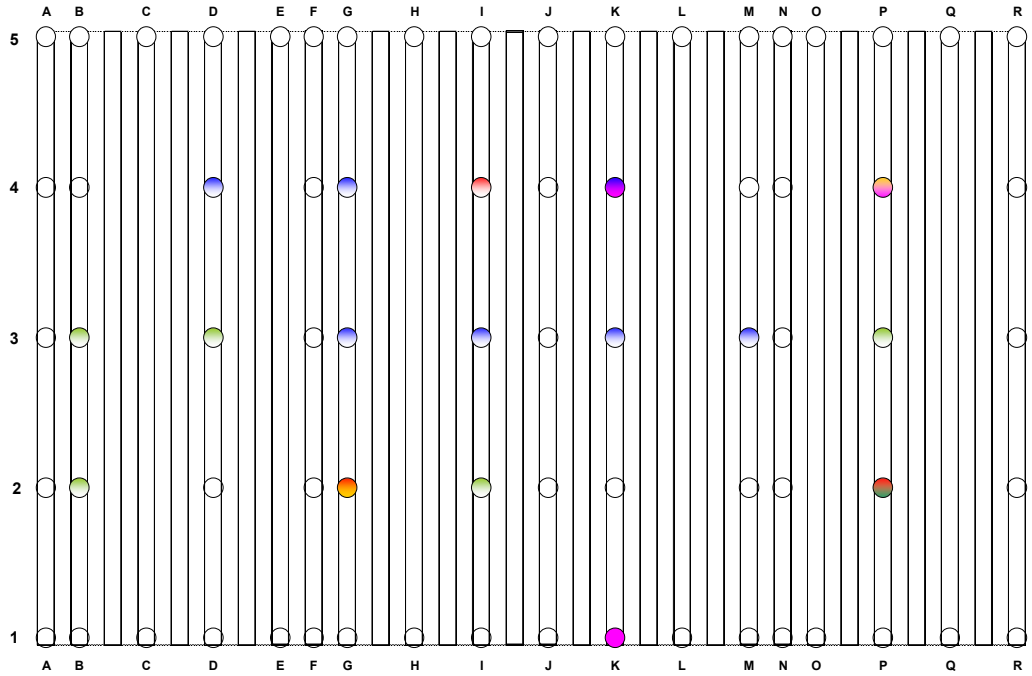

Figure B.2 - Schematic drawing of Specimen 31

Table B.2 - Damage summary of Specimen 31

Failures, in order of appearance: 11. Total number of fasteners: 68.

Cycles	Comments
0 - 1000	Fatigue crack around fastener in P2.
1000 - 2000	Fatigue crack around fastener in I4, G2.
2000 - 3000	Fatigue crack around fastener in K3, I3, G4.
3000 - 4000	Fatigue crack around fastener in M3, G3, D4.
4000 - 5000	Fatigue crack around fastener in I2, B2, D3,P3. Connector head lost in P2.
5000 - 6000	Fatigue crack around fastener in B3.
6000 - 7000	Fatigue crack around fastener in G2,K4,P4.
7000 - 8000	Propagation of previous fatigue cracks.
8000 - 9000	Propagation of previous fatigue cracks.
9000 - 10000	Connector separated from sheathing in P4.
10000 - 10200	Connector head lost in K1. Connector separated from sheathing in K1, K4. Test finished.

B.3. Specimen 32

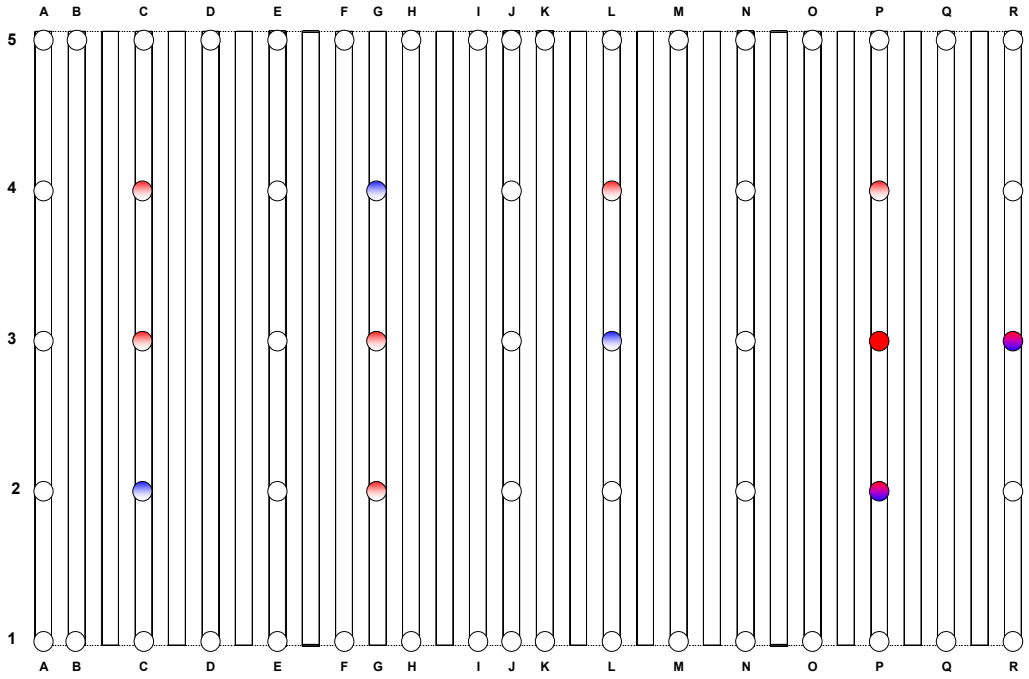

Figure B.3 - Schematic drawing of Specimen 32

Table B.3 - Damage summary of Specimen 32

Failures, in order of appearance: 7.5. Total number of fasteners: 61.

Lv.	Set	Comments
A	2	Connector head lost in P3.
A	3	Fatigue crack around fastener in P2. Connector head lost in R3.
A	4	Fatigue crack around fastener in G2, G3. Connector separated from sheathing in P3.
A	5	Fatigue crack around fastener in C4.
A	6	Fatigue crack around fastener in L4.
A	7	Fatigue crack around fastener in C3, P4.
B	1	Fatigue crack around fastener in G4, C2.
B	3	Connector separated from sheathing in R3.
B	4	Fatigue crack around fastener in L3. Connector separated from sheathing in P2.
C	8	Propagation of previous fatigue cracks. Test finished.

Level A Index: 5.0
Level B Index: 7.5
Level C Index: 7.5

B.4. Specimen 33

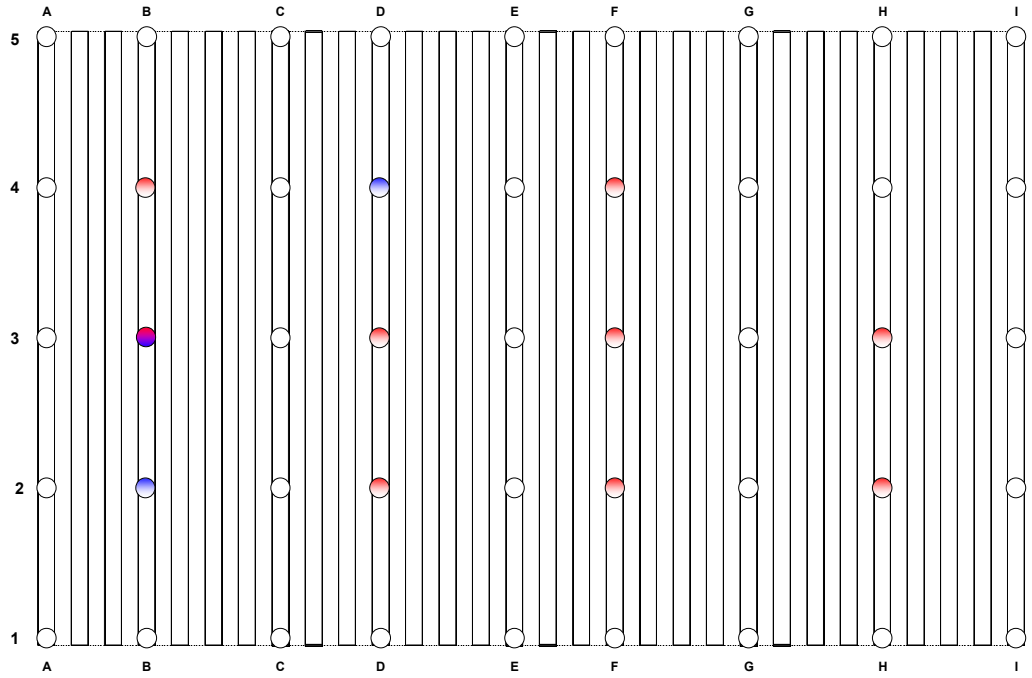

Figure B.4 - Schematic drawing of Specimen 33

Table B.4 - Damage summary of Specimen 33

Failures, in order of appearance: 6. Total number of fasteners: 45.

Lv.	Set	Comments
A	4	Fatigue crack around fastener in B3, F4, H2, H3. Connector head lost in B4.
A	5	Fatigue crack around fastener in D2, D3, D4.
A	8	Fatigue crack around fastener in F2, F3.
B	3	Connector separated from sheathing in B3.
B	4	Fatigue crack around fastener in B2.
B	6	Connector separated from sheathing in D4.
B	8	Propagation of previous fatigue cracks. Test finished.

Level A Index: 5.0
Level B Index: 6.5

B.5. Specimen 34

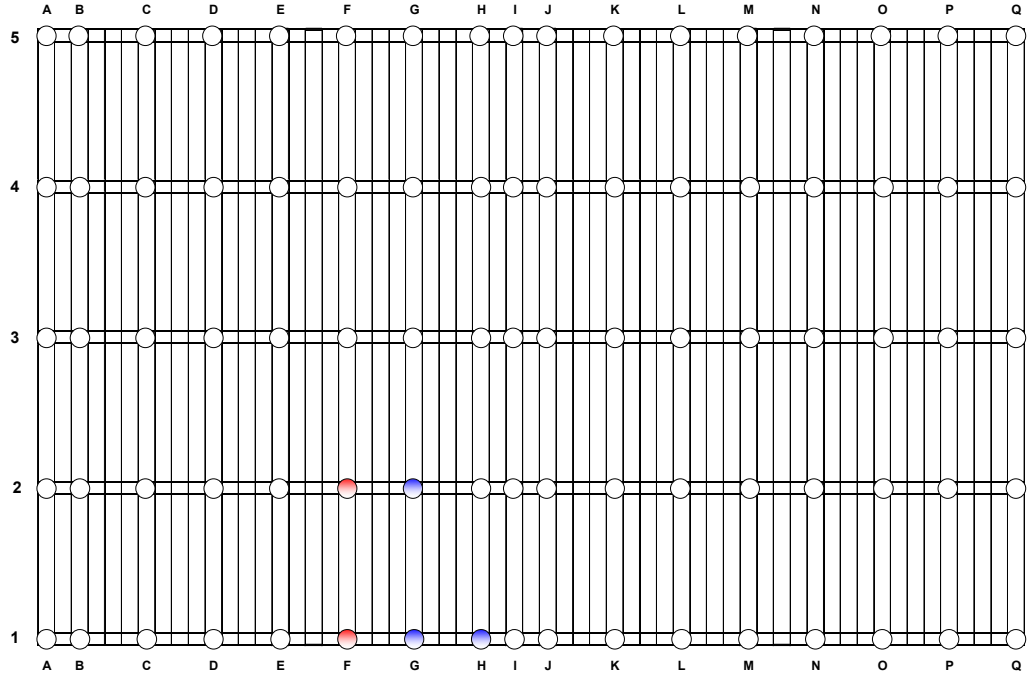

Figure B.5 - Schematic drawing of Specimen 34

Table B.5 - Damage summary of Specimen 34

Failures, in order of appearance: 5 Total number of fasteners: 85.

Lv.	Set	Comments
F	4	Fatigue failure of connector in F1 , F2.
G	3	Fatigue failure of connector in G1.
G	4	Fatigue failure of connector in G2. Straightening and withdrawal of connector in H1. Test finished.

Level F Index: 2.0
Level G Index: 5.0

B.6. Specimen 35

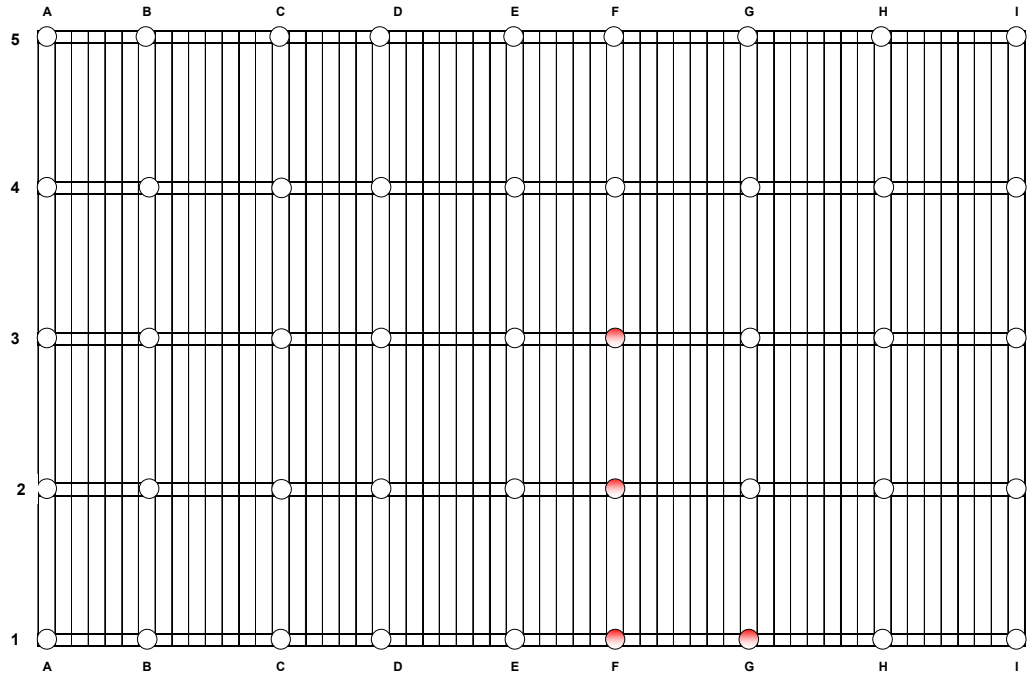

Figure B.6 - Schematic drawing of Specimen 35

Table B.6 - Damage summary of Specimen 35

Failures, in order of appearance: 4. Total number of fasteners: 45.

Lv.	Set	Comments
M	4	Connector withdrew from spacer in F1, F2, F3, G1. Test Finished.

Level F Index: 4.0

B.7. Specimen 36

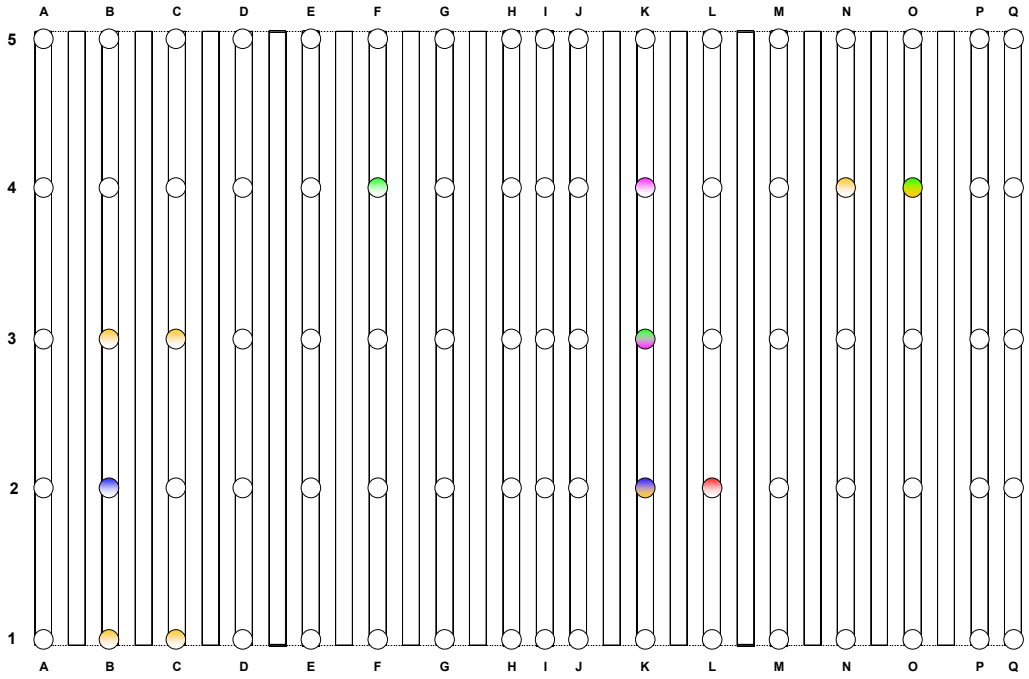

Figure B.7 - Schematic drawing of Specimen 36

Table B.7 - Damage summary of Specimen 36

Failures, in order of appearance: 7.5 Total number of fasteners: 85.

Lv.	Set	Comments
G	8	Connector head lost in L2.
K	4	Fatigue failure in B2 and K2.
L	2	Fatigue failure around connector in F4 and O4.
L	4	Fatigue failure around connector in K3.
M	2	Fatigue failure around connector in N4.
M	4	Fatigue failure around connector in B1, B3, C1, and C3.
M	8	Connector separated from sheathing in K2 and O4.
N	4	Connector separated from sheathing in K3. Fatigue failure around connector in K4. Test finished.

Level G Index:	0.5	Level K Index:	1.5
Level H Index:	0.5	Level L Index:	3.0
Level I Index:	0.5	Level M Index:	6.5
Level J Index:	0.5	Level N Index:	7.5

B.8. Specimen 37

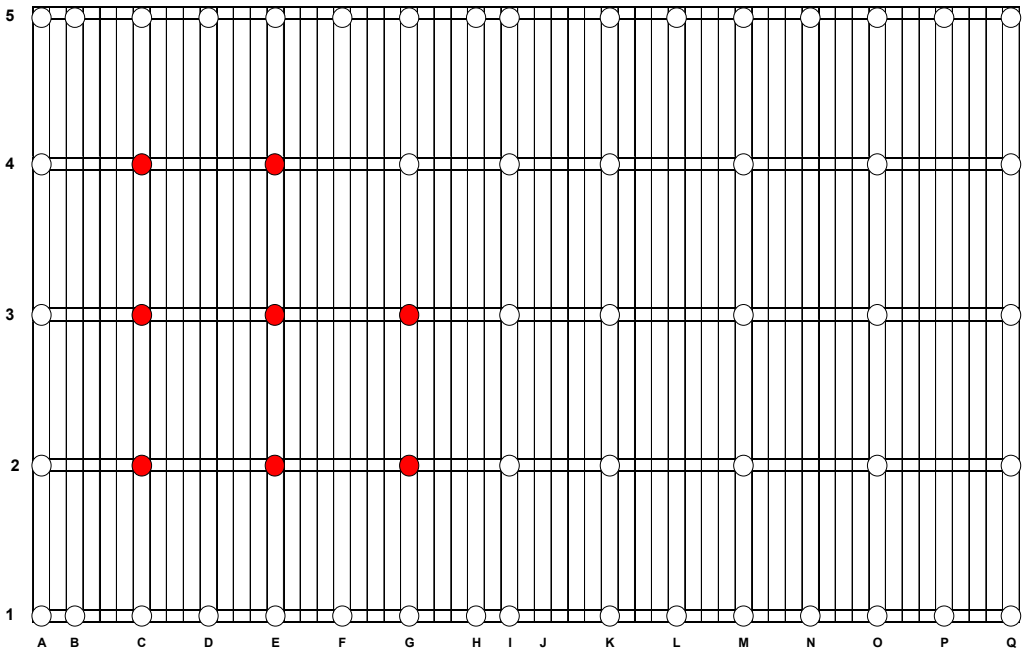

Figure B.8 - Schematic drawing of Specimen 37

Table B.8 - Damage summary of Specimen 37

Failures, in order of appearance: 8. Total number of fasteners: 59.

Lv.	Set	Comments
H	4	Connector withdrew from spacer in C2, C3, C4, E2, E3, E4, G2, G3. Test Finished.

Level H Index: 8.0

NOTE: Ultimate load from static load: 9.5 kips.

B.9. Specimen 38

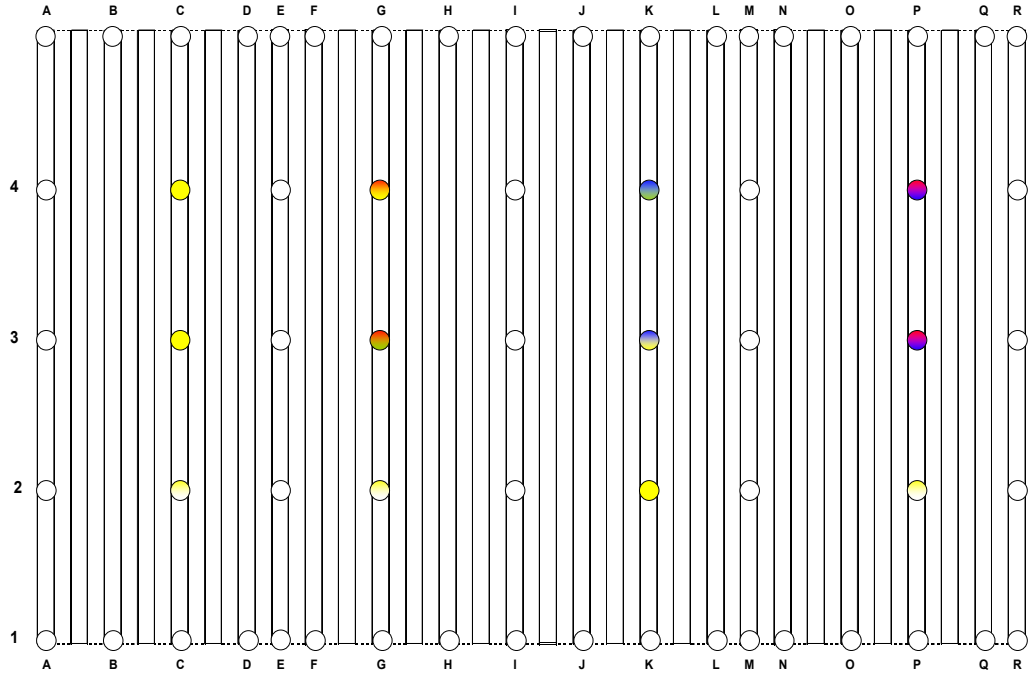

Figure B.9 - Schematic drawing of Specimen 38

Table B.9 - Damage summary of Specimen 38

Failures, in order of appearance: 10.5. Total number of fasteners: 63.

Lv.	Set	Comments
D	4	Fatigue crack around fastener in P3, P4.
D	8	Fatigue crack around fastener in G3, G4.
E	3	Fatigue crack around fastener in K3.
E	4	Connector head lost and separation of sheahing in P3, P4.
E	8	Fatigue crack around fastener in K4.
G	4	Connector separated from sheathing in G3, K4.
H	2	Fatigue crack around fastener in C2, K2, G4, P2.
H	3	Connector separated from sheathing in K3.
H	4	Connector separated from sheathing in C3, C4, K2. Fatigue crack around fastener in G2. Finished.

Level D Index: 2.0
Level E Index: 5.0
Level F Index: 5.0
Level G Index: 6.0
Level H Index: 10.5

B.10. Specimen 39

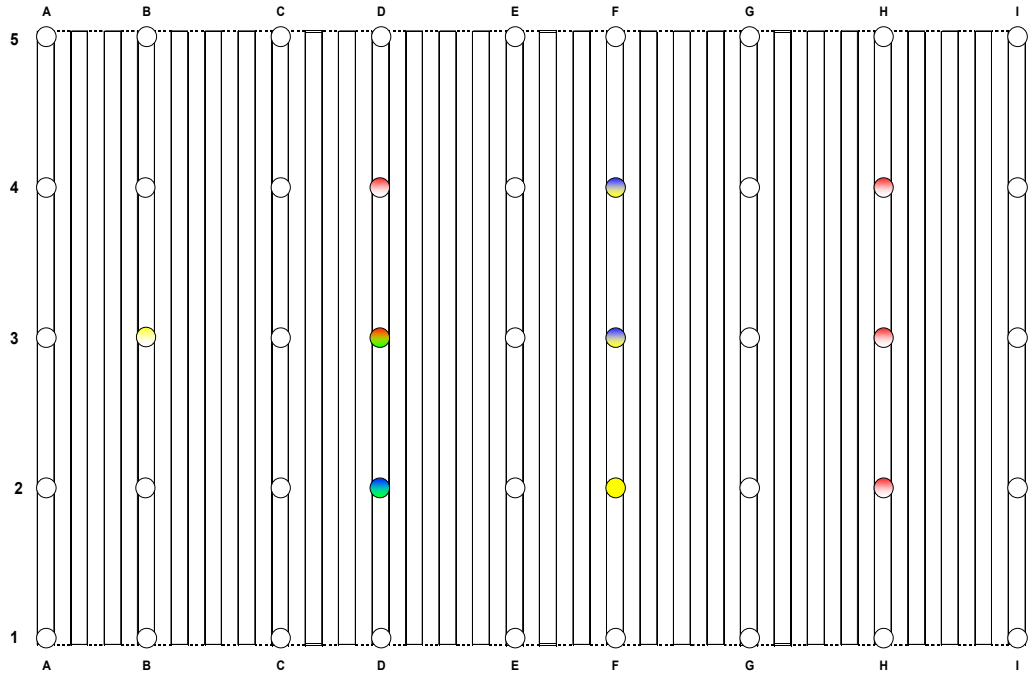

Figure B.10 - Schematic drawing of Specimen 39

Table B.10 - Damage summary of Specimen 39

Failures, in order of appearance: 8.5. Total number of fasteners: 45.

Lv.	Set	Comments
C	3	Fatigue crack around fastener in H3.
C	4	Fatigue crack around fastener in H2.
C	6	Fatigue crack around fastener in D3, H4.
C	8	Fatigue crack around fastener in D4.
D	4	Fatigue crack around fastener in F4.
D	8	Fatigue crack around fastener in D2, F3.
F	3	Connector separated from sheathing in D2.
F	4	Connector separated from sheathing in D3.
G	2	Fatigue crack around fastener in B3.
G	4	Connector separated from sheathing in F2, F3, F4. Test finished.

Level C Index: 2.5
Level D Index: 4.0
Level E Index: 4.0
Level F Index: 6.0
Level G Index: 8.5